

**THE EFFECT OF DIALYSIS ENVIRONMENT AND
REPROCESSING PROCEDURE ON THE MECHANICAL AND
STRUCTURAL STABILITY OF HIGH FLUX POLYSULFONE
MEMBRANE**

by

Bengi YILMAZ

B.Sc. in Chemical Engineering, METU, 2006

Submitted to the Institute of Biomedical Engineering
in partial fulfillment of the requirements
for the degree of
Master of Science
in
Biomedical Engineering

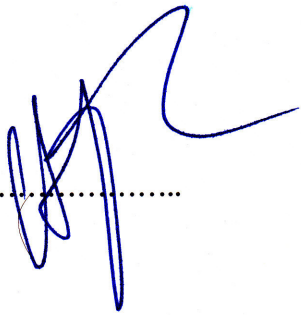
Bogaziçi University

August 2008

**THE EFFECT OF DIALYSIS ENVIRONMENT AND
REPROCESSING PROCEDURE ON THE MECHANICAL AND
STRUCTURAL STABILITY OF HIGH FLUX POLYSULFONE
MEMBRANE**

APPROVED BY:

Prof. Dr. A. Hikmet ÜÇİŞİK
(Thesis Advisor)

.....


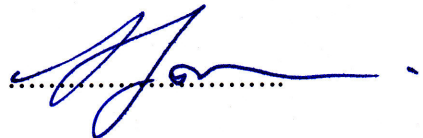
Prof. Dr. Cuma BİNDAL
(Thesis Co-advisor)

.....

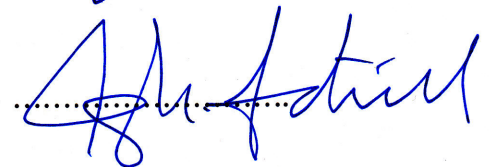

Assoc. Prof. Dr. Metin USTA

.....


Assoc. Prof. Dr. Albert GÜVENİŞ

.....


Assoc. Prof. Dr. Cengizhan ÖZTÜRK

.....


DATE OF APPROVAL: 19.08.2008

ACKNOWLEDGMENTS

Foremost, I would like to thank my thesis advisor, Prof. Dr. A. Hikmet ÜÇİŞİK. This thesis would not have been possible without his kind support and the remarkable patience.

I also like to express my sincere gratitude to Prof. Dr. Cuma BİNDAL from Sakarya University and Assoc. Prof. Dr. Metin USTA from Gebze Institute of Technology for giving the opportunity to carry out my experiments in their laboratories. I would like to express my sincere gratitude to Assist. Prof. Dr. A. Şükran DEMİRKİRAN and Fuat KAYIŞ from Sakarya University and Mızrap CANİBEYAZ from İstanbul Technical University for their support in laboratory works. It is a pleasure to thank Dr. Emin AKSOY from Ministry of Health İstanbul Health Management, Burhanettin ATAŞ from Taksim Education and Research Hospital, Prof. Dr. Semra BOZFAKİOĞLU from İstanbul Medical School of İstanbul University and Prof. Dr. Rezzan ATAMAN from Cerrahpaşa Medical School of İstanbul University for their interest. I am indebted to my student colleague Neslihan SARICA for providing a stimulating and fun environment during my thesis.

Finally, I would like to dedicate my M.Sc. thesis to my family on whose constant encouragement and love I have relied throughout my life. Especially I thank to my mother whose love is boundless and to my father for growing his daughters in an atmosphere full of science and art. I am grateful to my sister and her husband; Dr. Bilge YILMAZ KARA and Dr. Ekrem KARA, for the friendship, entertainment and caring they provided. And I am deeply grateful to Onur KARADELİ for his love, emotional support and patience.

This study is not funded nor influenced by any dialysis-products company or any other commercial agency.

ABSTRACT

THE EFFECT OF DIALYSIS ENVIRONMENT AND REPROCESSING PROCEDURE ON THE MECHANICAL AND STRUCTURAL STABILITY OF HIGH FLUX POLYSULFONE MEMBRANE

Although there are many clinical researches in the open literature, biocompatibility and performance of reprocessed hemodialysis membranes are not still well defined. This thesis aims to fulfill the deficiency in the experimental studies performed from an engineering point of view. In line with this aim, Fresenius FX80 polysulfone hemodialyzer membrane was exposed to formaldehyde and bleach after a dialysis session. The mechanical stabilities of virgin and used-processed fibers were investigated by tensile tests consisting of monotonic and cyclic loading. The surface features and morphology changes were examined by SEM and AFM. The crystallinity of the mechanically tested virgin and used-processed fibers was determined by XRD. The experiments showed that the ductility, toughness and strength of the used-processed fibers decrease. The microscopic studies depicted some morphological changes such as increase in pore size and deformation in pore shapes. The X-ray diffraction method demonstrated the increase in the crystallinity of monotonically loaded used-processed or virgin fibers. However, it is seen that the cyclically loaded fibers undergo some structural changes, although the crystalline portion in their structure does not increase. This result can be related with the loading cycles in the elastic region and further studies are needed to determine the behavior of polymeric material. In conclusion, reprocessing and dialysis structurally changes the hemodialyzer membrane, which may result in some complications during hemodialysis reuse.

Keywords: High Flux Polysulfone Hemodialyzer, Reuse, Formaldehyde, Bleach, Reprocessing, SEM, AFM, XRD, Tensile Test

ÖZET

DİYALİZ ORTAMININ VE TEKRAR KULLANILMAK ÜZERE HAZIRLAMA SÜRECİNİN YÜKSEK AKIM POLİSÜLFON MEMBRANLARININ MEKANİK VE YAPISAL STABİLİTESİ ÜZERİNDEKİ ETKİLERİ

Literatürde nefroloji ve hemodiyaliz konusunda gerçekleştirilmiş birçok klinik çalışma mevcut olmasına rağmen, hemodiyaliz membranlarının biyouyumluluk ve performansları hakkında yeterli sayıda laboratuvar çalışması bulunmamaktadır. Bu çalışma, ele alınan konuda, mühendislik bakış açısıyla yapılmış olan ilk araştırmalardan bir tanesidir. Bu çalışmada, Fresenius FX80 polisülfon diyaliz membranı, hasta tarafından kullanıldıktan sonra, formaldehit ve sodyum hipoklorite maruz bırakılmıştır. Elde edilen kullanılmış–tekrar işlenmiş membranlarla, hiç kullanılmamış membranın mekanik özellikleri monotonik ve tekrarlı yüklemelerle incelenmiş ve yapılan deneyler birbirleriyle karşılaştırılmıştır. Kullanılan membranların yüzeylerindeki ve morfolojilerindeki değişimler taramalı elektron mikroskobu ve atomik kuvvet mikroskobu ile incelenmiştir. Mekanik yüklemeye maruz bırakılan membranların yapılarındaki kristallik X–ışını difraksiyonu ile tayin edilmiş ve orijinal yapısı ile karşılaştırılmıştır. Elde edilen sonuçlara göre, kullanılmış–tekrar işlenmiş membranların tokluğu ve mukavemeti düşmüştür. Yapılan mikroskopik çalışmalar, söz konusu membranların por büyüklüğünde artma ve por şeklinde değişim olduğunu göstermiştir. Kristal yapıda artma, beklenildiği gibi monotonik olarak yüklenen fiberlerde görülmesine rağmen, tekrarlı olarak yüklenen fiberlerde görülmemiştir. Bunun sebepleri arasında tekrarlı yüklemelerin elastik bölgede kalması ve plastik deformasyona sebep vermemesi olabilir, ancak sonucun net olarak açıklanabilmesi için polimer davranışının tam olarak tespit edilebilmesini amaçlayan ileri çalışmalar gerekmektedir. Sonuç olarak, tekrar–işleme ve diyaliz, polisülfon hemodiyalizörler üzerinde, diyaliz sırasında komplikasyonlara sebep olması muhtemel yapısal değişikliklere sebebiyet vermektedir.

Anahtar Kelimeler: Polisülfon hemodiyalizör, Yüksek akımda diyaliz, Tekrar kullanım (Reuse), Formaldehit, Sodyum hipoklorit, SEM, AFM, XRD, Çekme Deneyi

TABLE OF CONTENTS

ACKNOWLEDGEMENTS.....	iii
ABSTRACT.....	iv
ÖZET.....	v
LIST OF FIGURES.....	viii
LIST OF TABLES.....	xi
LIST OF SYMBOLS.....	xii
LIST OF ABBREVIATIONS.....	xiii
1. INTRODUCTION.....	1
1.1 Objective Of The Thesis.....	1
1.2 The Kidney.....	1
1.2.1 Anatomy Of The Kidney.....	2
1.2.2 Filtration In The Kidney.....	3
1.2.3 Chronic Renal Failure.....	5
1.3 Hemodialysis.....	7
1.3.1 History of Hemodialysis.....	7
1.3.2 A Statistical Perspective.....	8
1.3.3 Principles Of Hemodialysis.....	11
1.4 Polysulfone Hemodialyzers.....	15
1.4.1 Hemodialyzers In General.....	15
1.4.2 General Properties Of Polysulfone.....	17
1.4.3 Fresenius FX Class Polysulfone Dialyzers.....	18
1.5 Reuse Procedure.....	22
1.5.1 Brief History.....	22
1.5.2 Reprocessing Solutions.....	23
1.5.3 Formaldehyde Bleach Reprocessing And Clearance.....	25
1.5.4 Advantages and Disadvantages Of Reuse.....	26
2. EXPERIMENTAL TECHNIQUES.....	29
2.1 Specimen preparation.....	30
2.1.1 Hemodialyzers.....	30
2.1.2 Cutting.....	32

2.1.3	Reprocessing.....	33
2.2	Stereomicroscopy.....	35
2.2.1	Introduction.....	35
2.2.2	Materials and Methods.....	35
2.2.3	Results And Discussion Of The Stereomicroscopic Studies.....	36
2.2.4	Conclusions.....	39
2.3	Mechanical Tests.....	39
2.3.1	Introduction.....	39
2.3.2	Materials and Methods.....	44
2.3.3	Results And Discussion Of Tensile Tests.....	45
2.3.4	Conclusions.....	51
2.4	Atomic Force Microscopy (AFM).....	53
2.4.1	Introduction.....	53
2.4.2	Materials and Methods.....	55
2.4.3	Results And Discussion Of AFM Studies.....	56
2.4.4	Conclusions.....	60
2.5	Scanning Electron Microscopy (SEM).....	61
2.5.1	Introduction.....	62
2.5.2	Materials and Methods.....	65
2.5.3	Results and Discussions of SEM Studies.....	66
2.5.4	Conclusions.....	73
2.6	X-Ray Diffractometry (XRD).....	74
2.6.1	Introduction.....	75
2.6.2	Materials and Methods.....	76
2.6.3	Results and Discussions of XRD Studies.....	77
2.6.4	Conclusions.....	83
3.	DISCUSSION.....	86
4.	CONCLUSION.....	91
	REFERENCES.....	92

LIST OF FIGURES

Figure 1.2.1.1	General organization of the kidneys and the urinary system.....	2
Figure 1.2.1.2	Basic tubular segments of the nephron (left), the relative lengths of the different tubular segments are not drawn to scale, Scanning electron micrograph of a glomerulus (right) $\times 300$	3
Figure 1.3.2.1	Total number of dialysis patients in the world and estimated increase in trend.....	8
Figure 1.3.2.2	The number of hemodialysis patients by years in Turkey.....	9
Figure 1.3.2.3	The renal replacement therapies modalities in prevalent ESRD patients as of the end of 2006 (left), incidence by gender in regular 11583 hemodialysis patients (right) in the year 2006.....	10
Figure 1.3.2.4	Etiology in prevalent hemodialysis patients in Turkey.....	10
Figure 1.3.3.1	Schema for hemodialysis.....	11
Figure 1.3.3.2	Mechanisms of solute removal in blood purification techniques.....	13
Figure 1.3.3.3	The mechanism of ultrafiltration in response to a trans–membrane pressure gradient.....	13
Figure 1.4.2.1	The chemical structure of polysulfone	17
Figure 1.4.3.1	Schematic representation of the components of the FX Class hemodialyzers. Top panel depicts the peculiar blood port and potting structure; middle panel describes the micro–ondulation of the fibers in the bundle; bottom panel depicts the special dialysate entrance with the pinnacle structure.....	20
Figure 2.1.1.1	The virgin hemodialyzer (upper) and the hemodialyzer after patient contact (lower).....	31
Figure 2.1.2.1	The diagram of cutting procedure.....	32
Figure 2.1.2.2	The picture of cutting the hemodialyzer which is mounted in a vise.....	33
Figure 2.1.3.1	The used top before rinse.....	34
Figure 2.1.3.2	The used fibers and tops in a glass plate, ready to be left in disinfectants.....	34
Figure 2.2.2.1	The Olympus U–PMTVC Stereomicroscope at ITU Materials Laboratories.....	36
Figure 2.2.3.1	The position of the dialyzer head under microscope (upper) and the microscopic views of head, showing the tapping material with the blood inlets of the fibers in two different magnifications (the two lower).....	37
Figure 2.2.3.2	Placing the sample under the microscope (left), the microscopic view of the conjunction part (right).....	38
Figure 2.2.3.3	A hallow fiber under microscope (left) and its microscopic view (right).....	38
Figure 2.3.1.1	(a) Schematic representation of tensile testing apparatus. (b) Initial portion of stress–strain curve plotted by an X–Y recorder, showing plastic yielding, causing the departure from linear elastic behavior.....	40
Figure 2.3.1.2	Typical non–equilibrium stress–strain curve in elongation.....	41

Figure 2.3.1.3	Non–equilibrium stress strain curves for some types of polymers.....	42
Figure 2.3.2.1	The fibers are mounted to the grips of Instron 5569 Universal Testing Machine individually.....	44
Figure 2.3.3.1	Tensile stress–strain curves of two initially identical virgin polysulfone hemodialyzer fibers, which are loaded monotonically or cyclically up to fracture.....	45
Figure 2.3.3.2	Tensile stress–strain curves of two initially identical used and processed polysulfone hemodialyzer fibers, which are loaded monotonically or cyclically up to fracture.....	47
Figure 2.3.3.3	Tensile stress–strain curves of virgin and used–processed polysulfone hemodialyzer fibers, which are loaded monotonically up to fracture.....	49
Figure 2.3.3.4	Tensile stress–strain curves of virgin and used–processed polysulfone hemodialyzer fibers, which are loaded cyclically for 4 times in elastic portion before the last loading up to fracture.....	50
Figure 2.4.1.1	The principle of atomic force microscope (AFM).....	54
Figure 2.4.1.2	a) An SEM image showing typical probe tip geometry b) The typical video camera view of a properly aligned cantilever ready to scan.....	54
Figure 2.4.2.1	The Q–Scope™ Universal SPM.....	56
Figure 2.4.3.1	The 3D AFM images of the exterior surface of the virgin and used–processed polysulfone hollow fibers: (a) virgin fiber in the range of 20 μm , (b) used–processed fiber in the range of 20 μm , (c) virgin fiber in the range of 40 μm , (d) used–processed fiber in the range of 40 μm	57
Figure 2.4.3.2	The 3D AFM images of the exterior surface of the virgin and used–processed polysulfone hollow fibers in the range of 3 μm : (a) virgin (height=619.1 nm), (b) used–processed (height=925.2 nm).....	58
Figure 2.4.3.3	The 3D AFM images of the exterior surface of virgin fiber at a scan size of 20 μm (left), used–processed fiber at a scan size of 20 μm (right).....	59
Figure 2.4.3.4	Height histograms of the images of virgin and used–processed hollow fibers (a) virgin (b) used–processed.....	59
Figure 2.5.1.1	The principle layout of Scanning Electron Microscope (SEM).....	62
Figure 2.5.1.2.	Field–Emission Scanning Electron Microscopy of the Helixone hollow fiber with relative dimensional parameters.....	64
Figure 2.5.2.1	JEOL JSM–6060LV Scanning electron microscope.....	65
Figure 2.5.2.2	Polaron SC7620 SEM sputter coater with CA7625 carbon accessory.....	66
Figure 2.5.3.1	SEM micrographs of the fracture surfaces of: (a) monotonically loaded virgin, (b) monotonically loaded used–processed, (c) cyclically loaded virgin, (d) cyclically loaded used–processed polysulfone hemodialyzer fiber at 500x magnification.....	67
Figure 2.5.3.2	SEM micrographs of the fracture surfaces of: (a) monotonically loaded virgin, (b) monotonically loaded used–processed, (c) cyclically loaded virgin, (d) cyclically loaded used–processed polysulfone hemodialyzer fiber at 2000x magnification.....	68

Figure 2.5.3.3	SEM micrographs of the lateral outer surfaces of: (a) virgin, (b) monotonically loaded virgin, (c) cyclically loaded virgin, (d) monotonically loaded used–processed, (e) cyclically loaded used–processed polysulfone hemodialyzer fiber at 2000x magnification.....	70
Figure 2.5.3.4	SEM micrographs of the lateral outer surfaces of the (untreated) virgin (left) and monotonically loaded used–processed (right) polysulfone hemodialyzer fiber at 1000x magnification.....	71
Figure 2.5.3.5	SEM micrograph of the lateral outer surface of monotonically loaded used–processed polysulfone hemodialyzer fiber at 8000x magnification.....	71
Figure 2.5.3.6	SEM micrographs of the lateral outer surfaces of the (untreated) virgin, cyclically loaded used–processed polysulfone hemodialyzer fiber at 1000x magnification.....	72
Figure 2.5.3.7	SEM micrograph of the lateral outer surface of cyclically loaded used–processed polysulfone hemodialyzer fiber at 8000x magnification.....	72
Figure 2.6.1.1	The principle of X–ray diffraction	75
Figure 2.6.2.1	Rigaku D–Max 2200 X–ray diffractometer.....	77
Figure 2.6.3.1	X–ray diffraction patterns of virgin polysulfone hemodialyzer fibers (upper belongs to the fiber on which monotonic tensile loading is applied).....	78
Figure 2.6.3.2	X–ray diffraction patterns of used–processed polysulfone hemodialyzer fiber on which monotonic tensile loading is applied (upper) and untreated virgin membrane (lower).....	79
Figure 2.6.3.3	The X–ray diffractograms of used–processed polysulfone hemodialyzer fiber after monotonic loading (upper), virgin polysulfone hemodialyzer fiber after monotonic loading (middle), and virgin polysulfone hemodialyzer fiber without any application (lower).....	80
Figure 2.6.3.4	The X–ray diffractograms of virgin polysulfone hemodialyzer fiber after cyclic loading (upper), and virgin polysulfone hemodialyzer fiber without any application (lower)	81
Figure 2.6.3.5	The X–ray diffractograms of used–processed polysulfone hemodialyzer fiber after cyclic loading (upper), and virgin polysulfone hemodialyzer fiber without any application (lower).....	82
Figure 2.6.3.6	The X–ray diffractograms of cyclically loaded polysulfone hemodialyzer fibers; used–processed fiber (upper) and virgin (lower).....	83

LIST OF TABLES

Table 1.2.3.1	Stages of chronic kidney disease and clinical action plan.....	6
Table 1.3.3.1	Comparison of dialyzing fluid with normal and uremic plasma	15
Table 1.4.1.1	Membrane types according to the given definitions.....	16
Table 1.4.3.1	Characteristics of Polysulfone FX80 Dialyzer Membrane.....	21
Table 1.4.3.2	In vitro performance data of FX80.....	21
Table 1.5.2.1	Automated bleach/formaldehyde reprocessing of hemodialyzers	24
Table 2.1.1.1	Dialyzer fibers categorized according to their history.....	31
Table 2.3.3.1	The fracture point stress and strain values and the energy/volume required to fracture the given membranes.....	46
Table 2.3.3.2	The fracture point stress and strain values and the energy/volume required to fracture the given membranes.....	58
Table 2.3.3.3	The fracture point stress and strain values and the energy/volume required to fracture the given membranes.....	49
Table 2.3.3.4	The fracture point stress and strain values and the energy/volume required to fracture the given membranes.....	51
Table 2.4.3.1	Surface characteristics and computed roughnesses.....	60
Table 2.6.3.1	The intensity values of the main peaks of the diffractograms of given membranes.....	80

LIST OF SYMBOLS

Å	Angstroms
°C	Degrees Celsius
d	The spacing between adjacent lattices
ε	Tensile Strain
θ	Diffraction angle
λ	X-ray wavelength
σ	Tensile Stress

LIST OF ABBREVIATIONS

A	Surface Area
A_0	The original specimen cross-sectional area and length
AAMI	Association for Advancement of Medical Instrumentation
AFM	Atomic Force Microscopy
A–V	Arterio–venous
BEI	Backscattered electron imaging
CDC	Centers for Disease Control and Prevention
cps	Counts per second
Cu	Copper
Da	Dalton
ESRD	End–Stage Renal Disease
FE–SEM	Field–Emission Scanning Electron Microscopy
GFR	Glomerular Filtration Rate
GYTE	Gebze Institute of Technology
HBsAg	Hepatitis B surface Antigen
HCFA	Health Care Financing Administration
HIV	Human Immune Deficiency Virus
ITU	Istanbul Technical University
K_f	Filtration coefficient
K_{uf}	Ultrafiltration coefficient
K_oA	Area mass transfer coefficient
KDOQI	Kidney Dialysis Outcomes Quality Initiative
l_0	The original specimen length
m^2	Squaremeter
MPa	Megapascal
N	Newton
NIH	National Institutes of Health
NKF	National Kidney Foundation
Pa	Pascal
PVP	Polyvinylpyrrolidone

PZT	A lead zirconate titanate piezoelectric ceramic
Q_B	Blood Flow
Q_D	Dialysate Flow
R_p	The maximum profile peak height
R_t	The maximum height of the profile
R_v	The maximum profile valley depth
R_z	The ten point height
RMS	Root-mean-squared
RRT	Renal Replacement Therapy
SEI	Secondary electron imaging
SEM	Scanning Electron Microscopy
SPM	Scanning Probe Microscopy
TMP	Trans Membrane Pressure
USA, U.S.	United States of America
USRDS	United States Renal Data System
US\$	United States Dollar
XRD	X-Ray Diffraction
2D	Two-dimensional
3D	Three-dimensional

1. INTRODUCTION

1.1 Objective Of The Thesis

The main purpose of this study is to evaluate the performance of a widely used hemodialysis membrane; Fresenius FX Class high flux polysulfone hemodialyzer with Helixone fibers, in terms of mechanical and structural stability under the effect of patient contact and reprocessing.

The reason beneath the prediction of the alteration in service performance is the fact that the hemodialyzer is mechanically and chemically stressed during reuse applications and consequently, the polymeric material undergoes ageing that affects the transport properties of the membrane. In order to clarify the tolerance for the stresses, in vitro experiments were performed to examine the behavior of polysulfone membrane by focusing on the possible drop in the mechanical properties, the change in the membrane porous structure and the alteration in the crystallinity.

The present study actually aims to fulfill the gap in knowledge about the effect of dialysis environment and reprocessing on the hemodialyzers and will be a reference for other synthetic dialysis membranes.

1.2 The Kidney

The kidney is one of the highly differentiated vital organs in the body. It has multiple functions in establishing the body homeostasis. Diseases of the kidneys are among the most important causes of death. Severe loss of kidney function requires removal of toxic waste products and restoration of body fluid volume and composition toward normal. This can be accomplished by dialysis with an artificial kidney [1], which is the main focus

of this thesis. This chapter covers the anatomy, functioning and malfunctioning of the kidney with the aim of providing introductory information.

1.2.1 Anatomy Of The Kidney

The kidneys are bean-shaped structures; each is about the size of a clenched fist, and they lie on the posterior wall of the abdomen, outside the peritoneal cavity [1, 2]. The medial side of each kidney contains an indented region called the hilum through which pass the renal artery and vein, lymphatics, nerve supply, and ureter, which carries the final urine from the kidney to the bladder, where it is stored until emptied. The kidney is surrounded by a tough, fibrous capsule that protects its delicate inner structures [1].

Figure 1.2.1.1 shows a longitudinal section of the kidney. The ureter branches inside the kidney into 2–4 major calyces, each of which in turn branches into several minor calyces, which collect urine from the tubules of each papilla. The kidney parenchyma is divided into renal cortex (1 cm thick) and medulla. The medulla is formed of 8–18 renal pyramids, which are conical-shaped [1, 2]. The walls of the calyces, pelvis, and ureter contain contractile elements that propel the urine toward the bladder [1].

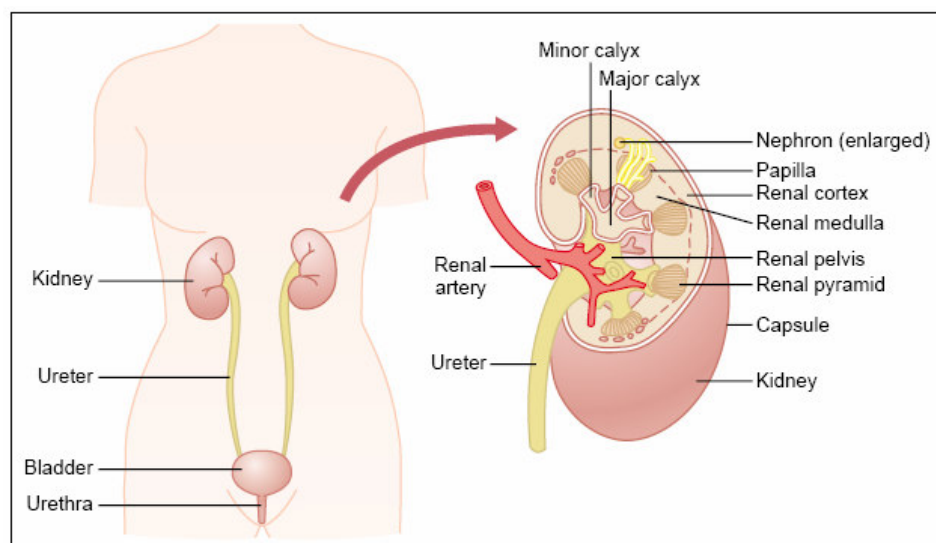


Figure 1.2.1.1 General organization of the kidneys and the urinary system [1].

The functional unit of the kidney is the nephron, each capable of forming urine, see Figure 1.2.1.2. Each human kidney contains about 0.4 to 1.2 million nephrons [3]. The kidney cannot regenerate new nephrons. Therefore, with renal injury, disease, or normal aging, there is a gradual decrease in nephron number [1]. The essential components of the nephron include the glomerulus, through which large amounts of fluid are filtered from the blood, Bowman's capsule, the proximal tubule, the thin limbs, the distal tubule, and the connecting segment or connecting tubule [1, 3].

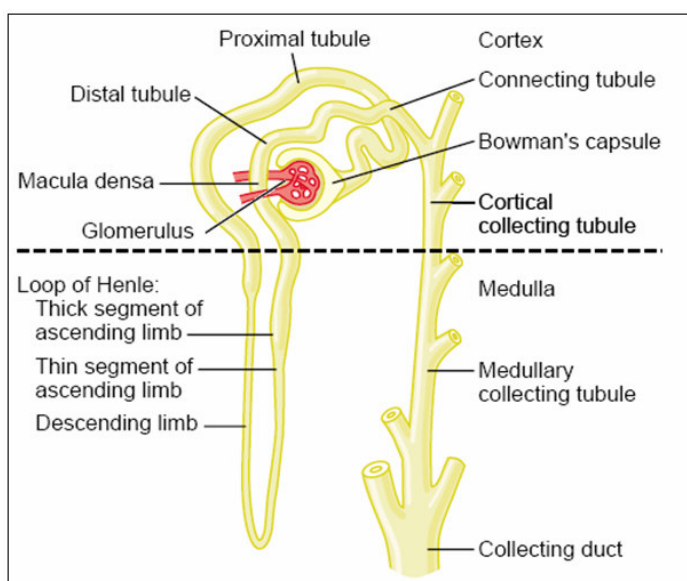


Figure 1.2.1.2 Basic tubular segments of the nephron; the relative lengths of the different tubular segments are not drawn to scale (left) [1] and scanning electron micrograph of a glomerulus at 300x (right) [3].

1.2.2 Filtration In The Kidney

The kidney serves multiple complex physiologic functions including; excretion of metabolic waste products and foreign chemicals, regulation of water and electrolyte balances, regulation of body fluid osmolality and electrolyte concentrations, regulation of arterial pressure, acid–base balance, secretion, metabolism, excretion of hormones and gluconeogenesis [1]. Most of these functions cannot be implemented by artificial kidney which basically goals to remove the toxins and excess fluid.

There are many differences between the native and artificial kidneys (hemodialyzers) in terms of structure and functioning. There are 1 to 2 million functioning elements, i.e. nephrons, in the two native kidneys. In general, the hollow fiber artificial kidney contains 8000 to 10000 fibers and provides a surface area for exchange as high as 1.8 to 2 m². The proximal tubule of the nephron is 40 μm in diameter and is 14 mm long [3], where each hollow fiber of Fresenius FX80 dialyzer has a membrane lumen of 185 μm. It is longer than 20 cm and has the surface area of 1.8 m² [4]. The blood flow rate into the kidney is about 1 L/min, accounting for about 20 to 25 % of the total cardiac output, although the kidney is less than 0.5 % of the total body weight [5] and the ultrafiltrate rate in human kidney changes in the range of 90–120 ml/min [2]. Whereas, in dialysis, the blood flow rate may range from 250–500 mL/min. The dialysis membranes have different ultrafiltration coefficients (i.e., mL removed/min per mmHg) [6] so that, fluid removal in hemodialyzer membranes can be varied.

Furthermore, in addition to being influenced by diffusive and convective forces, the renal tubules perform a great number of biochemical processes on the fluid that is filtered at the glomerulus whereas clearance in the artificial kidney is solely dependent on the physical forces of diffusion and convection across a semi-permeable membrane [3], which will be discussed in the Section 1.3.3.

Wearn and Richards first demonstrated about 80 years ago that the initial step in the process of urine formation is the filtration of a nearly protein-free fluid across the glomerular capillary walls to Bowman's capsule [1, 3]. Although proteins are excluded from the ultrafiltrate, the filtration barrier allows electrolytes, amino acids, glucose, creatinine, and exogenous molecules at least as large as inulin (5000 kDa, molecular radius ~14 Å) to pass virtually unimpeded. Studies demonstrated that all neutral molecules with molecular radii less than approximately 20 Å are filtered as freely as inulin (and hence water), whereas molecules larger than approximately 50 Å are virtually excluded from filtration [3]. The resulting concentration in the glomerular filtrate in Bowman's capsule is almost the same as in the plasma. After the filtered fluid leaves Bowman's capsule and passes through the tubules, it is modified by reabsorption of water and specific solutes back into the blood or by secretion of other substances from the peritubular capillaries into the tubules [1].

The hydrostatic pressure gradient across the glomerular capillary wall is the primary driving force for glomerular filtration [6]. The other forces are the hydrostatic pressure in Bowman's capsule, which opposes filtration; the osmotic pressure of the glomerular capillary plasma proteins, which also opposes filtration; and the osmotic pressure of the proteins in Bowman's capsule, which promotes filtration [1]. Approximately 20 % of the renal plasma flow is filtered into Bowman's space, and the ratio of glomerular filtration rate (GFR) to renal plasma flow determines the filtration fraction [6].

If it is expressed mathematically, the GFR equals the product of filtration coefficient and the net filtration pressure. Consequently, the filtration coefficient cannot be measured directly, but if it is estimated experimentally by dividing the rate of glomerular filtration by net filtration pressure and normal K_f is calculated to be about 12.5 ml/min/mmHg of filtration pressure [1].

1.2.3 Chronic Renal Failure

Diseases of the kidneys are among the most important causes of death and disability in many countries throughout the world. Severe kidney diseases can be divided into two main categories. The first one is acute renal failure, in which the kidneys abruptly stop working entirely or almost entirely but may eventually recover nearly normal function. The second one is chronic renal failure, in which there is progressive loss of function of more and more nephrons that gradually decreases overall kidney function [1]. The focus of this chapter will be on the chronic renal failure and end stage renal disease (ESRD), the majority of which require dialysis.

Firstly, the classification of chronic renal disease must be defined. Table 1.2.3.1 provides a widely accepted classification, based on recent guidelines of the National Kidney Foundation; Kidney Dialysis Outcomes Quality Initiative (KDOQI), in which the stages are defined according to the estimated GFR [6].

Table 1.2.3.1

Stages of chronic kidney disease and clinical action plan [3, 6].

Stage	Description	GFR (mL/min/1.73m ²)	Evaluation Plan
0	At increased risk	>90	Screening CKD risk reduction
1	Kidney damage with normal or increased GFR	=90	Diagnose and treat cause, slow progression, evaluate risk of cardiovascular disease
2	Kidney damage with mild decrease in GFR	60–89	Estimate progression
3	Moderate decrease in GFR	30–59	Evaluate and treat complications
4	Severe decrease in GFR	15–29	Prepare for renal replacement therapy
5	Kidney failure	<15	Initiate renal replacement therapy

The term chronic renal failure applies to the process of continuing significant irreversible reduction in nephron number, and typically corresponds to chronic kidney disease stages 3–5 and end stage renal disease (ESRD) is the stage 5 chronic renal disease [6], when the glomerular filtration rate falls below 15 mL/min/1.73m².

Some causes of chronic renal failure are; metabolic disorders (e.g. diabetes mellitus and obesity), hypertension, renal vascular disorders, immunologic disorders (e.g. glomerulonephritis), infections (e.g. tuberculosis), primary tubular disorders (e.g. nephrotoxins; analgesics, heavy metals), urinary tract obstruction, congenital disorders (e.g. polycystic disease) [1]. The etiology is similar in prevalent hemodialysis patients in Turkey and given in Section 1.3.2.

In ESRD, treatment options include hemodialysis, peritoneal dialysis, or transplantation. Although there are geographic variations, hemodialysis remains the most common therapeutic modality for ESRD. In contrast to hemodialysis, peritoneal dialysis is continuous, but much less efficient, in terms of solute clearance but the decision of which modality to select is often based on personal preferences and quality of life considerations [6]. In some cases, rather than being a preference, peritoneal dialysis becomes a useful method if hemodialysis is not possible, e.g. for the patients with vascular access problems.

Commonly accepted criteria for initiating patients on maintenance dialysis include the presence of uremic symptoms, the presence of hyperkalemia unresponsive to conservative measures, persistent extracellular volume expansion despite diuretic therapy, acidosis refractory to medical therapy, a bleeding diathesis, and a creatinine clearance or estimated glomerular filtration rate (GFR) below 10 mL/min per 1.73 m² [6]. KDOQI guidelines suggest that dialysis should be initiated at a creatinine clearance between 9 and 14 mL/min [3].

1.3 Hemodialysis

1.3.1 History Of Hemodialysis

Acute and chronic kidney failure, which can lead to death if untreated for several days or weeks, is an illness that is as old as humanity itself. In early Rome and later in the Middle Ages, treatments for uremia included the use of hot baths, sweating therapies, blood letting and enemas [7]. Today, while the number of patients keeps increasing, thanks to the breakthroughs in history, qualified dialysis procedures are being carried on.

The first historical description was published in 1913 by Abel and his colleagues who “dialyzed” anesthetized animals. By 1924, a German doctor Georg Haas dialyzed the patients with kidney failure, none of which survived. The first successful dialysis was performed by Willem Kolff, of the Netherlands, in 1945. Kolff used a rotating drum kidney to treat a 67 year old patient with acute kidney failure. The treatment continued for a week and allowed the patient to have normal kidney function. By proving that uremic patients could be successfully treated using artificial kidneys; Kolff sparked a flurry of activity around the world to develop improved and more effective dialyzers [7].

The birth of modern dialysis can be identified with a series of discoveries made in the 1960s. Based on the experience of Kolff and other investigators, Scribner et al. started the application of hemodialysis on a large scale in chronic renal failure. External arteriovenous (A–V) shunts were used as a vascular access. Kiil plate dialyzers were

employed and dialysis machines including systems for dialysate preparation and delivery were developed in Seattle. Subsequently, the shunt was modified into a silastic–teflon structure until 1966 when the internal A–V fistula was proposed by Brescia and Cimino. By the late 1960s, hollow fiber artificial kidneys were also manufactured and dialysis started to be performed out of hospital in self–care centers or even at home. Dialysis for chronic renal failure was no longer experimental. The problem of logistically organizing dialysis for all who needed it was the real challenge. The solution was in part offered by new technological advances that made dialysis more reliable and widely applicable [8].

1.3.2 A Statistical Perspective

Since the beginning of the therapy for end stage renal disease (ESRD) through dialysis or transplantation, the number of patients treated for terminal kidney failure worldwide has continued to grow at a rate that is far in excess of the growth rate of the general population [9].

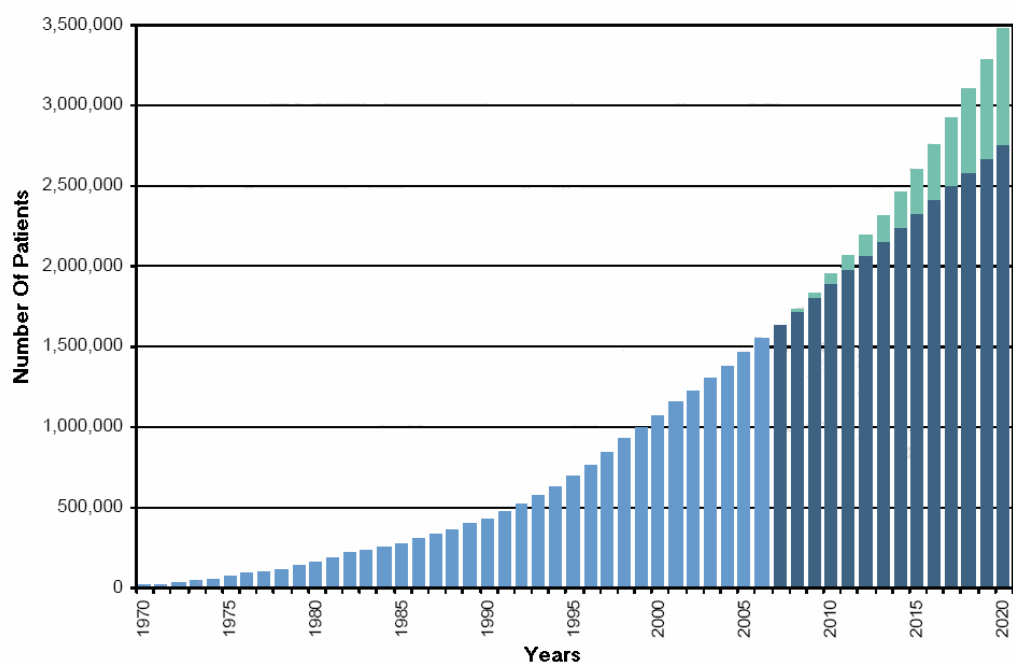


Figure 1.3.2.1 Total number of dialysis patients in the world and estimated increase in the trend, redrawn from [10].

Figure 1.3.2.1 shows the dialysis patient population throughout the world and the predictive increase in the number of patients up to year 2020. In addition, the upward trend is particularly similar in Turkey. According to the study of Turkish Society Of Nephrology, 2006, there is a mild increase in both incidence and prevalence of end stage renal disease needed renal replacement therapy [11]. Figure 1.3.2.2 gives the trend in the number of hemodialysis patients in Turkey by years.

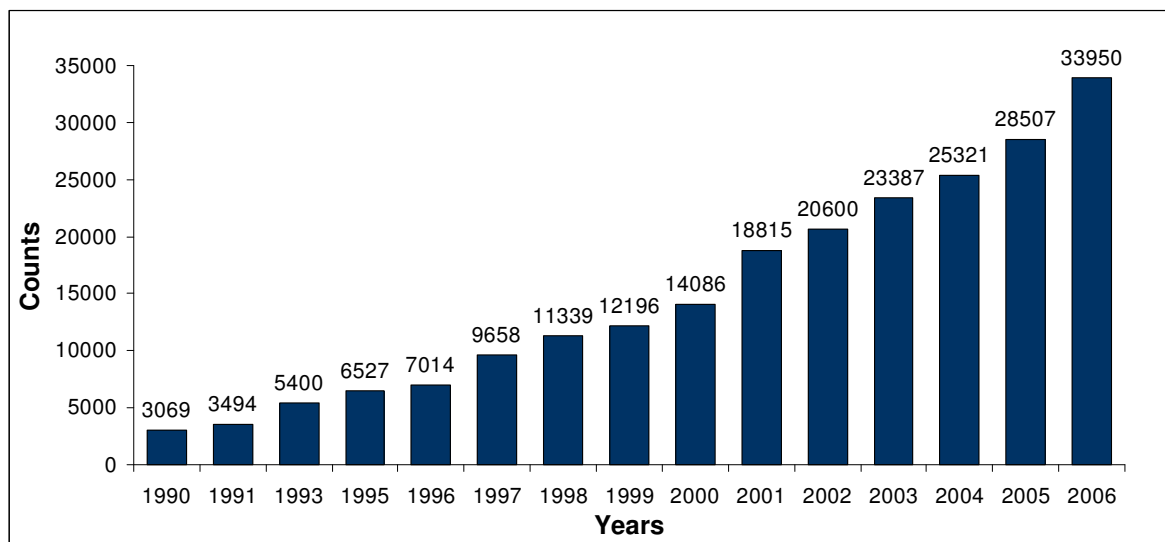


Figure 1.3.2.2 The number of hemodialysis patients by years in Turkey [11].

For 2005, the highest rate of incident ESRD is reported by Taiwan, at 404 per million population. The United States, Mexico, and the city of Shanghai report rates of 351, 302, and 275, respectively. Turkey, with the rate of 179 per million population, ranked eighth among the 37 regions and countries. Iceland, the Philippines, Finland, and Norway, in contrast, report rates of 67–99 per million population, while rates in Bangladesh and Russia are only 9 and 24 per million population [12].

Hemodialysis remains the most frequently used form of dialysis therapy in most parts of the world [12], as in Turkey. As of the end of 2006, 80.5 % of prevalent ESRD patients treated with hemodialysis, 9.7 % and 9.8 % with peritoneal dialysis and transplantation respectively [11], see Figure 1.3.2.3. The 57.3 percent of the regular hemodialysis patients was male in the year 2006.

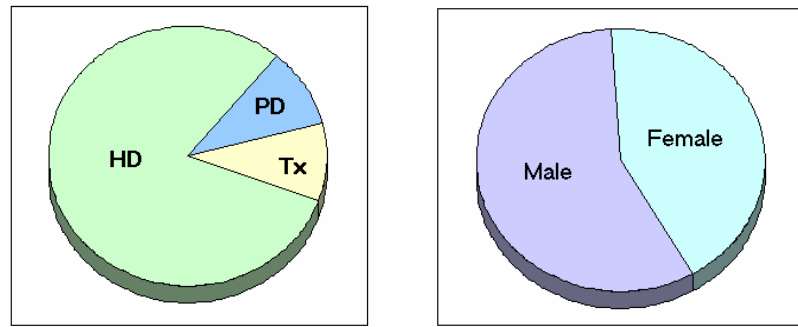


Figure 1.3.2.3 The renal replacement therapies modalities in prevalent ESRD patients as of the end of 2006 (left), incidence by gender in regular 11583 hemodialysis patients (right) in the year 2006, adapted from [11].

Figure 1.3.2.4 gives the etiology in prevalent hemodialysis patients in Turkey. In addition, with a rate of 50.4 %, cardiovascular diseases are the most common death causes in hemodialysis patients in Turkey.

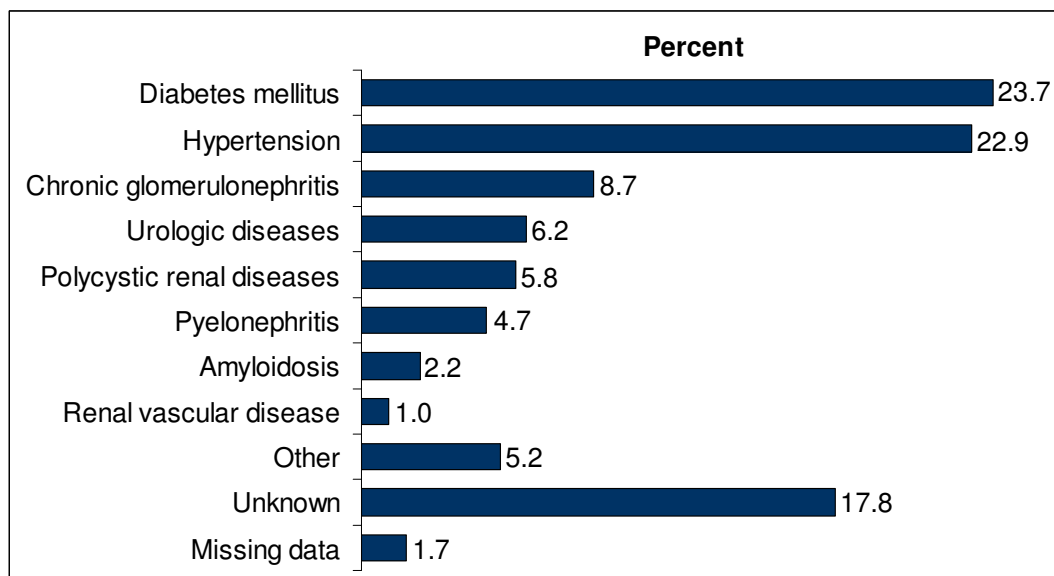


Figure 1.3.2.4 Etiology in prevalent hemodialysis patients in Turkey, adapted from [11].

Finally, the annual cost of hemodialysis per patient is US\$ 22759 in Turkey [13]. The majority of the hemodialysis expenses are for erythropoietin and dialyzers and the remaining part of this cost includes dialysate, heparin, A–V fistula, drugs (e.g. antihypertensives, antibiotics, vitamin D), electricity, staff salaries, equipment wear costs and rents for the dialysis centers etc. Additionally, the total cost of RRT in Turkey is calculated as being US\$ 488,958,709 for 1 year, which corresponds to nearly 5.5 % of Turkey's total health expenditure [13].

1.3.3 Principles Of Hemodialysis

Continuous hemodialysis is a treatment carried out over an extended period of time with a pump driven circuit [14], which is shown in Figure 1.3.3.1 The diagram labels basically the A–V fistula, blood and dialysate lines, blood pump, hollow fiber dialyzer, air detector and a series of monitors, such as arterial and venous pressure monitors, dialysate flow rate and conductivity monitors. The circuit also contains a heparin pump to prevent clotting, proportioning pumps to produce dialysate, a heater to warm the dialysate and audio and/or visual alarms and failsafe shutdown sequences to establish patient safety.

Briefly, during hemodialysis, the blood is drawn from the body at a flow rate depending on patient conditions and procedural requirements, heparinized and then pumped with a roller pump through the extracorporeal circuit that includes the dialyzer. The transport process of water, electrolytes, and simple metabolites between the blood and the dialysate takes place in the dialyzer [15] and the clean blood returns to body. The blood–flow compartment is monitored to control the pressures, flow, and accidental entry of air into the blood circuit; in the dialysis–fluid compartment, the composition of the dialysis fluid, flow, pressure, and accidental entry of blood into dialysate due to rupture of the dialyzer membrane need to be monitored [16].

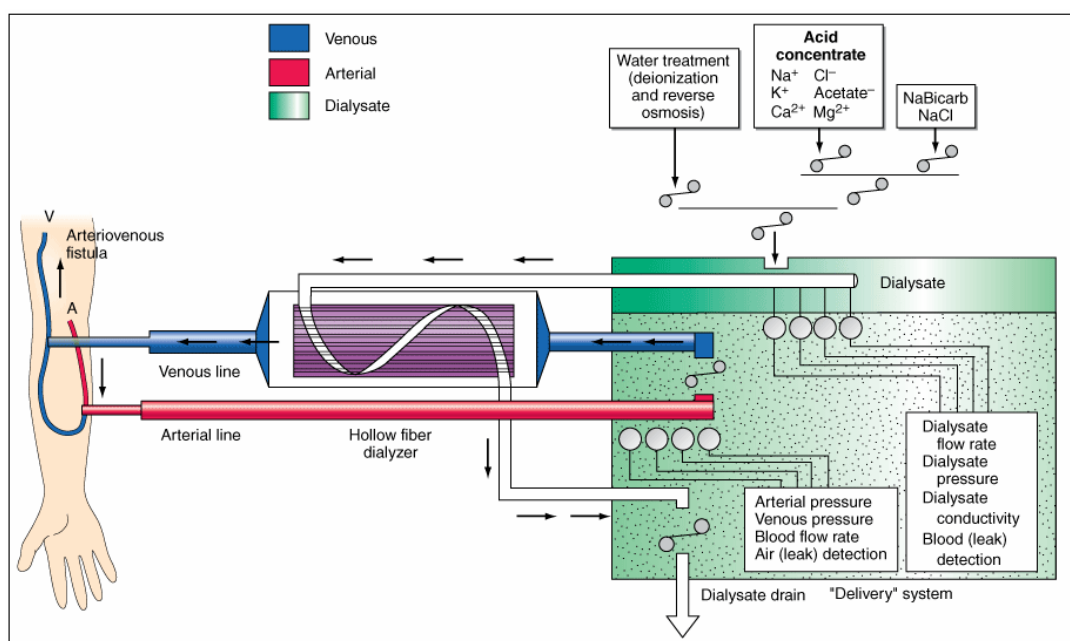


Figure 1.3.3.1 Schema for hemodialysis [6].

Other than hemodialyzers, the implants that undergo blood–surface interactions during hemodialysis are the grafts and catheters, which are used to obtain blood for hemodialysis and referred as dialysis access. On the other hand, a native fistula can be created by the anastomosis of an artery to a vein (e.g., the Brescia–Cimino fistula) results in arterialization of the vein. This facilitates its subsequent use in the placement of large needles to access the circulation [6].

However, the majority of patients undergo placement of an arteriovenous graft, i.e., the interposition of prosthetic material, usually polytetrafluoroethylene, between an artery and a vein. Unfortunately, arteriovenous (A–V) fistulas may not mature sufficiently to provide reliable access to the circulation, or they may thrombose early in their development [6].

Grafts and catheters tend to be used among persons with smaller–caliber veins or persons whose veins have been damaged by repeated puncture, or after prolonged hospitalization. The most important complication of arteriovenous grafts is thrombosis of the graft and graft failure and they are associated with much higher rates of infection than fistulas [6]. According to Turkish Society Of Nephrology, main intravenous route in routine hemodialysis patients as of the end of 2006 is A–V fistula by 85.7 % [11].

Dialysis membranes are classified according to their ultrafiltration coefficient and solute sieving profile as high flux and low flux [14]. On the other hand, there are four categories of dialysis membranes; cellulose, substituted cellulose, cellulose-synthetic, and synthetic [6], according to the material used. The types of dialyzer membranes are discussed in Section 1.4.1 in detail. In this section, the mechanisms of solute and water transport across the hemodialyzers will be considered. These mechanisms are diffusion, convection and ultrafiltration.

Diffusion is a process of transport in which the molecules that are present in a solvent and can freely cross the membrane tend to move from the region at higher concentration into the region at lower concentration [14], see Figure 1.3.3.2.

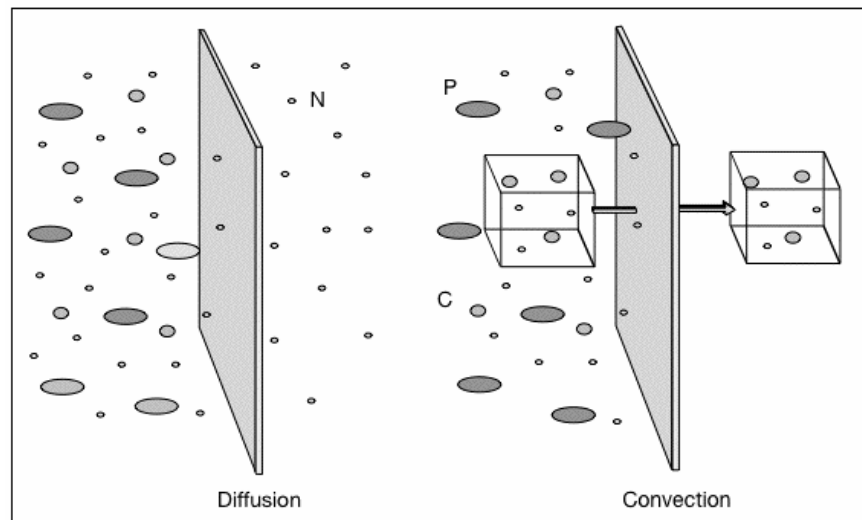


Figure 1.3.3.2 Mechanisms of solute removal in blood purification techniques [14].

The rate of diffusive transport increases with the increase in the concentration gradient across the membrane, the membrane surface area (A), and the mass transfer coefficient of the membrane times the surface area (K_oA) [17].

Convection is a form of transport that requires a movement of fluid across the membrane as a consequence of a trans-membrane pressure gradient (TMP) [14]. The fluid transport from the blood to the dialysate as a result of TMP existing between the blood and dialysate compartments is defined as ultrafiltration [18]. High rates of fluid transport by ultrafiltration is associated with further solute clearance through convective transport by dragging the solutes.

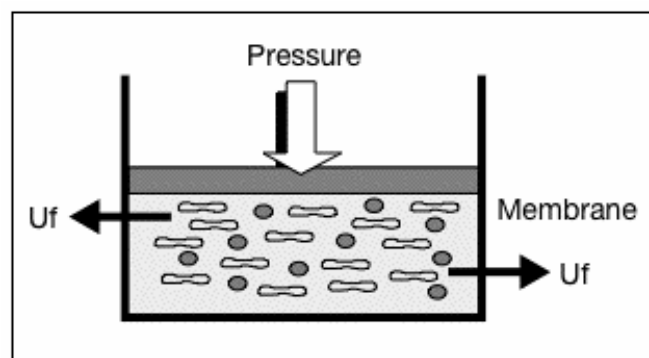


Figure 1.3.3.3 The mechanism of ultrafiltration in response to a trans-membrane pressure gradient [14].

In mathematical expression, TMP is the hydrostatic pressure of blood minus the hydrostatic pressure of dialysate, and the oncotic pressure generated by plasma proteins in the blood [14]. Figure 1.3.3.3 shows the ultrafiltration mechanism occurring due to the difference in these pressures. Convective transport is measured in terms of the sieving coefficient. The sieving coefficient is the permeability of dialysis membranes to a particular solute and not its diffusability. It is defined as the ratio of solute concentration in the ultrafiltrate to that of the plasma [17]. Based on the above-mentioned concepts, the dialyzer can be thought of as the mass transfer analog of a shell and tube heat exchanger [19].

The solute transport characteristics of a dialyzer may be expressed as clearance, analogous to the use of this term in renal physiology. Clearance is defined as the amount of solute removed from the blood per unit of time, divided by the incoming blood concentration. The clearances of solutes depend on membrane permeability and the flow rate of blood [16].

The removal of small solutes, such as urea and creatinine, is influenced to a greater extent by the flow rates of blood and dialysis fluid than by the diffusive resistance of the dialyzer membrane. The removal of large solutes such as vitamin B₁₂ (MW 1355 Da) is, however, mainly influenced by the diffusive resistance of the membrane and to a much smaller extent by blood and dialysate flow rates [16]. Therefore, while small solutes are flow limited, large solutes are membrane limited [17]. High flux membranes have a comparatively low diffusive resistance, and greater clearances of larger solutes are achieved by such dialyzers [16]. Clearance data for the high flux polysulfone dialyzer used in this study is given in the Section 1.4.3.

Furthermore, the concentrations of ions and other substances in dialyzing fluid are not the same as the concentrations in normal plasma or in uremic plasma. Instead, they are adjusted to levels that are needed to cause appropriate movement of water and solutes through the membrane during dialysis [1]. Table 1.3.3.1 lists the constituents in a typical dialyzing fluid with those in normal plasma and uremic plasma.

Table 1.3.3.1

Comparison of dialyzing fluid with normal and uremic plasma [1].

Constituent	Normal Plasma	Dialyzing Fluid	Uremic Plasma
Na ⁺ (mEq/ L)	142	133	142
K ⁺ (mEq/ L)	5	1.0	7
Ca ⁺⁺ (mEq/ L)	3	3.0	2
Cl ⁻ (mEq/ L)	107	105	107
HCO ₃ ⁻ (mEq/ L)	24	35.7	14
HPO ₄ ⁻ (mEq/ L)	3	0	9
Urate ⁻ (mEq/ L)	0.3	0	2
Sulfate ⁻ (mEq/ L)	0.5	0	3
Glucose	100	125	100
Creatinine	1	0	6
Urea	26	0	200

1.4 Polysulfone Hemodialyzers

1.4.1 Hemodialyzers In General

The two main categories of dialysis membranes are cellulosic and synthetic membranes according to the material used. Over the past three decades, there has been a gradual switch from cellulose-derived to synthetic membranes, such as polysulfone, since they are more biocompatible because of the absence of hydroxyl groups [6], in their structure. The hydroxyl groups on the surface of cellulose membranes, makes them hydrophilic and are responsible for the activation of alternative complement system on contact with blood, contributing to the bioincompatibility. Substitution of some of the hydroxyl groups with benzyl or acetate groups reduces complement activation [20]. Accordingly, polysulfone membranes are now used in more than 60 % of the dialysis treatments in the United States [6].

Both cellulose and synthetic membranes can be either low flux or high flux [21]. Classic cellulosic membranes, such as Cuprophan, are typically low flux membranes

strongly hydrophilic and remarkably thin. On the other hand, classic high flux synthetic membranes are hydrophobic, strongly asymmetric and with a thick wall. However, recently manufactured synthetic membranes are designed with reduced wall thickness. This permits their use in new techniques such as high flux hemodialysis [8]. The new design of high flux polysulfone membrane will be discussed in the Section 1.4.3.

Dialyzer membranes can be classified as low flux or high flux in accordance with their ultrafiltration coefficient (K_{uf}) and large-molecule clearance [21, 14]. Ultrafiltration coefficient is a measure of the hydraulic permeability of the dialyzer, and defined as the volume of ultrafiltrate formed per hour per mmHg trans-membrane pressure. It depends not only on membrane characteristics, but also on membrane surface area [16].

In 1997, the HEMO Study defined low flux dialyzers as having a mean clearance of β_2 -microglobulin less than 10 mL/min during the first use and high flux dialyzers as having an ultrafiltration coefficient (K_{uf}) greater than 14 mL/h/mmHg and a mean β_2 -microglobulin clearance greater than 20 mL/min during the first use or over the lifetime of the dialyzer model with a given reprocessing method [21, 18]. The other recommended classifications are listed in Table 1.4.1.1.

Table 1.4.1.1

Membrane types according to the given definitions [22].

Definitions	Membrane Type	Specification
Flux as a measure of ultrafiltration capacity (based on the ultrafiltration coefficient)	Low flux	$K_{uf} < 10$ mL/h/mmHg
	High flux	$K_{uf} > 20$ mL/h/mmHg
Permeability as a measure of the clearance of the middle molecular weight molecule	Low permeability	β_2 -microglobulin clearance <10 mL/min
	High permeability	β_2 -microglobulin clearance >20 mL/min
Efficiency as a measure of urea clearance (based on the urea K_oA value)	Low efficiency	$K_oA < 500$ mL/min
	High efficiency	$K_oA > 600$ mL/min

High flux dialyzers may provide a therapeutic advantage over low flux dialyzers in the treatment of end stage renal disease [23]. High flux dialyzers, made of synthetic membranes like polysulfone, have ultrafiltration coefficients up to 60 ml/min per mmHg. In addition, water-soluble toxins of low and middle molecular weight are most effectively removed by high flux hemodialyzers [24]. Additionally, these dialyzers have greater convective permeability to molecules of 5000 to 25000 Da, allowing faster removal of larger solutes from the blood [16]. Another feature of high flux dialyzers is that higher blood and dialysate flows used during hemodialysis.

1.4.2 General Properties Of Polysulfone

Polysulfone thermoplastics came into commercial use around 1970. The basic monomer contains stable linkages of benzene rings, see Figure 1.4.2.1.

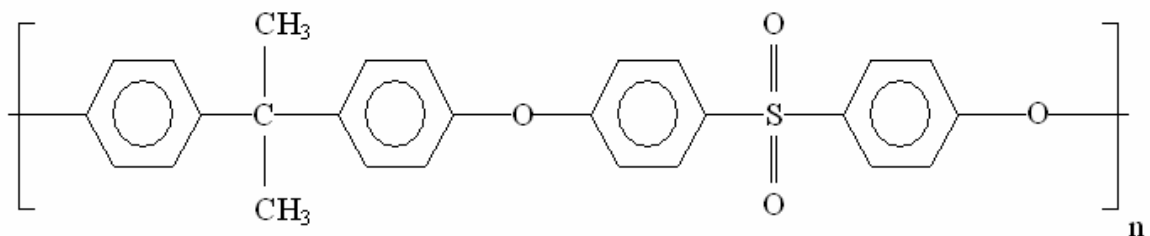


Figure 1.4.2.1 The chemical structure of polysulfone [25].

Polysulfone is an amorphous, hydrophobic, thermoplastic material made from dichlorodiphenylsulfone and bisphenol A [25].

The mechanical properties of polysulfones are similar to nylons at room temperature, but useful strength and rigidity are maintained to temperatures as high as 180 °C. Polysulfones have relatively good optical clarity and lower moisture absorption. The continuous use temperature, as high as 160°C, is significantly above other clear plastics, such as polystyrene, acrylics, and polycarbonate. Polysulfone is above the other materials in cost, but it is less expensive than some of the clear engineering plastics such as polyethersulfone [25], which is also used in manufacture of hemodialyzers.

The property combination of good strength at elevated temperatures and transparency make this material popular in the health field. It is used for medical containers and supplies that must withstand repeated sterilization. Polysulfone retains its strength after repeated autoclave cycles, and it is very resistant to degradation by hot water. The elevated temperature properties allow polysulfone sterilization by heating [25]. However, in the case of hemodialyzers, these properties are needed to be investigated profoundly before defining the material as disinfection and stress tolerant.

1.4.3 Fresenius FX Class Polysulfone Dialyzers

The main aim of the developments in the artificial kidneys is to mimic the ability of kidney to completely remove metabolic wastes by making the fiber more identical to the organ itself [26]. For this purpose, dialyzer-related developments have concentrated upon the improvement of performance and biocompatibility. The focus of these developments was predominantly on the membrane itself [27].

In a newly developed high flux dialyzer with a polysulfone membrane; Helixone, both the fiber and the fiber bundle structure were refined with the aim of improving overall performance and biocompatibility and also to reduce dialysate consumption [27]. The development of this membrane takes the advantage of nanotechnology fabrication principles to result in membrane characteristics with minimal resistance to the removal of large molecular weight substances, and a membrane claimed to be closer in structure to that of the human glomerulus [28].

As stated above, these polysulfone dialyzer membranes are produced by nanotechnology membrane fabrication procedures (Nano Controlled Spinning Technology) [4]. In the manufacturing process, firstly, the fibers are produced when polymers are extruded out of a spinnerette. The whole process is called spinning, and through careful control of speeds, temperatures and materials, the result is a hollow fiber that has pores through its walls that are just the right size for letting toxins leave the blood, while keeping albumin and blood cells behind [29].

The case and end-caps are made from plastic resin, which is polypropylene in FX Class. The polypropylene case is filled with a fiber bundle made up of thousands of Helixone fibers. Then, liquid polyurethane is fed into case, and centrifugal force makes the polyurethane run to each end where it flows around every fiber, sealing each one tightly in place. The polyurethane then hardens, forming the potting material that holds the fibers firmly in place. Finally, the end-caps are attached to each end of the dialyzer casing, and then the dialyzer is sterilized [29], by inline steaming.

According to the manufacturer, this technology provides fibers with a highly defined pore structure and distribution at the innermost, separating region of the membrane. The modulation of the Helixone structure, at the nanoscale level, facilitates the targeted elimination of larger ureamic toxins [4].

Besides the developments of the membrane itself, there are many design related improvements of FX Class polysulfone hemodialyzer, see Figure 1.4.3.1. In the conventional dialyzer design, dialysate enters straight through the dialysate port (and only from one side) into the actual fiber compartment. This often leads to an inappropriate dialysate distribution, with the dialysate flowing directly from the inlet to the outlet leading to poor coverage of large parts of the fiber bundle.

However, in the design of the polysulfone dialyzer, the special pinnacle structure of the housing acts as a more homogeneous dialysate distributor and ensures that dialysate enters from all sides into the fiber bundle at similar flow rates [27]. This is confirmed by the experimental studies, which also demonstrate the significant increase in solute clearance [30].

By taking all of these into consideration, high flux polysulfone membranes, which have very common use around the world, are highly concentrated on both first and reuse treatments and ongoing experiments by medical society. Therefore, in this study, the high flux polysulfone membrane; Fresenius FX80, which also has wide application and acceptance in our country, was chosen to be investigated.

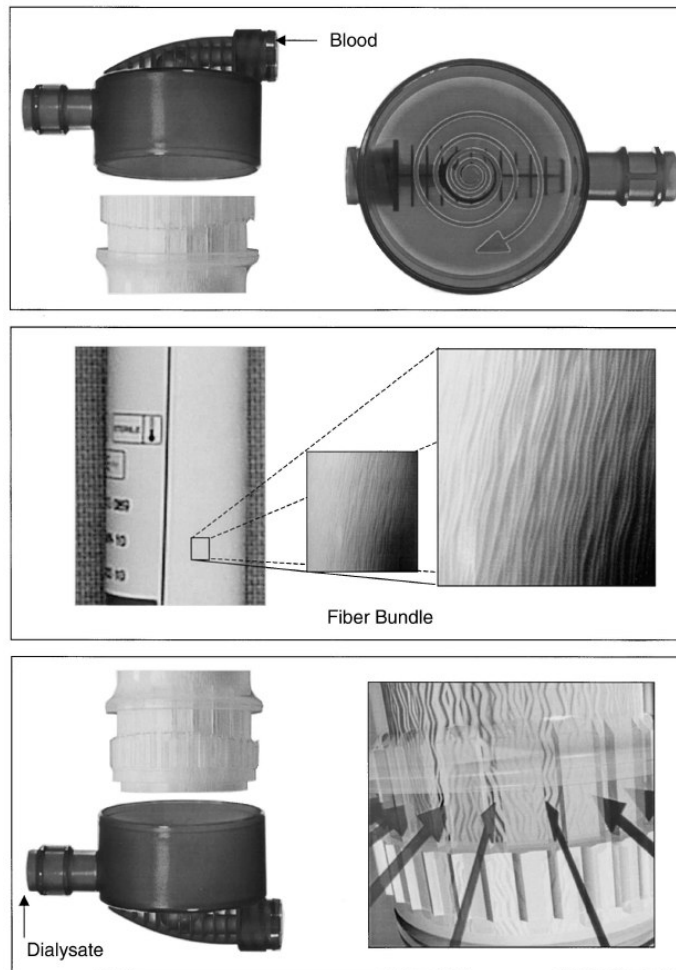


Figure 1.4.3.1 Schematic representation of the components of the FX Class hemodialyzers. Top panel depicts the peculiar blood port and potting structure; middle panel describes the micro-ondulation of the fibers in the bundle; bottom panel depicts the special dialysate entrance with the pinnacle structure [31].

It should be noted that the FX class high flux polysulfone membranes are manufactured with different surface areas and labeled as FX40, FX50, FX60, FX80, and FX100. FX class dialyzers are made up of same fibers (Helixone) but the number of fibers packed in each hemodialyzer differs and that results different effective surface areas, blood filling volumes, also clearances. The dialyzer used in this thesis is FX80, which is one of the most widely used FX class hemodialyzers. However, the results of this study will be a reference for the other polysulfone hemodialyzers as well as for the other types of synthetic membranes. Table 1.4.3.1 and Table 1.4.3.2 show the characteristics and performance data of the hemodialyzer investigated in this study.

Table 1.4.3.1

Characteristics of polysulfone FX80 dialyzer membrane, adapted from [4, 31].

Characteristics / Dialyzer	FX80
Sieving coefficient ($Q_B = 300$ mL/min, $Q_F = 60$ ml/min)	Inulin 1
	β_2 -microglobulin 0.8
	Albumin 0.001
Effective surface area (m^2)	1.8
Blood filling volume (mL)	95
Wall thickness/inner diameter (μm)	35/185
Membrane	Helixone
Housing material	Polypropylene
Potting compound	Polyurethane
Sterilization method	INLINE steam

Table 1.4.3.2

In vitro performance data of FX80, adapted from [4].

Performance Data /Dialyzers	FX80
Ultrafiltration coefficient (mL/h•mmHg)	59
Clearances Q_B 300 (mL/min)	Urea 276
	Creatinine 250
	Phosphate 239
	Vitamin B ₁₂ 175
	Inulin 125
Clearances Q_B 400 (mL/min)	Urea 326
	Creatinine 287
	Phosphate 272
	Vitamin B ₁₂ 190
	Inulin 133

The in vitro performance data were obtained with $Q_D = 500$ mL/min and $T = 37$ °C

The ultrafiltration coefficients were measured using human blood, Hct 32 %, protein content 6 %.

1.5 Reuse Procedure

Reuse of hemodialyzers can be defined as the cleaning and disinfection of a hemodialyzer for multiple uses by a given patient and it is practiced in many countries to reduce costs in the treatment of end stage renal disease (ESRD) [32]. Reuse of hemodialyzers is obviously advantageous from economical point of view; however, knowledge of the performances of reused hemodialyzers is still incomplete and being questioned. This study takes no position for or against the practice of dialyzer reuse since the impact of reused dialyzers on patient safety is not completely determined.

1.5.1 Brief History

In 1964, the storage of used dialyzers and reuse was first described by Shaldon and coworkers in London using twin coil dialyzers for hemodialysis [33, 34]. Their aim was to reduce the cost of daily dialysis in a hospital and to avoid the residual blood loss in the dialyzer. They stored the entire blood circuit and contained anticoagulated blood in a refrigerator between dialyses [33].

At the end of 1970s, researches (e.g. Gotch–1969, DePalma–1974, Ahmad–1975 and Hardy–1976) about manual or automatic cleaning of coil, parallel plate, and hollow fiber type dialyzers were highly common in literature [34, 35]. In the early 1980s, the National Kidney Foundation (NKF) published an interim standard for the reuse of dialyzers [34]. After that, especially with the development of hollow fiber dialyzers, the reuse procedure became widespread in many countries.

In 1983, the first standards about reuse were published in USA, by AAMI (Association for Advancement of Medical Instrumentation) and in 1988 it was approved by HCFA (Health Care Financing Administration) and enforced in dialysis facilities. Then, these standards are improved by National Kidney Foundation in KDOQI (Kidney Dialysis Outcomes Quality Initiative) by means of preprocessing and the values of total cell volume and fiber bundle volume [35].

Based on the data collected annually by the Centers for Disease Control and Prevention (CDC), in 1996, it appears that 2261 of 2808 (81 %) dialysis facilities were practicing dialyzer reuse in United States. In 1993, there were approximately 180,000 patients being treated in U.S. dialysis facilities, of whom 143,000 (almost 79 %) were in centers that reprocess dialyzers. In Europe, only about 10 % of dialyzers are reused (still far behind the extent of reuse in the United States), and there has been a real proliferation in the development of automated systems. However, by far, dialyzer reprocessing in the United States is the rule, not the exception [34]. In our country, although it has been tried in some university hospitals, such as in İstanbul and Atatürk Universities, it has never become widespread.

1.5.2 Reprocessing Solutions

The choice of a disinfection agent is often made on the basis of the compatibility with a membrane, the environmental comfort, the biocompatibility effects, and the maintenance of adequate dialyzer clearances, including β_2 -microglobulin removal [36]. Additionally, the decontamination possibility of the disinfecting agent after reprocessing and the effect of disinfection agent on the membrane's mechanical and structural properties should also be included in the basis of choice. For reprocessing hemodialyzers, the following disinfecting agents with the given concentrations are in current use;

- Formaldehyde 0.5–4 % (concentration is dependent on whether heat is used) and usually preceded by bleach [38], e.g. 4 % formaldehyde then 5 % bleach [32],
- Peracetic acid mixture (~0.08 %), usually used alone but sometimes preceded by exposure to bleach (~0.6–1.0 %) [37] or 1.0 % hydrogen peroxide [38],
- Gluteraldehyde alone or preceded by bleach [37] (usually 3 %),
- Heat sterilization with hot citric acid (1.5 % at 95 °C for 20 hours) [37],
- Renalin (a solution including hydrogen peroxide, peracetic acid and acetic acid), or some other brands, such as Sporicidin.

Among these, formaldehyde and bleach combination is one of the most widely used reprocessing methods. The used membrane treatment can be done according to the protocol shown in Table 1.5.2.1, with formaldehyde and bleach in an automated dialyzer-reprocessing machine. In automated reprocessing, the hemodialyzers are tested for the reduction in ultrafiltration and total bundle volume and more importantly for possible leakages.

Table 1.5.2.1

Automated bleach/formaldehyde reprocessing of hemodialyzers [32].

Step	Description
1	Water, bleach, water rinse for cleaning
2	Reverse ultrafiltration
3	Test A, ultrafiltration
4	Test B, total bundle volume
5	Test C, fiber/resin leak test
6	Fill with formaldehyde for disinfection
7	Label and document

Formaldehyde (HCHO) solution has nominal concentration 37 % by weight (w/w) or 40 % by volume (w/v). Generally the solution contains 8 % to 16 % methanol for stabilization. A dilution of 1 part of formaldehyde with 9 parts of water yields 4 % (w/v), also called formalin [18]. The NKF standards consisted of the recommendation that formaldehyde should be used at room temperature in a concentration of 4 % [34], during dialyzer reprocessing. Additionally, if less than this concentration is used, then dialyzers should be disinfected at 40 °C for 24 hours or overnight [34].

In this study, the dialyzers are reprocessed manually with 4 % formaldehyde since there is no ongoing reuse treatment and available automated machines in our country. The reprocessing was carried out for 14 hours with formaldehyde and 6 hours with bleach. The procedure is explained in detail in Section 2.1.3.

1.5.3 Formaldehyde/Bleach Reprocessing And Clearance

There are many studies on formaldehyde and bleach reprocessing with varying membrane types in literature. For example, in 1994, Held and colleagues reported an analysis of data of approximately 33,000 prevalent patients and found no significant increased risk of death for patients treated with dialyzers reprocessed with formaldehyde [39, 40].

Additionally, Collins and coworkers studied 38,057 hemodialysis patients in 1994 and found that using formaldehyde for reprocessing was associated with a 6 % lower relative risk of death than with no reuse [33].

In the article of National Institutes of Health (NIH), hemodialysis (HEMO) study about the effects of reprocessing on dialyzer function has shown that the use of bleach with formaldehyde produced the greatest increase in clearance when compared to bleach with Renalin and Diacide. With the less permeable dialyzer type used in the study, 20 reuses increased β_2 -microglobulin clearance by 163 %, with formaldehyde and bleach compared to the initial values [37].

However, there are some experiments showing that formaldehyde reprocessing without bleach (alone) causes a reduction in β_2 -microglobulin clearance and there is a limitation in reuse number with certain dialyzers reprocessed with this technique [41]. Therefore, in terms of enhancing β_2 -microglobulin clearance, the combination of formaldehyde and bleach is more effective, although it may have negative effects because of the increase in pore size.

Murthy et al. reported that the effect of bleach/formaldehyde reprocessing on dialyzer clearances of urea and creatinine might vary depending on the type of the dialysis membrane. They reported that dialyzer reprocessing in 20 reuses led to decrease in clearances of urea and creatinine for a type of polysulfone dialyzer (F80B). Additionally, in some dialysis sessions, albumin was detected in the dialysate with this polysulfone dialyzer [42], which indicates leakage. On the other hand, in another publication, urea

clearance for both polysulfone and cellulosic membranes, has found to be unaffected by various specific methods of reprocessing including formaldehyde method [37].

In conclusion, there is a great need for further studies in order to determine the performances of reprocessed dialyzers in terms of clearances.

1.5.4 Advantages And Disadvantages Of Reuse

Today, more than 60 % of dialysis patients in U.S., and about 10 % of dialysis patients in Europe are treated with reprocessed dialyzers, in this wise, the cost of dialysis is reduced by almost half [43]. According to Twardowski Z.J., although single dialyzer use and reuse by chemical reprocessing are both associated with some complications in dialysis patients, there is no definitive advantage to either [40], from clinical perspective.

Erek, E., reported that the reuse application has the advantage of reducing the effect of first–use syndrome, e.g. allergic symptoms [44]. The first–use syndrome is characterized by complex symptoms including chest tightness, back pain, dyspnea, angio edema or laryngeal edema, peripheral numbness and tingling, flushing of the skin and nausea and vomiting, occurring within minutes of the initiation of dialysis with a new dialyzer. Although usually mild in nature, in extreme cases the symptoms may progress to respiratory arrest and death. The etiology of first–use syndrome is not completely understood. However, the term usually is considered to include anaphylactoid reactions [18].

By reusing the dialyzers, it is reported that some of the complications, such as nausea, irritation, languor, hypotension, and also complement activation and cytokine formation can be reduced [44]. At this point, it must be noted that this advantage is restricted with the type of the membrane. Since the first–use syndrome is related with the blood–membrane interactions due to the usage of relatively bioincompatible membranes, such as cellulosic membranes, the symptoms can also be reduced by using more biocompatible membranes, such as synthetic membranes.

On the other hand, the sterilants and/or the procedures for reuse processing may be responsible for dialyzer reactions. In an extensive study by the Centers for Disease Control and Prevention (CDC), the number of pyrogenic reactions was clearly higher in dialysis units applying reuse [24]. However, in this kind of studies, the potential confounding factors must also be considered. For example, for this study, the centers applying reuse at the same time also applied more high flux dialysis and hemodiafiltration. Additionally, it should be stressed that many of the negative reactions have been depicted with the hardware applied in the early 1990s and that the newer technology might offer a possibility to avoid these reactions [24].

In sufficient quantities, all sterilants, such as sodium hypochlorite, formaldehyde, and peracetic acid, are toxic [24]. In hollow fiber dialyzers, potting material has been shown to absorb formaldehyde, which is leached out and infused to patients. Even if there is no acute reaction to formaldehyde infusion, there may be long-term consequences like production of anti-N-like antibody and hemolytic anemia [40].

The bioincompatibility of reused membranes must be also considered from dialyzer performance point of view. As stated before, for polysulfone hemodialyzers, removal of β_2 -microglobulin is important when dialyzers are reused with bleach, which is attributed to modifications of the membrane structure and possible increase in pore size. Similarly, transdialyzer protein losses is reported to gradually increase with the number of bleach reuse procedures, with losses up to 20g/dialysis once dialyzers are reused more than 20 times [21]. The delivered dose of dialysis depends on the performance of the dialyzers in terms of clearance and may decrease as a result of dialyzer reuse.

Reprocessing of dialyzers actually aims to achieve cost saving. As stated in the Section 1.3.2, the cost of renal replacement therapy in Turkey is US\$ 488,958,709 for 1 year, which corresponds to nearly 5.5 % of Turkey's total health expenditure [13], which is an important amount for a growing economy. It is reported that the use of same filter reduces the cost of dialysis by 30–50 % depending on the type and cost of the membrane [43]. From this point of view, reuse has a great advantage over single use. At the same time, fewer oil based waste products would disperse to the environment by reusing the same dialyzers.

In the case of dialyzer reuse, the risk for infection and pyrogenic reactions, toxicity from disinfectants, reduced dialyzer performance, impaired removal of large molecules and the validity of the dialyzer blood volume measurement are the criteria for assessing dialyzer function [21]. Whether the outcome will be positive or negative depends both on the membrane and the disinfecting agent and also on the quality of reprocessing. Because both reuse and dialysis practices continue to change over time, large observational studies are needed to continue monitoring for potential risks and benefits associated with dialyzer reuse agents and choice of dialyzer membrane [45]. Therefore, the advantages and disadvantages of reused membranes must be determined by convincing scientific evidence of further studies.

2. EXPERIMENTAL TECHNIQUES

The characteristics of hemodialysis membranes and the effect of disinfecting agents on their structure are the issues that are not still well defined because of the paucity of experimental studies performed from an engineering point of view. There are many clinical researches about biocompatibility and ultrafiltration abilities of several hemodialysis membranes but there is no publication in the open literature, which covers all of the experimental techniques used in this study to the best of our knowledge.

The aim of the experiments performed in this thesis is to evaluate the performance of a well known hemodialysis membrane; high flux polysulfone hemodialyzer with the fibers named Helixone, in terms of the mechanical and structural stability. The reason for including reprocessed fibers is the great need of information about the reuse application which is very common in many countries, such as USA, Thailand, China and Singapore [44], but new and almost unattempted in our country.

Many clinical researches have proven that reuse of the dialysis membranes reduces the effect of first-use syndrome including allergic symptoms and increases the biocompatibility [3]. Despite the low cost advantage and the increasing use of new reuse hemodialysis modalities, there are still some uncertain issues. The possible loss of mechanical toughness, alteration in morphology and crystallinity are some of these issues.

In order to clarify these uncertainties, in addition to the tensile testing and crystallinity determination, several types of microscopical studies are necessary for analyzing the dialysis fiber surfaces. This thesis aims to give the clear answers of the questions about the polysulfone membranes for both first-use and reuse processes.

2.1 Specimen Preparation

2.1.1 Hemodialyzers

The surface features, morphology and mechanical behavior of virgin and used-processed Fresenius polysulfone high flux FX80 hemodialyzer fibers were studied in this study. In fact, all FX class high flux dialyzers are made up of the same type of hollow fibers named Helixone. The difference between these hemodialyzers is based on the packing properties, like the number of fibers that affects the surface area, blood filling volume, ultrafiltration coefficient and maximum blood flow. Therefore, by investigating the performance of the Helixone membrane, the performance of all FX class dialyzers can be estimated.

Figure 2.1.1.1 shows the virgin (unused) dialyzer and a dialyzer after one dialysis session. Dialyzers labeled as virgin were received from the manufacturer in sterile packages. The used dialyzers were provided by Diamed Dialysis Clinic (Kozyatağı, İstanbul).

The dialyzers that were chosen for this study, were used by the patients who were HIV (-), HBsAg (-) and had no other contagious disease. The dialysis machine was Fresenius 4008B and Renasol dialysate solution was used. The patient blood flow rate was in the range of 350–360 ml/min and one dialysis session took 4 hours.

Cutting and reprocessing operations for the used fibers were started in 1.5h following the patient contact. The used dialyzers were carried from one place to another in ice bath and refrigerated at 4 °C when necessary.



Figure 2.1.1.1 The virgin hemodialyzer (upper) and the hemodialyzer after patient contact (lower).

The virgin and used–processed fibers are mechanically tested and the testing method is described in the Section 2.3. After mechanical tests, different types of fibers according to their history are obtained in order to determine and compare the differences. Table 2.1.1.1 lists the fiber categories after mechanical testing.

Table 2.1.1.1

Dialyzer fibers categorized according to their history.

Category	Description
1	Virgin
2	Virgin, on which tensile test (monotonic loading) is applied
3	Virgin, on which tensile test (cyclic loading) is applied
4	Used and processed
5	Used, which is bleach/formaldehyde processed and on which tensile test (monotonic loading) is applied
6	Used, which is formaldehyde/bleach processed and on which tensile test (cyclic loading) is applied

2.1.2 Cutting

In order to obtain fiber samples from the dialyzers, a proper cutting procedure was needed to be performed. Figure 2.1.2.1 shows the cutting planes on the hemodialyzer, consecutively.

Following the given order, firstly, the blood inlet end-cap of the virgin hemodialyzer was totally removed by using a sharp saw; see Figure 2.1.2.1 (1). The dialyzer was cut again about 1.5 cm away from the cap in order to separate the top of the fibers that are potted in polyurethane and the gasket (2). The picture of step 2 is given in Figure 2.1.2.2. After that, to reach the free (unstuck) fiber bunch, another length of 1.5 cm was cut (3). The other end of the dialyzer was cut in the half of the dialyzer diameter to form 16 cm lengths of fibers that can be removed easily from the polypropylene case without damaging (4). The fiber samples from hemodialyzers with patient contact were obtained by cutting according to the same procedure.

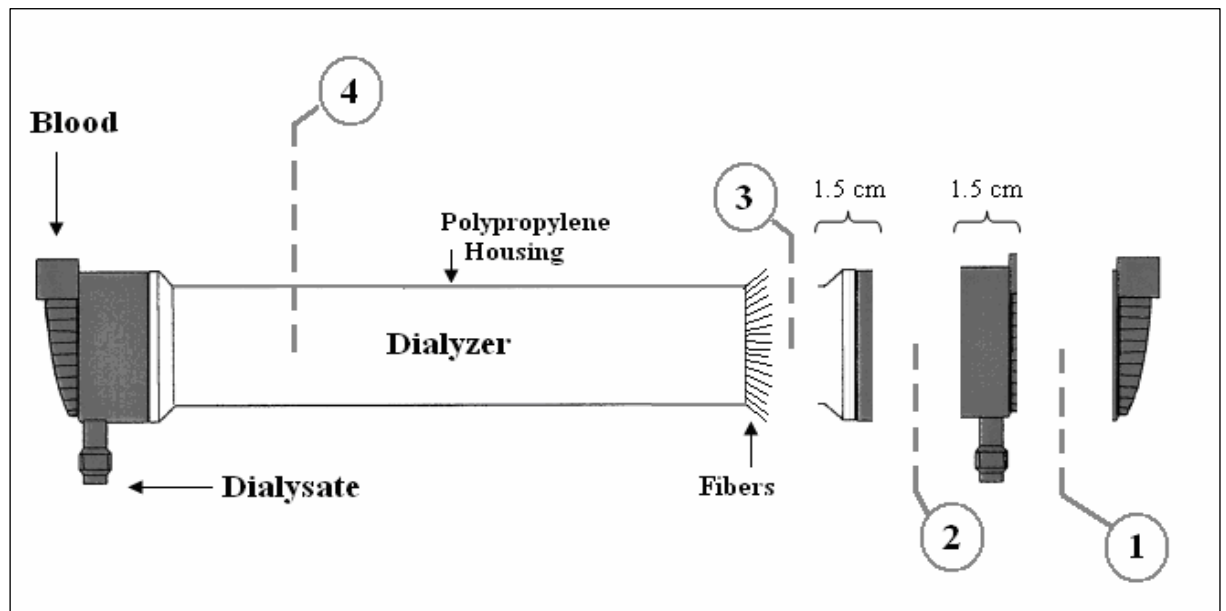


Figure 2.1.2.1 The diagram of cutting procedure.



Figure 2.1.2.2 The picture of cutting the hemodialyzer which was mounted in a vise (Step – 2 in Figure 2.1.2.1).

2.1.3 Reprocessing

The used fibers were firstly rinsed with isotonic sodium chloride solution (0.9 per cent w/v) in order to remove the visible clotted blood. Figure 2.1.3.1 shows one of the potted tops of the fibers before rinsing.

Since commercially available formaldehyde solution is 40 % by (w/v), it was diluted to 4 % with ultra-pure water. After that, the dialyzer fibers were disinfected manually by leaving in 4 % formaldehyde solution for 14 hours and again rinsed extensively with isotonic solution and high quality water. Then, the fibers were rinsed with 5 % aqueous sodium hypochlorite (commercial bleach without fragrances or scents) and stored in the solution for 6 hours. Figure 2.1.3.2 shows the glass plate where the used fibers and the stuck tops were left in disinfectants. The residual disinfectant was removed by rinsing the fibers with isotonic solution. The room temperature was kept constant at 24 °C during reprocessing.



Figure 2.1.3.1 The used top before rinse.

A similar disinfection process in automated machines was applied by Cornelius and his colleagues on the used fibers of another type of polysulfone high flux hemodialyzer while investigating the effectiveness of formaldehyde/bleach reprocessing in removing the bound material from the blood contacting surface. Briefly, the dialyzers were rinsed extensively using high quality water, cleaned with 5 % aqueous sodium hypochlorite (bleach), and again rinsed extensively with water. The dialyzers were then disinfected with 4 % formaldehyde, removed from the reprocessing machine, and recapped [32].



Figure 2.1.3.2 The used fibers and tops in a glass plate, which are ready to be stored in disinfectants.

2.2 Stereomicroscopy

Stereomicroscopes are valuable in three dimensional observation of specimen structure and perception of depth and contrast. In this study, the stereomicroscope is used for initial examination of fibers at relatively low magnification compared to scanning electron and atomic force microscopes.

2.2.1 Introduction

Microscopy is the study of the fine structure of an object by using a microscope. The limitations of the human eye as an instrument for the study of fine detail are overcome by three important attributes of a microscope: resolution, contrast and magnification. It is clear that magnification is a prime requirement, resulting in a significantly enlarged image. In optical microscopy, magnifications up to 1000× can be used. Information regarding size, shape, and arrangement of features can be obtained [46]. However, the microscope used in this study cannot attain magnifications as high as 1000×. Therefore, it is not possible to display the pores of the dialyzer fibers, which are about a few micrometers, through simple lenses of the optical microscopes. Thus, the optical microscopy studies emphasized the necessity of scanning electron and atomic force microscopes for this study.

The different parts of hemodialyzers can be observed under the microscope without any other special specimen preparation explained above. Instead of transmitting through the specimen, the light is reflected from the surface of the specimen during the observation; therefore, the hemodialyzers was not dissected further.

2.2.2 Materials And Methods

The stereographic microscope used in this experiment was an Olympus SZ with a U-PMTVC type adapter and a CCD camera, which was a CS Lilin PIH 735, attached to a PC at İstanbul Technical University (ITU) Materials Laboratories (Figure 2.2.2.1).

The pictures of virgin fibers were taken up to 10× since stereomicroscopy can provide relatively scant pictures at relatively low magnification and macro level. Instead of the fibers, the disk made up of the stuck ends of the fibers was preferred to study.



Figure 2.2.2.1 The Olympus Stereomicroscope at İstanbul Technical University (ITU) Materials Laboratories.

2.2.3 Results And Discussions Of The Stereomicroscopic Studies

The distribution of the fibers in the potting material and their places relative to each other are the constituents responsible for the adequate distribution of blood flow. In longitudinal direction, the Helixone hemodialyzers are designed such as to distribute the blood flow in the spiral configuration. The entrance in the potted fiber region compartments of the dialyzers, which are arranged according to this aim, were examined by the optical microscope as shown in Figure 2.2.3.1.

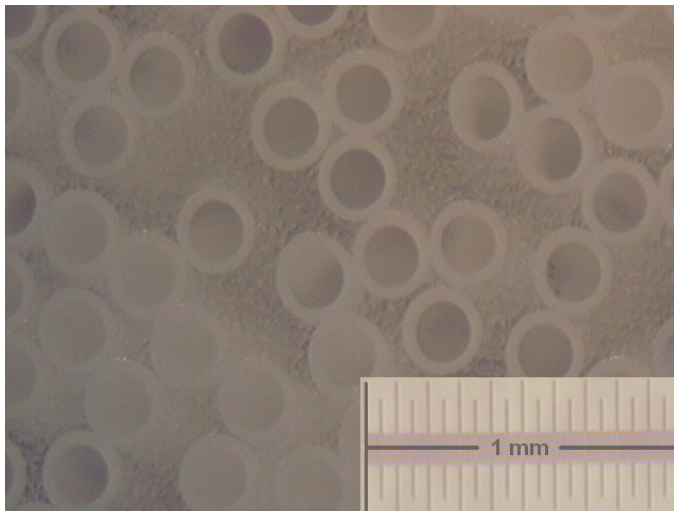
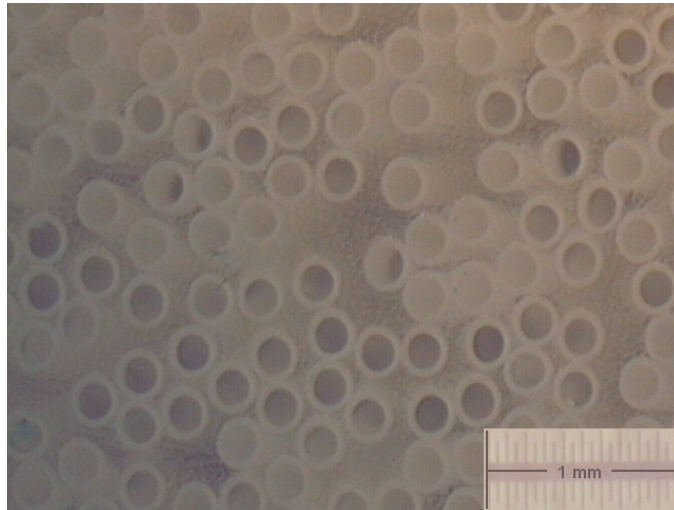
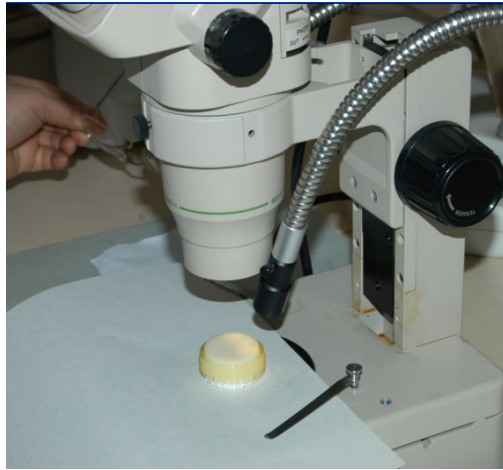


Figure 2.2.3.1 The position of the dialyzer head under microscope (upper) and the microscopic views of head, showing the tapping material with the blood inlets of the fibers in two different magnifications (the two lower).

The conjunction of the adherent part and the individual fibers was observed by placing the sample under the microscope as shown in Figure 2.2.3.2. From this figure, the polyurethane potting compound is seen as it is properly adhered to the hemodialyzer fibers.

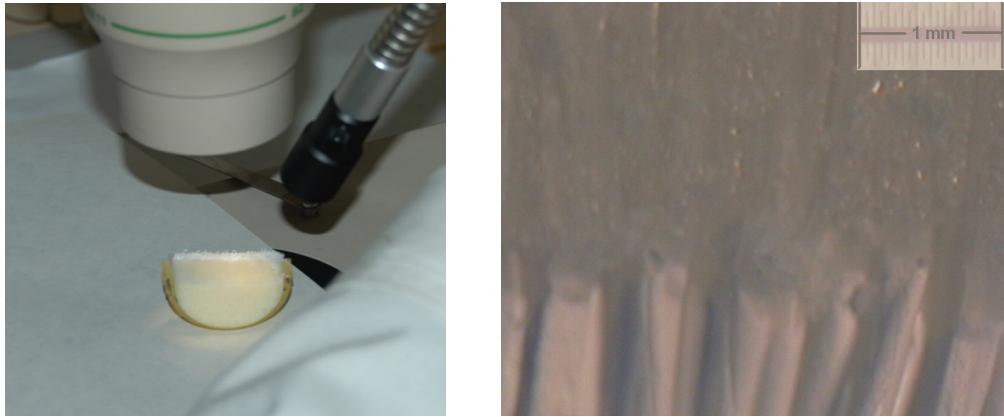


Figure 2.2.3.2 Placing the sample under the microscope (left), the microscopic view of the conjunction part (right).

Figure 2.2.3.3 shows the hallow fiber placed under the microscope and its outer (dialysate) side's microscopic view.

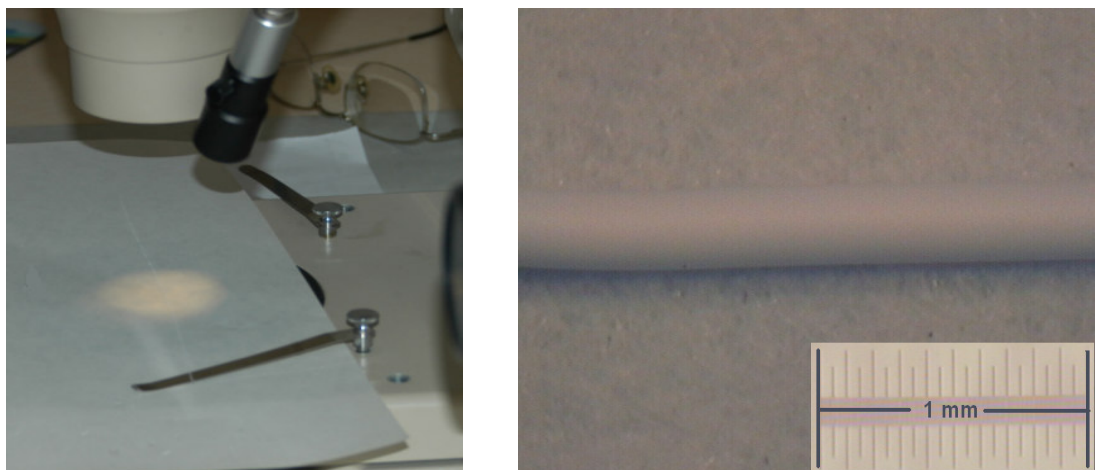


Figure 2.2.3.3 A hallow fiber under microscope (left) and its microscopic view (right).

2.2.4 Conclusions

As stated in the Section 1.4.3, FX class hemodialyzers have many improvements in the fiber itself, fiber bundle structure and outer housing. These innovations are important for blood and dialysate entrance, pathway and proper distribution. In addition, the diameter of the fibers is important in flow velocity, wall shear rates, pressure drop, convection and therefore, filtration [30]. In this study, general information about the structure of polysulfone hemodialyzer (including the measurement of fiber diameter, the distribution of fibers in the potting material and the general view of a single fiber) was obtained. However, optical microscopy studies were not sufficient in determining the micro structure of the membrane. Therefore, pore size, shape and distribution and the effect of patient contact, disinfection and tensile stress on these properties were investigated by scanning electron and atomic force microscopes.

2.3 Mechanical Tests

The mechanical properties of virgin and used–processed polysulfone hemodialyzers were determined by tensile test, which can be considered as the most fundamental type of mechanical tests. Conducting a tensile test, in other words, pulling the fibers in a properly controlled way gives important information, e.g. their elastic and plastic deformation behaviors, toughness and ductility characteristics, yield and tensile strengths.

2.3.1 Introduction

A tensile test is carried out on a machine that can exert sufficient force to stretch the specimen of interest. One end of the specimen is attached through a suitable linkage to a load cell, and the other is attached to a movable crosshead, which is driven by either large screws or by a hydraulic piston [47]. A screw–driven machine is illustrated schematically in Figure 2.3.1.1(a).

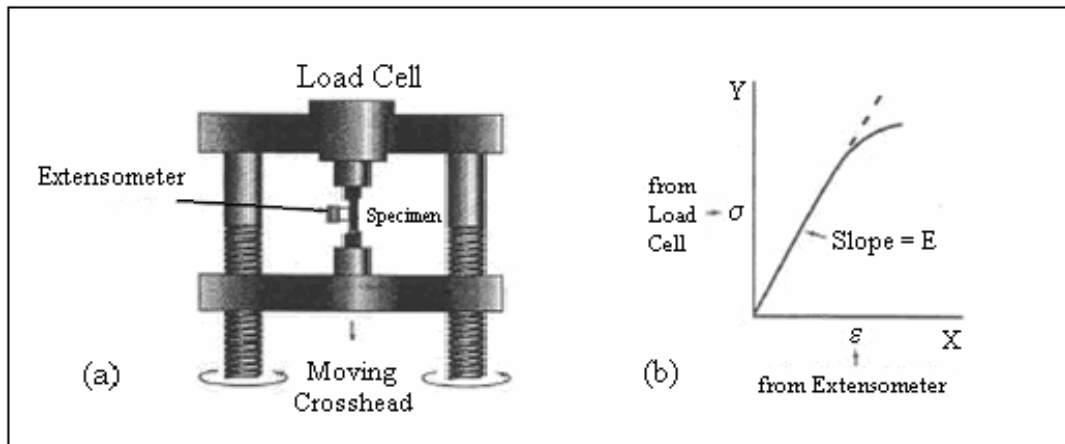


Figure 2.3.1.1 (a) Schematic representation of tensile-testing apparatus (b) Initial portion of stress-strain curve plotted by an X-Y recorder, showing plastic yielding, causing the departure from linear elastic behavior [47].

An extensometer, which is a displacement transducer, provides an electronic reading of the displacement [47, 48]. The voltage outputs from the load cell and the extensometer are displayed as the stress-strain curve, as illustrated in Figure 2.3.1.1 (b), where σ and ϵ denotes stress and strain, respectively.

The engineering stress and strain are determined from the measured load (F) and elongation (Δl) divided by the original specimen cross-sectional area and length A_0 and l_0 , respectively [47, 48].

$$\text{Stress } (\sigma) = \frac{F}{A_0} \quad (2.3.1.1)$$

$$\text{Strain } (\epsilon) = \frac{\Delta l}{l_0} \quad (2.3.1.2)$$

Stress has dimensions of force per unit area (N/m^2 or pascal, Pa) and strain is dimensionless [47]. When the stress σ is plotted against the strain ϵ , an engineering stress-strain curve is obtained. The modulus is a direct measure of a material's resistance to deformation [49]. In the early (low strain) portion of the curve, shown in Figure 2.3.1.1(b), many materials obey Hooke's law (Eq. 2.3.1.3) to a reasonable approximation, so that

stress is proportional to strain with the constant of proportionality being the modulus of elasticity or Young's modulus [48], denoted by E :

$$\sigma = E\varepsilon \quad (2.3.1.3)$$

Elasticity is the property of complete and immediate recovery from an imposed displacement on release of the load [48]. In the elastic range of stress–strain curve, the slope, i.e. Young's modulus, is an indicator of stiffness. The higher the value of E represents the stiffer the material [48].

The total engineering stress–strain curve is actually plotted beyond the elastic limit, as shown in Figure 2.3.1.2.

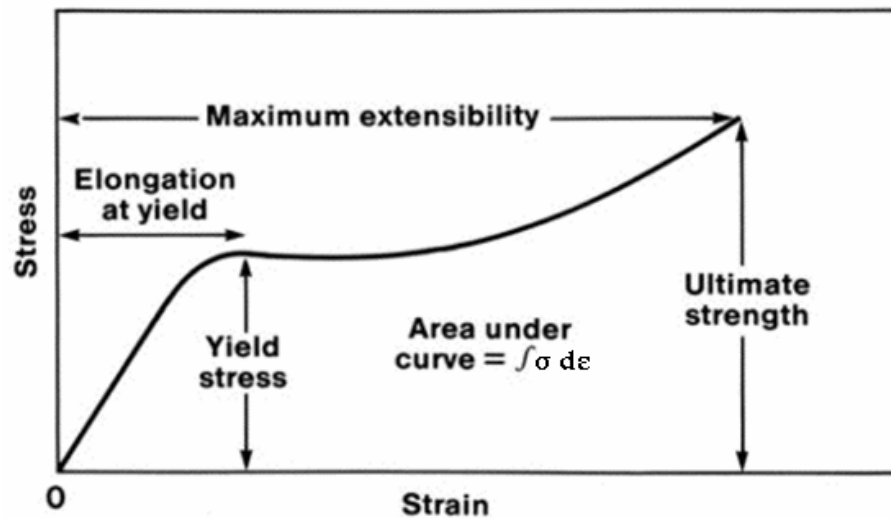


Figure 2.3.1.2 Typical non–equilibrium stress–strain curve in elongation, adapted from [49].

The stress–strain curve becomes nonlinear for many materials at a value called ‘yield’, where the stress is equal to yield stress [48, 49]. This nonlinearity is usually associated with stress–induced “plastic” flow in the specimen. At this point, the material is undergoing a rearrangement of its internal molecular or microscopic structure, in which atoms are being moved to new equilibrium positions. These microstructural rearrangements associated with plastic flow are usually not reversed when the load is removed [48], i.e. at stress levels higher than yield stress, which is needed to induce plastic deformation, the material cannot retake its original shape.

For the case in Figure 2.3.1.2, the curve increases monotonically until rupture occurs. The stress at this point is called the “ultimate strength”. The area under the curve corresponds to the integral of $\sigma d\epsilon$, and is therefore the work or energy required for rupture. It is the standard measure of toughness [49]. Therefore, for any stress–strain curve, the larger the total area under the curve up to fracture means the tougher the material.

As an example, curves for typical polymeric materials are shown in Figure 2.3.1.3. The term “soft” refers to the fact that the initial slope is small which means a low value of the modulus. “Weak” refers to the low value of the ultimate strength. “Hard” refers to the fact that the initial slope and modulus are large, and “brittle” refers to the fact that the maximum extensibility is very small [49].

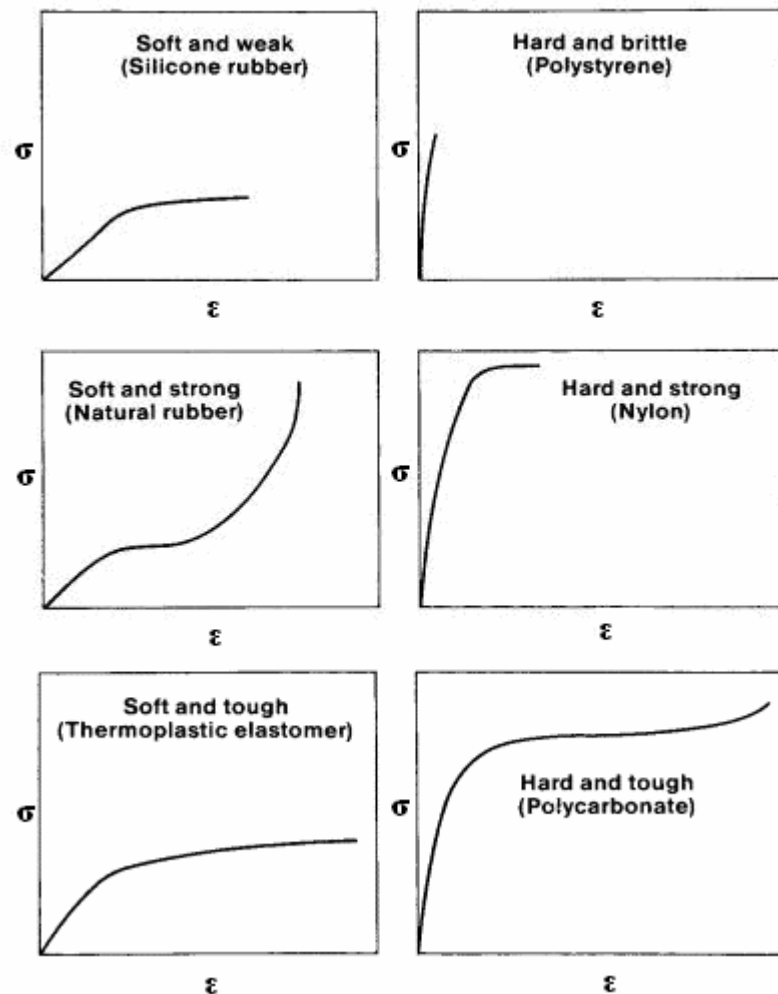


Figure 2.3.1.3 Non–equilibrium stress–strain curves for some types of polymers, adapted from [49].

In this study, fractures due to tensile overstress are important because the service characteristics of hemodialysis membranes are affected by the failures due to crack formations, which can also be investigated by microscopic techniques like SEM and AFM.

It is known that the formation of cracks strongly depends on the microstructure of a crystalline or amorphous solid, applied loading and environment. The microstructure plays a very important role in a fracture process due to dislocation motion, precipitates, inclusions, grain size, and type of phases making up the microstructure. All these microstructural features are imperfections and can act as fracture nuclei under unfavorable conditions [50]. In particular, the imperfections in the dialysis membranes are the pores that are coming from the materials original morphology and desirable from filtration point of view. The microstructural geometrical discontinuities, such as notches, holes, and the pores, are sources for crack initiation when the stress–concentration is sufficiently high.

During dialysis, the load and stress on the dialyzer varies because of the fluctuating pressure, which depends on the flow rates of blood and dialysate. In order to prevent muscle cramp, which is a common complication of the dialysis procedure, the volume removal from the patient, therefore, the flow rate can be reduced [6]. Additionally, the symptoms that may be related to air embolism, e.g. sudden dyspnea, cough, and cyanosis, followed by unconsciousness, must be thwarted by stopping the dialysis immediately and placing the patient head and chest down, and turned on the left side [16]. In some cases, the sudden drop of flow rate may be followed by a sudden raise, if the dialysis is stopped and continued again. Furthermore, the turbulence of blood content (especially red blood cells) creates frictional forces on the surface. Under these circumstances, the almost circular form of pores may become elliptic and it is expected to have high amount of stress concentration at the ends of the axes of the ellipses. This situation is predicted to be followed by merging of pores and even fracture.

Fracture of hemodialysis membranes would result in inadequate solute removal, inefficient dialysis, more importantly, blood leakage. From this point of view, determination of mechanical properties of the hemodialyzer membranes is critically important and can be regarded as a precaution in dialysis risks.

2.3.2 Materials And Methods

The mechanical tests were performed at Materials Laboratories of Gebze Institute of Technology (GYTE) by using Instron 5569 Universal Testing Machine connected to a PC (see Figure 2.3.2.1). The virgin fibers, with an outer diameter of 0.255 mm, were cut to a length of 5 cm and loaded monotonically or cyclically until fracture. The cycling loading experiments were repeated four times until 50 % of the maximum load of fracture obtained during monotonic loading and the last (fifth) loading was continued until fracture. All of the first four cycles were in the elastic range. All these tests were performed by uniaxial loading and run at room temperature in laboratory conditions. Crosshead speed was kept constant during each test at 50mm/min and load cell was 5kN. These tensile tests were performed with the same procedure at the same conditions also for the used samples in order to compare with the virgin fibers.

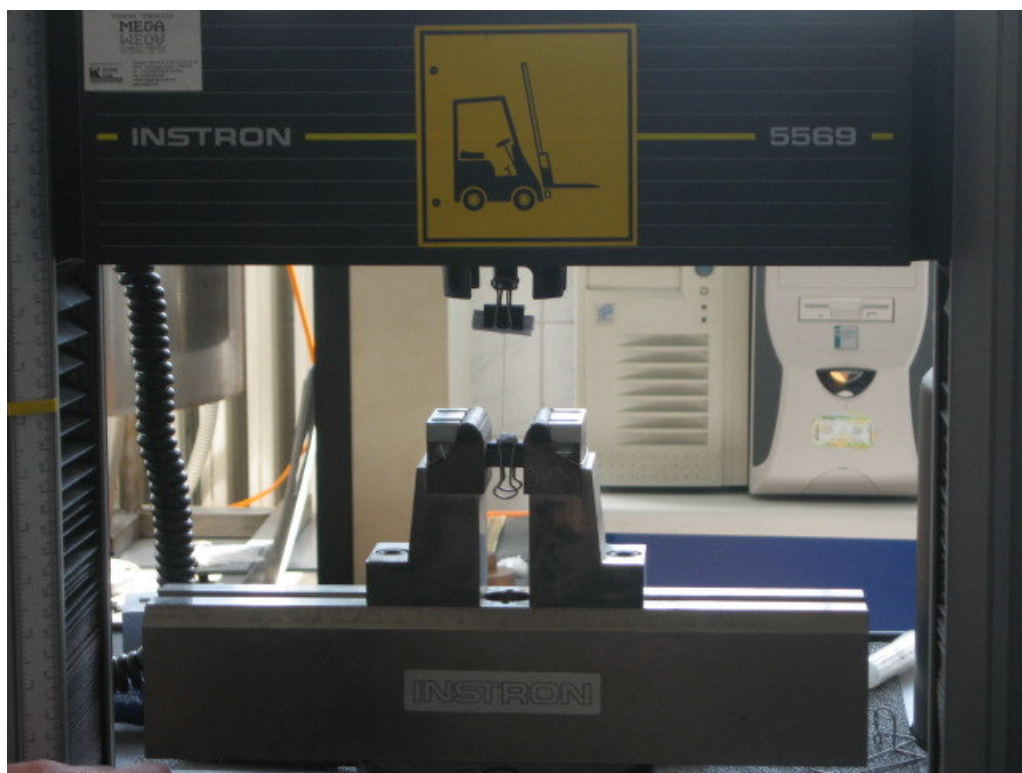


Figure 2.3.2.1 The fibers are mounted to the grips of Instron 5569 Universal Testing Machine individually.

2.3.3 Results And Discussions Of Tensile Tests

The measured load per area and extension of the polysulfone fibers during tensile tests are plotted as stress–strain curves depicting the mechanical behavior of the membrane. There is more than one sample from each fiber category to increase the reliability. However, the trends are the same for each category, so that, one sample chosen from each of them to demonstrate the equated mechanical behavior.

Figure 2.3.3.1 shows the tensile stress (MPa) versus tensile strain (% elongation) curves of two initially identical virgin polysulfone hemodialyzer fibers, which are loaded monotonically or cyclically. The fifth loading, which was continued until fracture, is plotted in the following figure to compare with the stress–strain curve of monotonic loading.

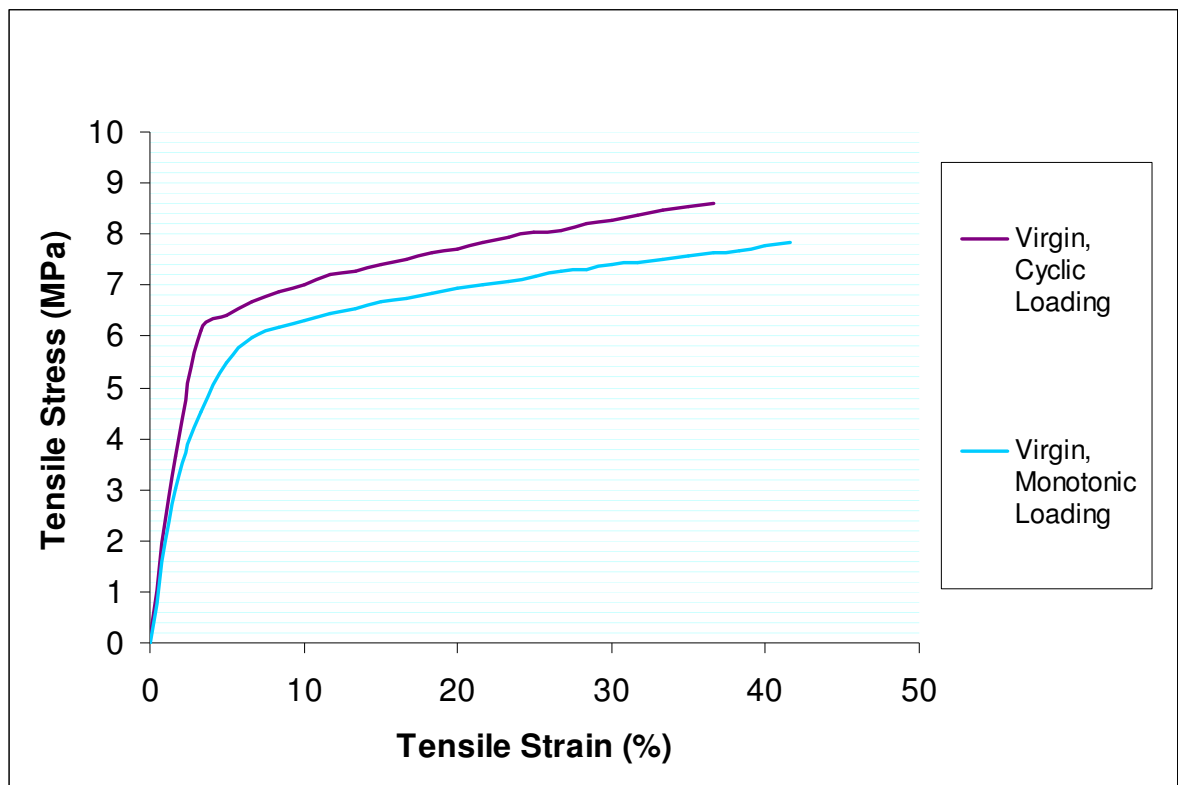


Figure 2.3.3.1 Tensile stress–strain curves of two initially identical virgin polysulfone hemodialyzer fibers, which are loaded monotonically or cyclically up to fracture.

As stated in Section 2.3.1, the area under any stress–strain curve is the energy per unit volume absorbed by the material, which determines the toughness. To calculate the area under the curves, first, the curves were fitted to polynomial regression curves whose equations were obtained from Microsoft EXCEL. Then these curves were integrated from zero to fracture points in MATLAB and the calculated absorbed energy values are given in Table 2.3.3.1.

Table 2.3.3.1

The fracture point stress and strain values and the energy/volume required to fracture the given membranes.

Fiber Type	Fracture Point		Energy/Volume (MPa)
	Stress (MPa)	Strain (%)	
Virgin fiber which is loaded monotonically	7.8	41.7	219.46
Virgin fiber which is loaded cyclically	8.6	36.7	173.79

Since toughness is the amount of energy per volume that a material can absorb before rupturing, it is the resistance to fracture of a material under tension. From Table 2.3.3.1, it is seen that the toughness of cyclically loaded virgin polysulfone fiber is lower than the monotonically loaded virgin fiber.

If the fracture point stress and strain values of cyclically and monotonically loaded virgin fibers are compared, it is seen that the cyclically loaded fiber fractures at higher stress and lower strain. Additionally, strain hardening is slightly more in cyclically loaded fiber than in monotonically loaded one.

In addition, from Figure 2.3.3.1, the slope of the linear part of the curve (i.e. modulus of elasticity) of the cyclically loaded fiber is higher than the modulus of elasticity of monotonically loaded fiber. For the case of uniaxial tension, modulus of elasticity is directly proportional to the stiffness and can be thought of as a measure of it. Therefore, when compared to the fiber that is exposed to monotonic loading, the cyclically loaded

fiber becomes stiffer that results in an increase in the resistance of the fiber to elastic deformation.

Figure 2.3.3.2 shows the tensile stress (MPa) versus tensile strain (% elongation) curves of two initially identical used and processed polysulfone hemodialyzer fibers, which were loaded monotonically or cyclically. The cycling loading experiments were performed four times until 50 % of the maximum load of fracture in the elastic range. The curve of fifth loading, which was continued until fracture, is compared with the monotonic loading curve, as follows:

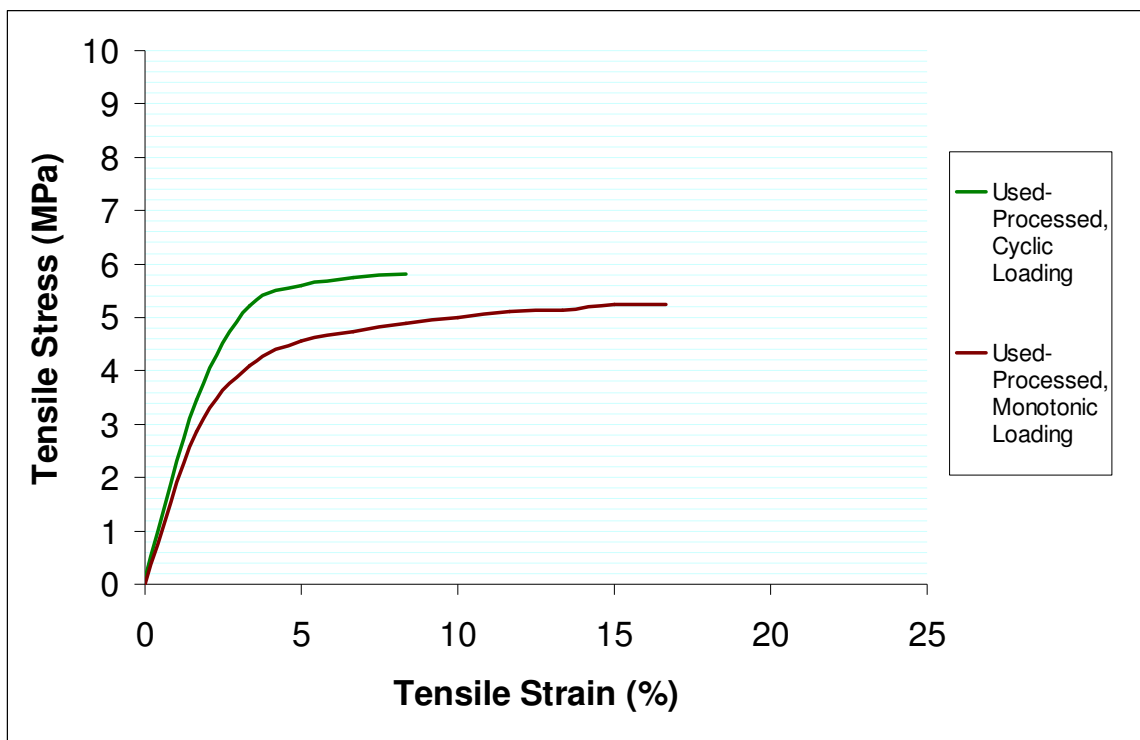


Figure 2.3.3.2 Tensile stress–strain curves of two initially identical used and processed polysulfone hemodialyzer fibers, which are loaded monotonically or cyclically up to fracture.

From Figure 2.3.3.2, it is seen that the cyclically loaded fiber fractures at higher stress and lower strain, as in the case of virgin fibers. The modulus of elasticity of the cyclically loaded used–processed fiber is higher than that of monotonically loaded fiber. It can be concluded that both of the virgin and used–processed fibers that are exposed to cyclic loading becomes stiffer.

The curves, shown in Figure 2.3.3.2 are fitted to polynomial regressions and integrated from zero to fracture points and the absorbed energy values are given in Table 2.3.3.2.

Table 2.3.3.2

The fracture point stress and strain values and the energy/volume required to fracture the given membranes.

Fiber Type	Fracture Point		Energy/Volume (MPa)
	Stress (MPa)	Strain (%)	
Used–Processed fiber which is loaded monotonically	5.2	16.7	140.13
Used–Processed fiber which is loaded cyclically	5.8	8.3	40.45

From Table 2.3.3.2, it is seen that the toughness of cyclically loaded used–processed polysulfone fibers is lower than the monotonically loaded used–processed ones. A similar case is observed for the virgin samples of polysulfone fibers. Therefore, it can be said that cyclic loading decreases the toughness of the fibers.

Figure 2.3.3.3 shows the tensile stress–strain curves for virgin and used–processed polysulfone hemodialyzer fibers, which are both monotonically loaded up to fracture.

From Figure 2.3.3.3, it can be said that ultimate tensile stress and yield strength decrease in the used–processed fiber and it becomes more brittle.

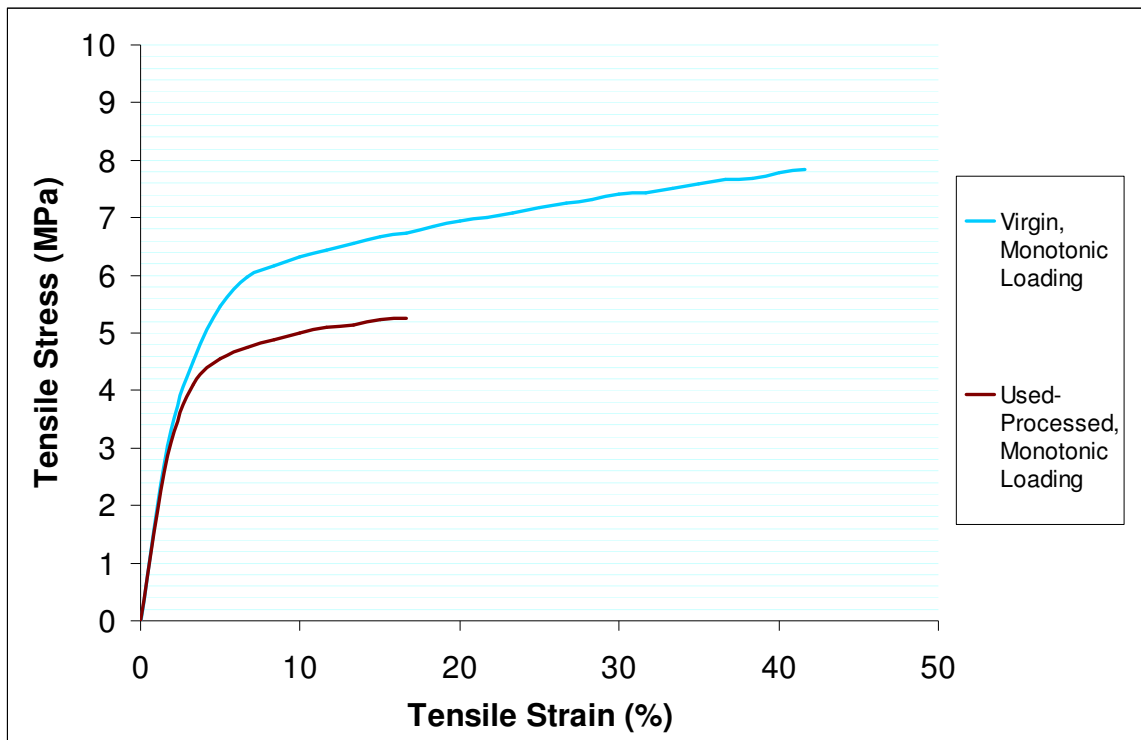


Figure 2.3.3.3 Tensile stress–strain curves of virgin and used–processed polysulfone hemodialyzer fibers, which are loaded monotonically up to fracture.

The curves, shown in Figure 2.3.3.3 are fitted to polynomial regressions and integrated from zero to fracture points and the absorbed energy values are given in Table 2.3.3.3.

Table 2.3.3.3

The fracture point stress and strain values and the energy/volume required to fracture the given membranes.

Fiber Type	Fracture Point		Energy/Volume (MPa)
	Stress (MPa)	Strain (%)	
Virgin fiber which is loaded monotonically	7.8	41.7	219.46
Used–Processed fiber which is loaded monotonically	5.2	16.7	140.13

From Table 2.3.3.3, although they are both monotonically loaded, it is seen that the toughness of used–processed polysulfone fiber is lower than the virgin one. The energy absorbed by the used–processed fiber is only 63.9 % of the energy needed to fracture the virgin fiber. Here, the effect of chemical environment including blood and disinfecting agents is seen.

Figure 2.3.3.4 shows tensile stress–strain curves for virgin and used–processed polysulfone hemodialyzer fibers. Both fibers were cyclically loaded again four times at about 50 % of the maximum load of fracture and these cycles were remained again in the elastic range. The last loadings, which were continued up to fracture, are plotted for virgin and used–processed fibers.

Similarly, the areas under the curves, shown in Figure 2.3.3.4, are calculated by taking the integral of polynomial regression curves form zero up to fracture point and given in Table 2.3.3.4.

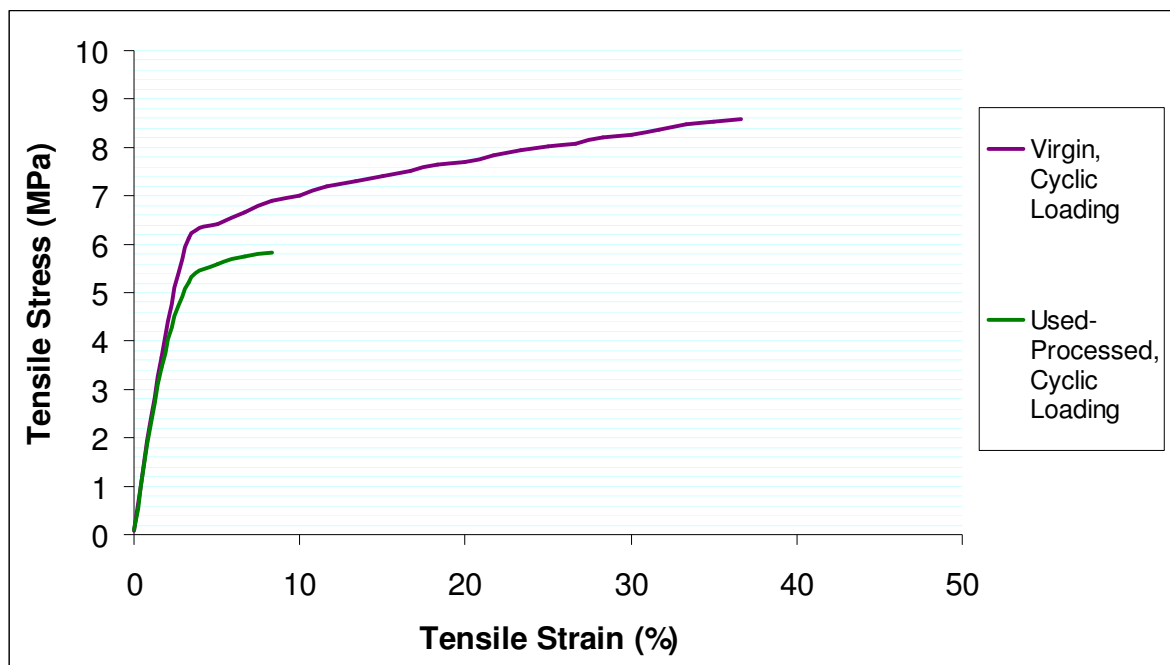


Figure 2.3.3.4 Tensile stress–strain curves of virgin and used–processed polysulfone hemodialyzer fibers, which are loaded cyclically for 4 times in elastic portion before the last loading up to fracture.

Table 2.3.3.4

The fracture point stress and strain values and the energy/volume required to fracture the given membranes.

Fiber Type	Fracture Point		Energy/Volume (MPa)
	Stress (MPa)	Strain (%)	
Virgin fiber which is loaded cyclically	8.6	36.7	173.79
Used–Processed fiber which is loaded cyclically	5.8	8.3	40.45

From Figure 2.3.3.4, it is seen that the ultimate tensile stress and yield strength decreases after patient contact and disinfection and the material becomes more brittle. It is concluded that, virgin membranes can resist higher loads compared to used–processed membranes.

From Table 2.3.3.4, it is seen that the toughness of used–processed polysulfone fiber is lower than the virgin one, although they are both cyclically loaded. Here, again, the effect of chemical environment including blood and disinfecting agents is seen. It can be concluded that reprocessing the used fibers decreases the toughness of the polysulfone hemodialyzer membranes.

2.3.4 Conclusions

The typical monotonic loading tensile properties of commercially available polysulfone resins are given as tensile strength is equal to 70.3 MPa and tensile elongation at break is 50–100 % by the manufacturer [51]. These values are obtained by monotonic loading under ideal conditions (any chemical exposure or time related effects) and reasonably higher than the values of monotonically loaded virgin polysulfone membrane, which are determined in this study.

FX Class hollow fiber dialyzers, also used in this study, have modified and improved polysulfone fibers named Helixone, are produced by a technique called nano-controlled spinning technology. The production process these membranes includes micro-crimping and addition of a hydrophilic substance polyvinylpyrrolidone (PVP) [20, 52], that causes the mechanical properties of the membrane to depart from the commercial polysulfone. Additionally, the pores of the membrane have a great impact on the material's behavior under tensile stresses, likely to decrease the resistance to fracture as being defects.

By taking these into consideration, polysulfone hemodialyzer membranes cannot be considered to have the same tensile properties with commercial nonporous polysulfone and this study is important for the determination of its performance under tensile stresses.

The experiments of Causserand and colleagues showed that an exposure to sodium hypochlorite produces chain breaking in the polysulfone molecules, which leads to changes to the membrane texture on the microscopic scale, and which is closely related to changes in the membrane mechanical properties [53].

Similarly, Gaudichet-Maurin et.al, also performed tensile tests on bleach aged polysulfone film and hollow fiber with internal skin. The fact that the engineering yield stress of films is greater than fibers is not a surprising finding, since strong stress concentration in pore walls are accepted in these latter [54]. The main experimental fact of their study is that the existence of an embrittlement process in both fibers and films.

In the tensile tests, cyclically loaded fibers are fractured at higher stress and lower strain compared to same type of fibers that are monotonically loaded. Additionally, strain hardening is more in cyclically loaded fibers than in monotonically loaded ones. The fibers that are exposed to cyclic loading become stiffer than the monotonically loaded ones for both virgin and used-processed type of fibers. They become more brittle and embrittlement is a problem resulting in pore tip breakage, crack initiation and propagation and also rupturing. Additionally, cyclic loading causes a decrease in the toughness of the polysulfone fibers.

It can be said that ultimate tensile stress and yield strength decrease in both monotonically and cyclically loaded used–processed fibers and they become more brittle compared to virgin ones. Additionally, the toughness of used–processed polysulfone fibers is lower than the virgin ones for all cases. The effect of chemical environment including blood and disinfecting agents together with tensile loading can be seen clearly in the used–processed fibers.

To conclude, virgin membranes can resist higher loads compared to used membranes. Patient contact together with disinfection reduces the membrane's toughness, yield and ultimate tensile stresses. The membrane becomes more brittle and possibility of membrane damage increases.

2.4 Atomic Force Microscopy (AFM)

Atomic force microscopy (AFM) is used to study the surfaces and the architecture of virgin and used–processed fibers. In contrast to SEM, which provides the two dimensional visualization of the surface structures, AFM allows precise determination of the depth of these structures with three dimensional images. When these techniques are combined, the surface topography of the hemodialyzer fibers can be completely revealed in microscale. Therefore, the three dimensional map of the surface features belonging to virgin and used–processed fibers were obtained by AFM to determine the effects of the dialysis session with disinfection process on the fiber structure.

2.4.1 Introduction

Atomic force microscopy was first applied to polymer surfaces in 1988, shortly after its invention [55]. The atomic force microscope (AFM), described in Figure 2.4.1.1, is a useful tool to investigate the various pore sizes on the fiber surface [56].

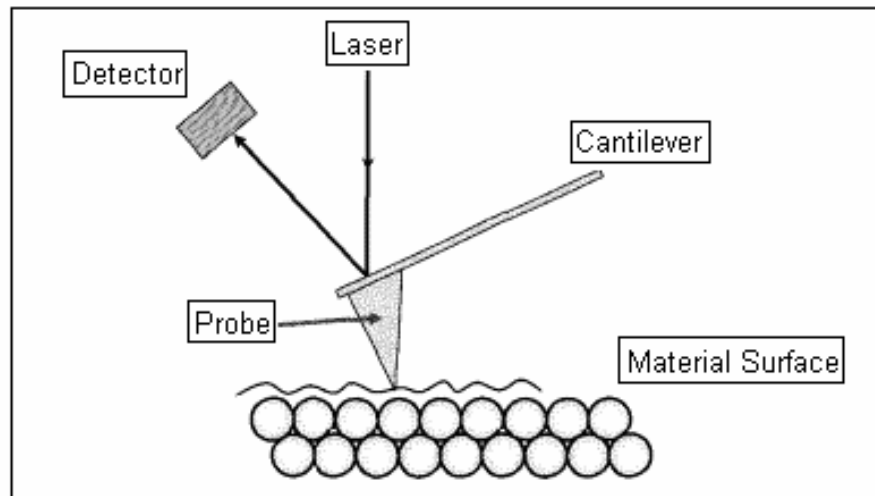


Figure 2.4.1.1 The principle of atomic force microscope (AFM) [56].

In AFM, an atomically sharp probe (a few μm long and often less than 5 nm in diameter, made of diamond or SiN), mounted on a very soft spring or metal-coated micro-fabricated cantilever (length: 100 – 200 μm), is drawn across a surface [46] (see Figure 2.4.1.2).

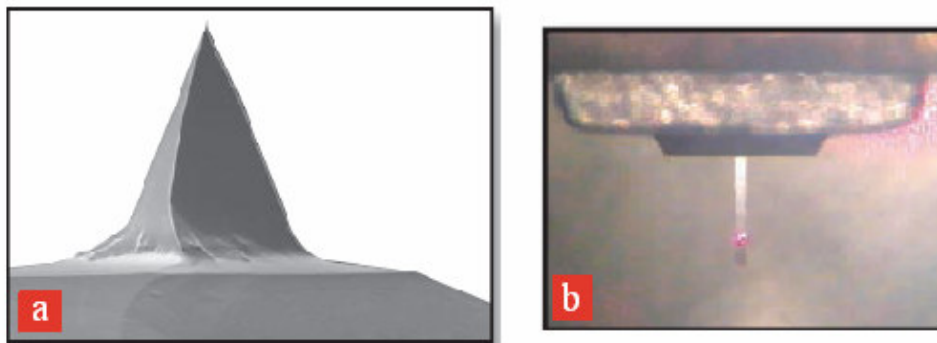


Figure 2.4.1.2 a) An SEM image showing typical probe tip geometry b) The typical video camera view of a properly aligned cantilever ready to scan. Adapted from [57].

AFM maps surface topographic features by constructing digitised images from the measurement of the attractive or repulsive probe and specimen surface interactions [46]. Depending on the sample surface–tip interaction, there are two main modes of operation: contact mode, non-contact mode. In contact mode, the tip is in almost physical contact with the sample surface from a few Ångstroms away [46].

Contact mode can generate images with high resolution; however, the drawback is a possible damage of material surface which is significant when soft materials are analyzed [56]. On the other hand, in the non-contact AFM mode, the tip is kept at a constant distance from the sample, typically tens to hundreds of Å [46]. Therefore, non-contact AFM is desirable in studying the membrane surface, because polymeric surfaces are soft [55] and damageable.

In contrast to SEM, AFM allows precise determination of the depth of surface structures, i.e. three dimensional views instead of two dimensional. Since AFM data stain height information, the determination of the surface features as a bump or pit is easier [46].

Another advantage of AFM is that the polymeric materials can well be characterized without coating the surface with a conductive material. However, AFM requires an isolation chamber to prevent the effects of building vibrations, interior acoustic noise, and thermal drift caused by room air movement.

2.4.2 Materials And Methods

Figure 2.4.2.1 shows the Q-Scope™ Universal SPM (Ambios Technology, Inc.), that can be run in either AFM or STM imaging modes. The AFM instrument comprises the following components: scanning system (e. g. piezoelectric tube scanner), probe, probe motion sensor and controller electronics [46]. The acoustic and vibration isolation is also seen in the Figure 2.4.2.1.

The exterior of the hollow fibers were examined by choosing AFM WaveMode™ on the SPM. Throughout the surface analysis, the probe is set to non-contact mode. The 3D AFM images are constructed by ScanAtomic™ image acquisition and analysis software. It allows mesh analysis on the scanned areas. The height histograms and roughness parameters are obtained by using this software.

The examined fibers are selected from the batches of the used–processed fibers and virgin fibers, separately. More than 10 hollow fibers from each batch are cut to a length of 1 cm and mounted side by side to form a module to put on the observation area of the atomic force microscope.

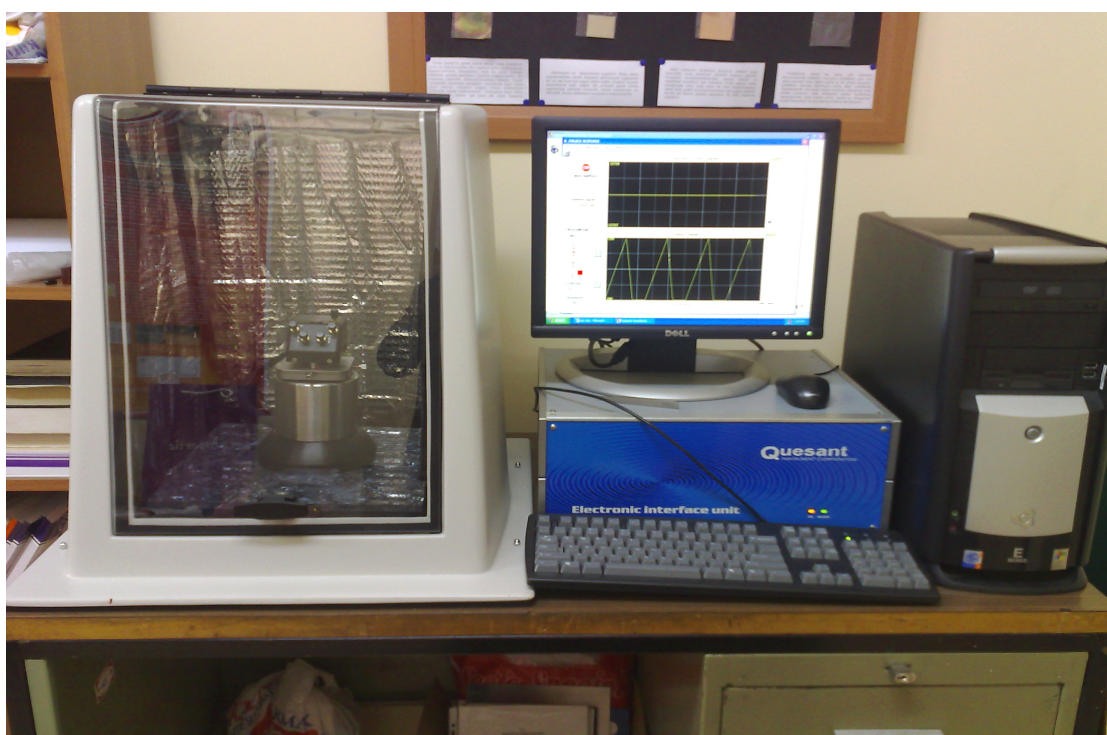


Figure 2.4.2.1 The Q-Scope™ Universal SPM.

2.4.3 Results And Discussions Of AFM Studies

The changes in the membrane surface morphology between virgin and used–processed fibers are determined by the AFM studies. Figure 2.4.3.1 and Figure 2.4.3.2 show the 3D AFM images of the exterior surface of the virgin and used–processed polysulfone hollow fibers.

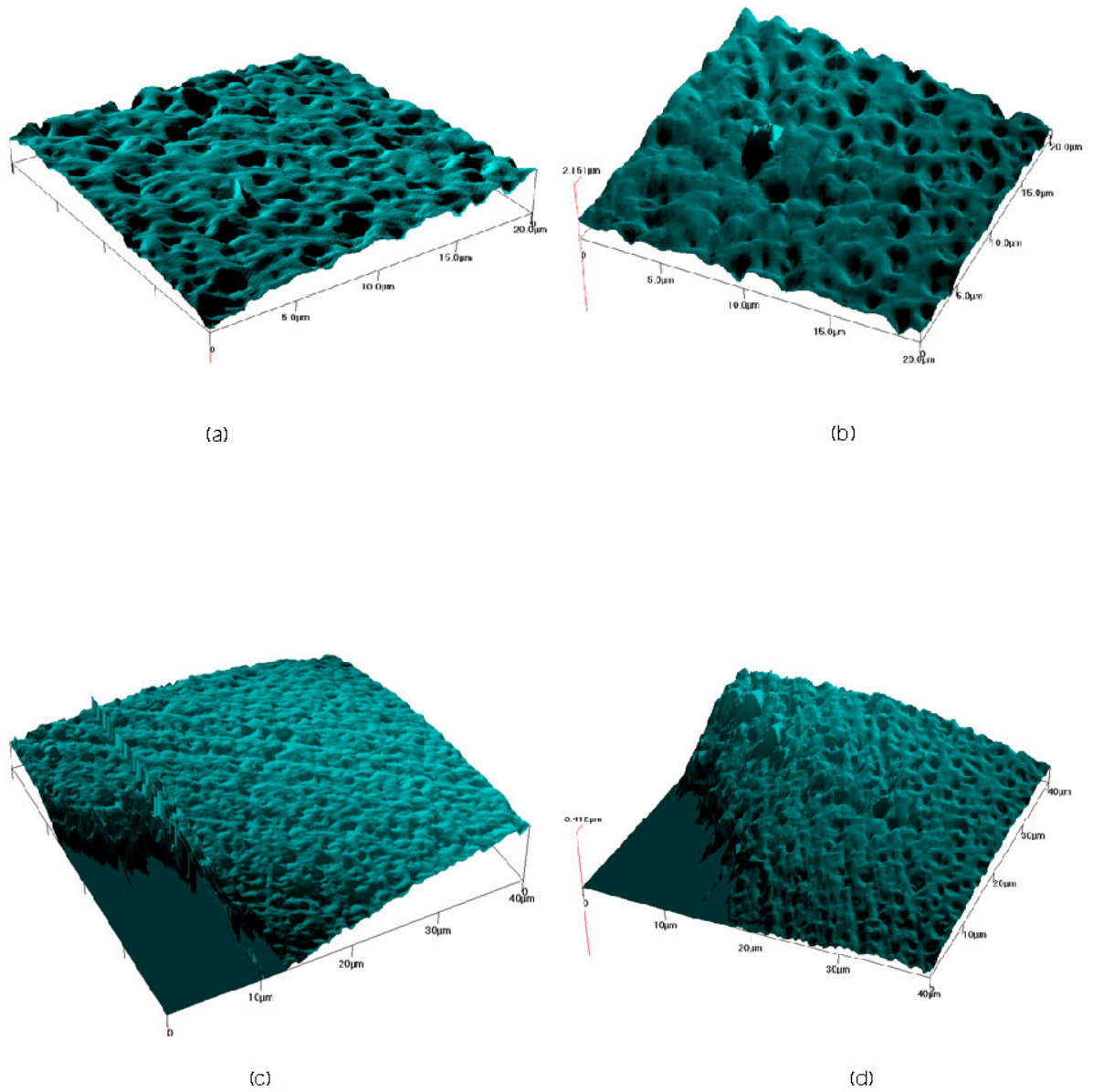


Figure 2.4.3.1 The 3D AFM images of the exterior surface of the virgin and used-processed polysulfone hollow fibers: (a) virgin fiber in the range of 20µm, (b) used-processed fiber in the range of 20µm, (c) virgin fiber in the range of 40µm, (d) used-processed fiber in the range of 40µm.

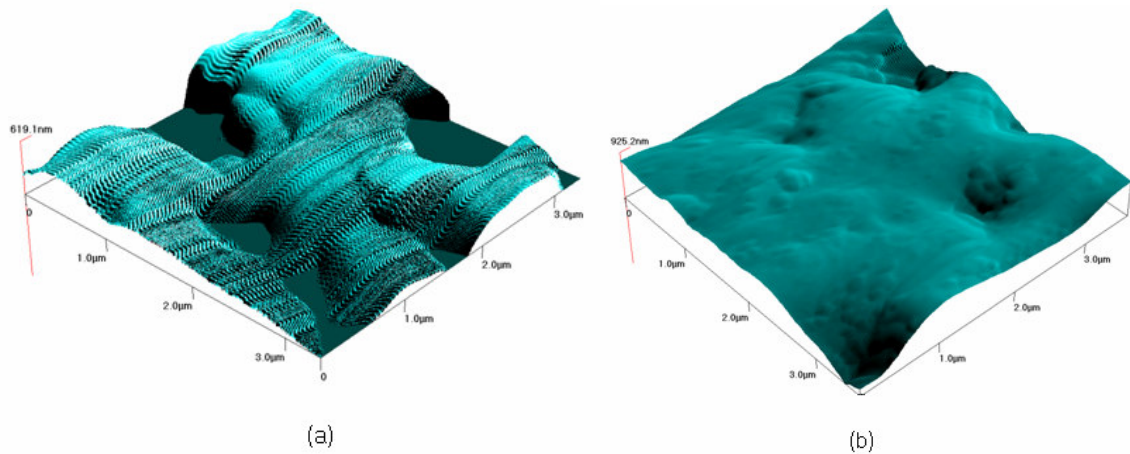


Figure 2.4.3.2 The 3D AFM images of the exterior surface of the virgin and used–processed polysulfone hollow fibers in the range of 3 μm : (a) virgin (height = 619.1 nm), (b) used–processed (height = 925.2 nm).

The dark bands in the Figure 2.4.3.2 (a) might be caused by air currents that results in temperature changes in the PZT (a lead zirconate titanate piezoelectric ceramic) and the metal components of the instrument head. This situation occurs when the acoustic cover and vibration isolator of the AFM is not sufficient. However, the image is not damaged in this case and the pores are seen clearly.

In AFM images shown in Figure 2.4.3.1 and Figure 2.4.3.2, lighter areas represent raised domains, and darker areas represent relatively deep areas of the surface. From Figure 2.4.3.2 (a), the appearance of interconnected cavity channels in the AFM images of virgin polysulfone hollow fiber can be seen obviously. However, this is probably due to the alterations resulting from reprocessing procedure combined with patient contact by means of the decrease in the number of clearly open channels. This result confirms the conclusions from the SEM data.

In order to demonstrate the difference in the degree of roughness, mesh view is applied to the images in the range of 20 μm , which are shown in Figure 2.4.3.1 (a) and (b). The mesh views are given in Figure 2.4.3.3, and the heights of the images are; 1.595 μm for the virgin fiber, 2.151 μm for the used–processed fiber.

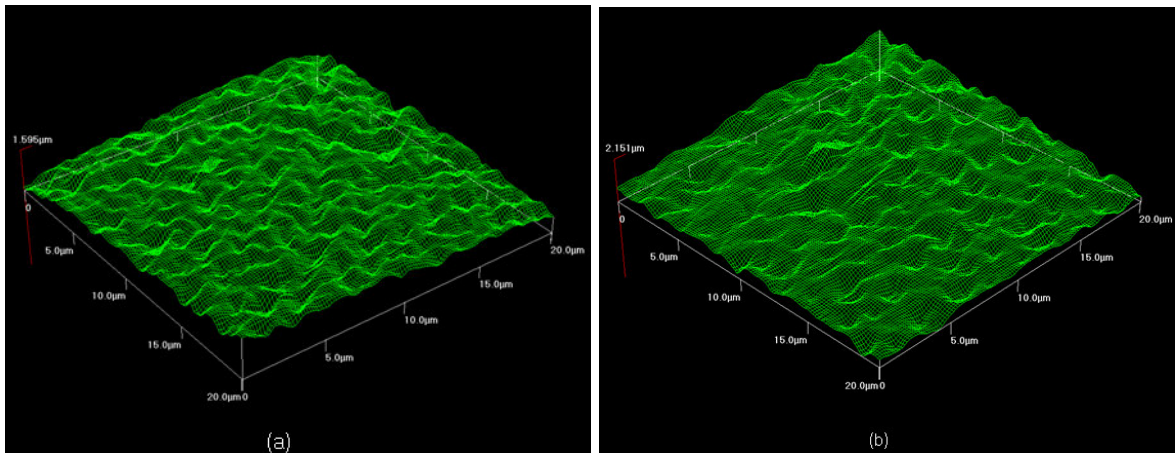


Figure 2.4.3.3 The 3D AFM images of the exterior surface of virgin fiber at a scan size of 20 μm (left), used-processed fiber at a scan size of 20 μm (right).

In addition to three dimensional image analyses, detailed information about the surface roughness of the fibers can be obtained from height histograms. The height histograms of the images shown in Figure 2.4.3.3 is given as follows:

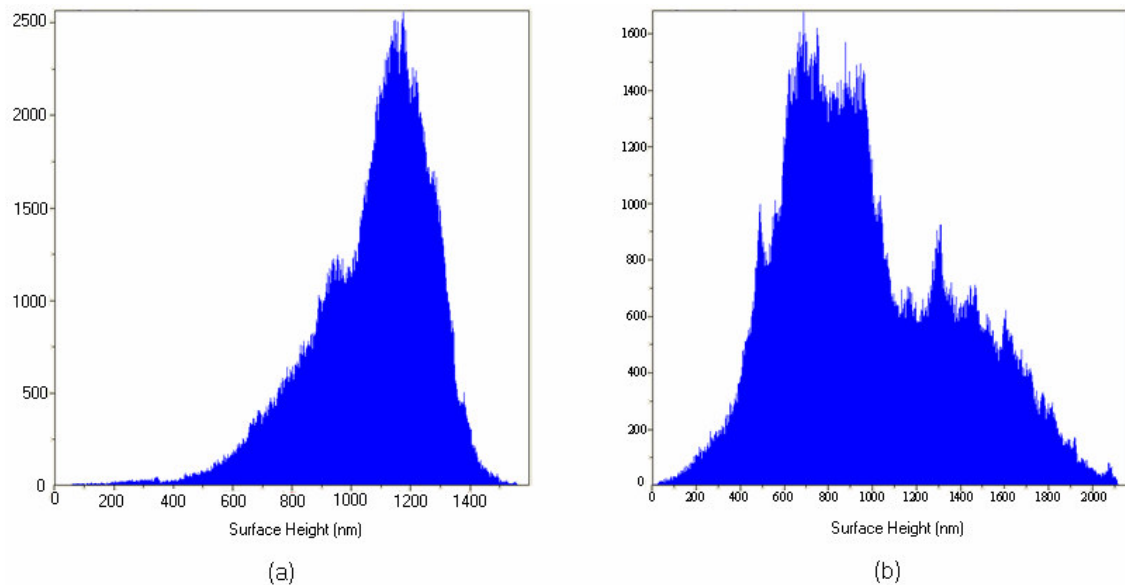


Figure 2.4.3.4 Height histograms of the images of virgin and used-processed hollow fibers (a) virgin, (b) used-processed fiber.

The height histogram of virgin fibers is relatively collective, it give a distinct peak (more uniform) while the height histogram of used-processed fibers depict a more scattered structure. The surface characteristics and the computed roughness parameters of the histograms in Figure 2.4.3.4 are summarized in the Table 2.4.3.1.

Table 2.4.3.1

Surface characteristics and computed roughnesses.

Parameters	Surface of Virgin Fiber	Surface of Used–Processed Fiber
Average Height	1.068 μm	0.975 μm
RMS Deviation	0.204 μm	0.398 μm
Mean Deviation	0.159 μm	0.327 μm
Skewness	– 0.988	0.478
Kurtosis	1.388	– 0.483
Max. Deviation	1.068 μm	1.176 μm
R _p	0.526 μm	1.176 μm
R _t	1.595 μm	2.151 μm
R _v	1.068 μm	0.975 μm
(10 pt. mean) R _z	1.595 μm	2.151 μm

From the Table 2.4.3.1, it is seen that the maximum height of the profile (R_t), the maximum profile peak height (R_p) and the ten point height (R_z) are greater in the surface of the used–processed fiber than in the virgin, while the maximum profile valley depth (R_v) is greater in virgin fiber. The negative skewness in the height histogram of virgin fiber indicates that the holes are dominant on the surface. However, these parameters are not sufficient in determining the difference between roughnesses of these surfaces. Additionally, the root–mean–squared (RMS) roughness, which is the most accurate definition in characterizing the roughness [58], is greater in the surface of used–processed fiber. To conclude, the surface morphology of the polysulfone hemodialyzer fibers become rougher after dialysis and reprocessing procedure.

2.4.4 Conclusions

Atomic force microscopy is an effective tool to investigate the surface structure of membranes and to measure the roughness parameters, which can be used for the comparison of different membrane surfaces [55]. In this study, the microstructure of the both used–processed and virgin polysulfone hemodialyzer fibers was examined in three dimensions and the surface roughness of the fibers is determined with the help of atomic force microscopy.

Cornelius et. al., who studied the morphology of a polysulfone hemodialyzer fiber (Fresenius F80B) before and after the reprocessing procedure, reported that the processing and reuse of dialyzers does alter the membrane surface [32]. In addition, it is known that the membrane post-treatments change the surface roughness. For example, by etching the surface, roughness increases, and by heating, the roughness decreases [55]. Since hemodialyzer fibers function under stress and are exposed to chemical agents during reprocessing, the increase in the surface roughness of used-processed fibers is an expected result.

AFM micrographs confirmed the surface degradation in the polysulfone hemodialyzer fiber after patient contact and disinfection procedure, which is important for the performance, adsorption deterioration and compatibility [59].

2.5 Scanning Electron Microscopy (SEM)

In this study, the mechanically and chemically treated polysulfone hemodialyzer fibers are compared to the virgin fibers, by the use of SEM, which is one of the most widely used techniques in characterization of materials and their structures. SEM and AFM are complementary techniques for surface investigations. Their image formation mechanisms are quite different, resulting in different types of information about the surface structure [46].

It is known that pores play an important role in determining the physical and chemical properties of porous substances and have a deterministic effect on the performance of membranes. Therefore, the microstructure of the membranes is investigated by using both of these techniques, which can provide detailed and magnified images of the fibers from which pore size and its distribution can be determined [56].

2.5.1 Introduction

The original idea of scanning electron microscopy dates back to the 1930's, however, commercial SEM's appeared in 1965, based on the work of C. W. Oatley et al. of Cambridge University [46]. The principle layout of SEM is shown in Figure 2.5.1.1.

In SEM, an electron beam is accelerated by holding the tungsten filament at a large negative potential between 1kV and 50kV and whilst the specimen is grounded. When the electron beam impinges on the material surface, backscattered electrons (BE), secondary electron (SE) and X-rays escape from the material surface. In the display of SEM system, SE is captured by the detector, amplified and displayed for producing the images (SEI) [46, 56]. SEI is the principal imaging mode, providing the best spatial resolution, and deriving contrast mainly from surface topography. Backscattered electron imaging (BEI) is a utility for analyzing material composition, density, and surface geometry [46].

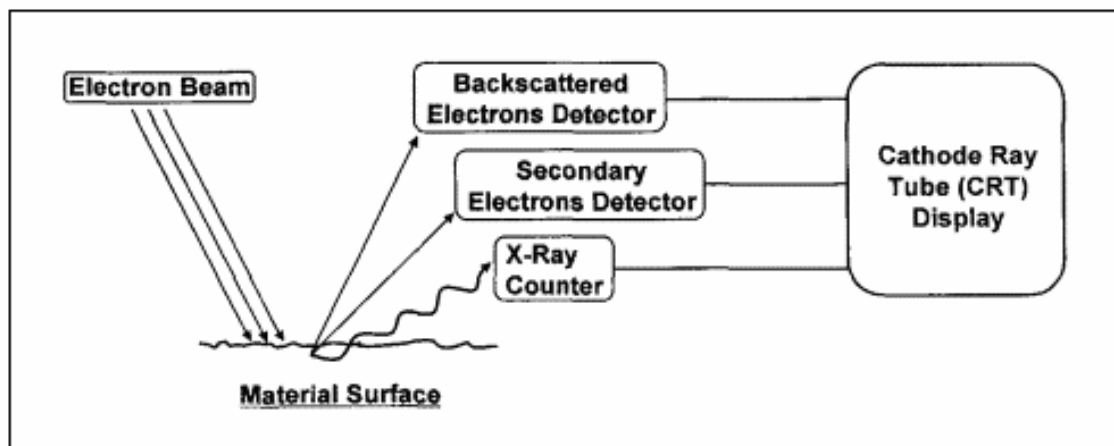


Figure 2.5.1.1 The principle layout of scanning electron microscope (SEM) [56].

In SEM, better visualization of objects such as fibers, fracture surfaces and powder particles is achieved with improved statistical interpretation. Information can be gathered concerning size, shape and texture of many solid specimens [46]. The resolution of the SEM approaches a few nanometers, and the instrument can operate at magnifications that are easily adjusted from 10 to over 300,000× [60].

SEM requires little sample preparation as the information required concerns only the surface structure. Small samples of up to several millimeters and sometimes even larger can be investigated directly in the SEM if the sample material has a sufficiently high electric conductivity to prevent charging produced by electron bombardment. However, SEM observation of nonconductive samples, such as polymers, is not possible without a metallic or carbon conductive layer on their surface. Such a coating avoids build-up of an electric negative charge in the specimen, which would induce “imaging artifacts” [46]. In this study, since polymer fibers require conductive coating, gold was selected as coating material due to its ease to vapor deposit and on bombardment with high energy electrons it gives a high secondary yield. Generally, the thickness of gold coating is around 25 nm [56].

The main advantages of SEM are the high lateral resolution (1–10 nm), large depth of focus (typically 100 μm at 1000 \times) and the numerous types of electron specimen interactions that can be used for imaging or chemical analyses purposes. SEM has the ability to cover a wide magnification range (e. g. 10 \times to 10⁵ \times or higher), so that, an area first observed at a low magnification can be studied at high magnification and resolution [46]. It is a wide applicable non-destructive method with minimal sample requirements.

The principal limitations of SEM are cost and instrumental complexity because a vacuum system is required. Problems in analysis of polymers by SEM are also related to sample preparation, beam penetration effects, charging, beam damage and outgassing of low molecular weight components. Moreover, SEM offers only vague vertical information [46], which makes AFM a necessary complementary method.

There are some previous studies showing the micro morphology of dialyzer fibers. Ronco, C. and his colleagues determined the fine structure of the Helixone membrane [31], which is the membrane type investigated in this study. Instead of standard SEM imaging, field-emission scanning electron microscopy (FE-SEM), which provides higher resolution images, was used. Additionally, the membranes are frosted in liquid nitrogen. Cross-sections of the frosted membranes were prepared by fracturing. Figure 2.5.1.2 depicts the typical structure of the fiber and the most internal skin layer.

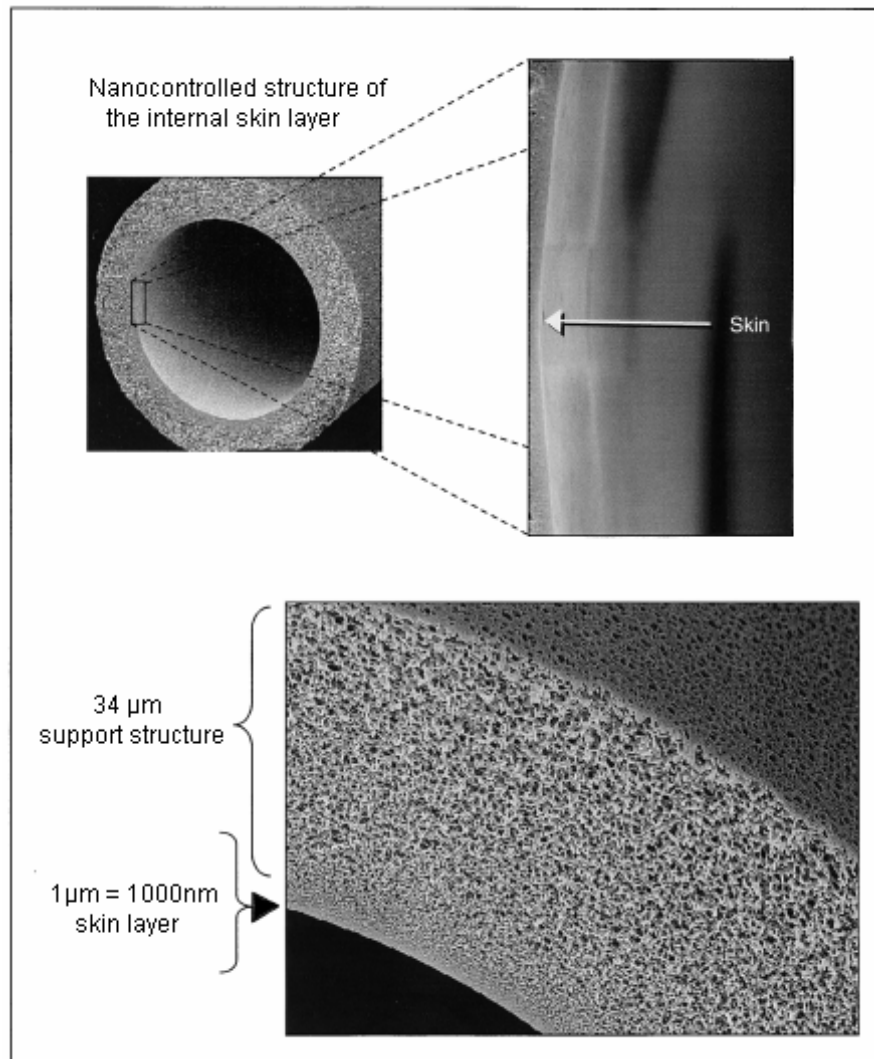


Figure 2.5.1.2 Field-emission scanning electron micrographs of the Helixone hollow fiber with relative dimensional parameters [31].

It is known that, for polymers, good cross-sections can usually be obtained by breaking the specimen at liquid nitrogen temperatures [46], as it is done in the work of Ronco, C. and his colleagues. In laboratory work of this thesis, the fibers were already fractured in the tension tests for the purpose of investigating the mechanical effects. However, only for gathering a general idea about the morphology of the dialyzer fiber, some virgin fibers, without any treatment, were fractured after freezing in liquid nitrogen. Unfortunately, from standard SEM images, it is observed that the fracture surfaces of these fibers adhered during fracturing and the images are not illustrative of the original texture of the fiber, therefore, they are not included.

2.5.2 Materials And Methods

JEOL JSM-6060LV scanning electron microscope was used to study side and fracture surfaces of the fibers at the Material Laboratory of Sakarya University, see Figure 2.5.2.1. To view the surfaces of the virgin and used-reprocessed fiber samples (both mechanically tested and not) in SEM, 0.5 cm lengths of the fibers were fixed to a sample puck using double sided adhesive conductive carbon tapes. The samples were firstly coated with gold by using a Polaron SC7620 SEM sputter coater with CA7625 carbon accessory (Quorum Technologies Ltd.) and a RV3 model vacuum pump (Edwards Ltd.), Figure 2.5.2.2.

The virgin fibers, the fibers tested mechanically (both virgin and used-processed) and the fibers fractured in liquid nitrogen were studied under SEM from 500× up to 20,000× magnification.



Figure 2.5.2.1 JEOL JSM-6060LV scanning electron microscope.



Figure 2.5.2.2 Polaron SC7620 SEM sputter coater with CA7625 carbon accessory.

2.5.3 Results And Discussions Of SEM Studies

Previous studies hypothesized that hemodialyzer reprocessing results in increased pore size and increased potential for loss of proteins, such as albumin [61]. This situation probably results in some complications during hemodialysis, for example, tissue edema. From this point of view, determination of the characteristics of the used–processed hemodialyzer membranes is a very important issue.

Figure 2.5.3.1 shows the scanning electron micrographs of the fracture surfaces of the monotonically or cyclically loaded virgin and used–processed fibers, together.

The blood flow takes place in the lumen of the hollow fibers, where dialysate flows in the outer side. The fracture surface of the monotonically loaded virgin fiber, shown in Figure 2.5.3.1 (a), is not circular and probably occurred because of specimen mounting. However, the fracture surface is not damaged and the effect of monotonic tensile loading can be seen.

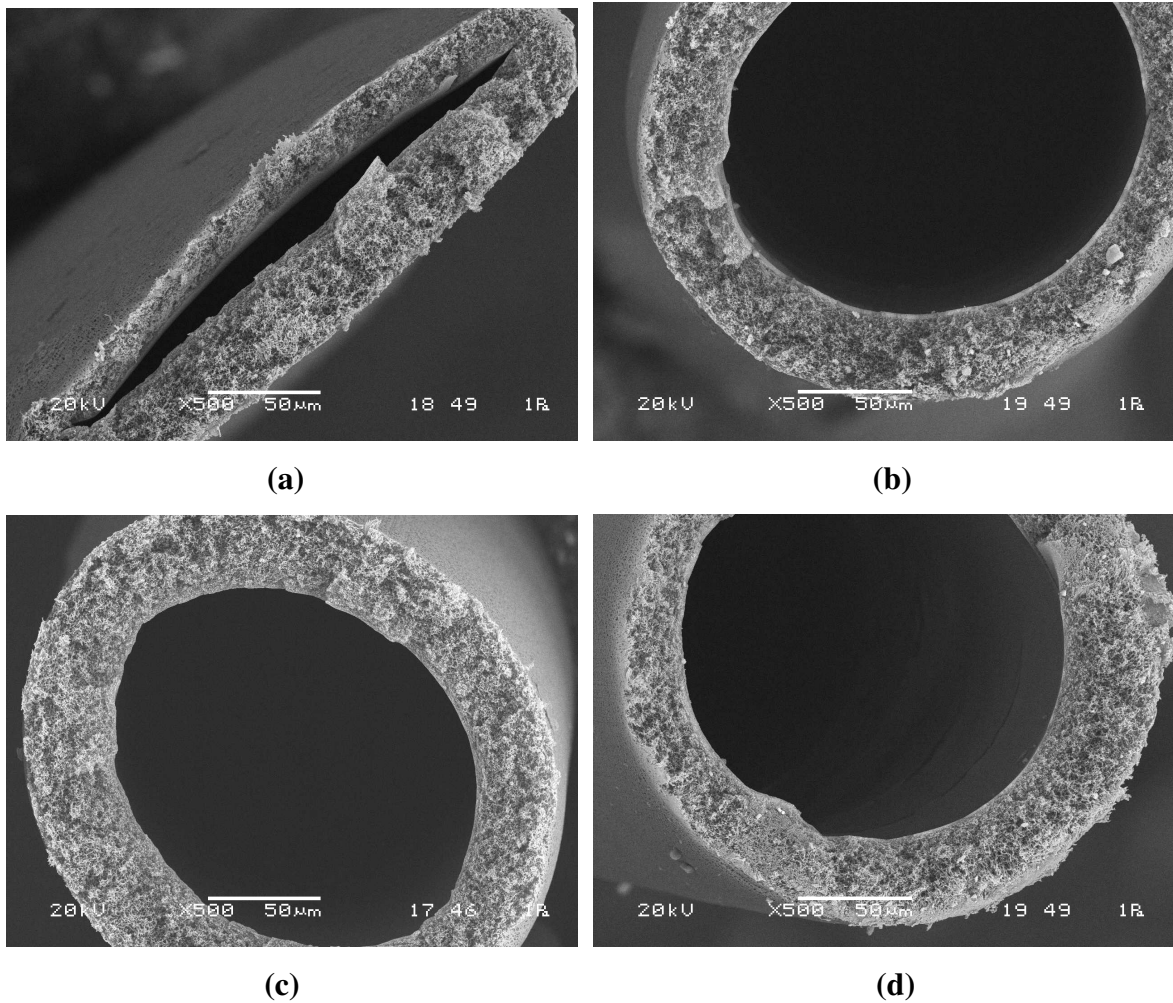


Figure 2.5.3.1 SEM micrographs of the fracture surfaces of: (a) monotonically loaded virgin, (b) monotonically loaded used-processed, (c) cyclically loaded virgin, (d) cyclically loaded used-processed polysulfone hemodialyzer fiber at 500× magnification.

The innermost layers, with increased number of pores, can be seen as grey skins in the walls of the lumen of each membrane. The porosity decreases toward the exterior of the membrane to form a support structure. However, the decrease in the number of pores in these mechanically tested fibers is not only from the original structure. In the original structure, up to a point, the gradual decrease in pore size is a desirable result of ‘nano controlled spinning technology’ applied to these hemodialyzer fibers to achieve reasonable separation properties. On the other hand, from Figure 2.5.1.2 and Figure 2.5.3.2, compared to the initial structure of the fiber (i.e. before mechanical tests and chemical exposure), these fibers have greater pores without uniform gradual increase in size. The darker areas show the merging of pores.

The most damaged fiber is the cyclically loaded used–processed fiber, which is shown in Figure 2.5.3.1 (d). In addition, some ruptures are seen in the lumen perimeter belonging to cyclically loaded used–processed fiber.

The fracture surfaces of surfaces of the monotonically or cyclically loaded virgin and used–processed fibers can be seen at a greater magnification in the Figure 2.5.3.2. The blood sides of the fibers are indicated in images, dialysate flows in the other sides of the walls.

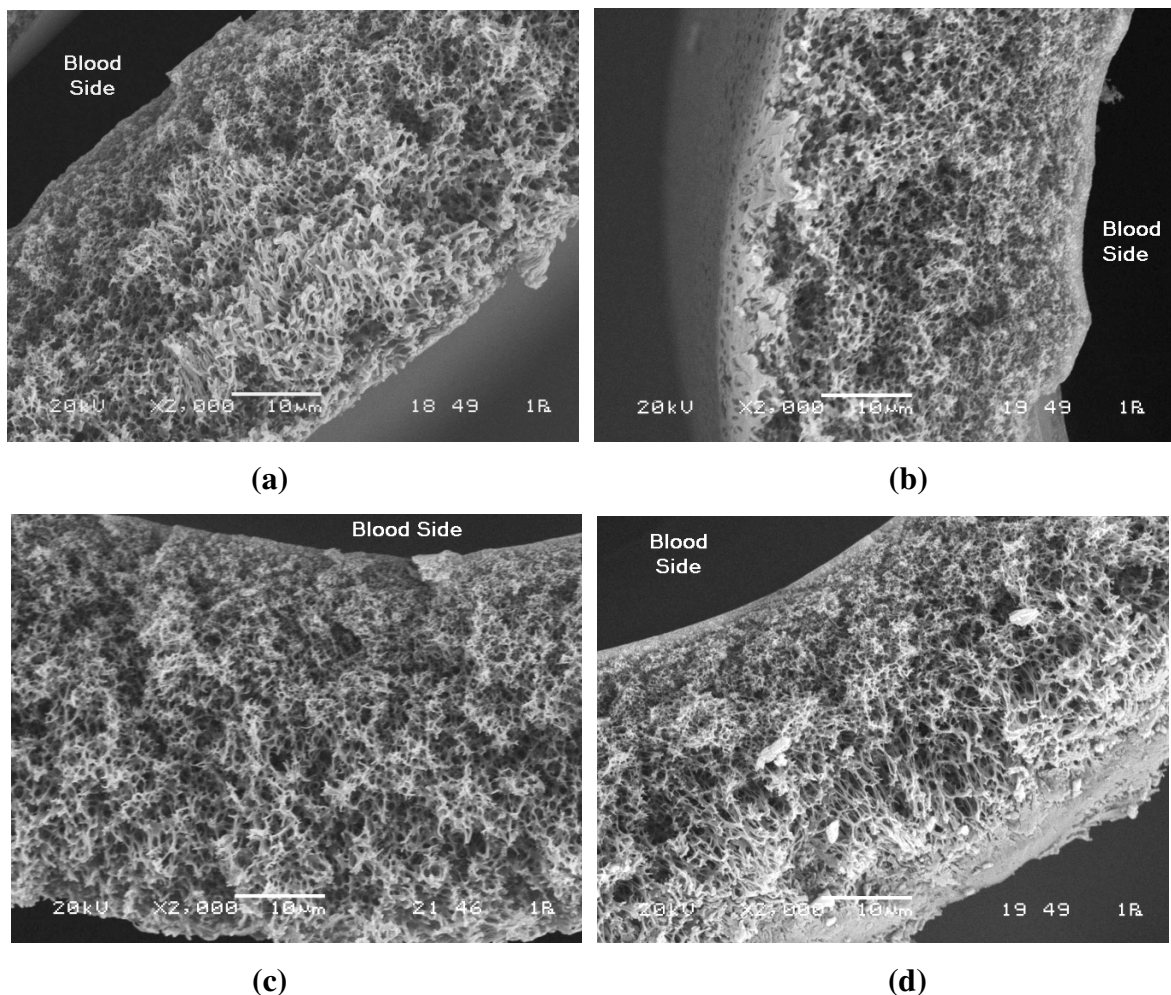


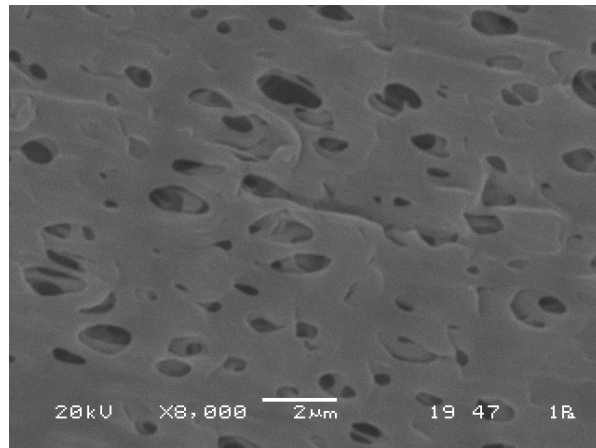
Figure 2.5.3.2 SEM micrographs of the fracture surfaces of: (a) monotonically loaded virgin, (b) monotonically loaded used–processed, (c) cyclically loaded virgin, (d) cyclically loaded used–processed polysulfone hemodialyzer fiber at 2000× magnification.

The two dimensional SEM micrographs do not give illustrative information about depth as much as AFM. However, it is clearly seen that the ruptures are concentrated on the outermost side because of the greater pore size. The virgin fibers demonstrate the pure mechanical effects while the used–processed fibers demonstrate both of the chemical and mechanical effects of the dialysis.

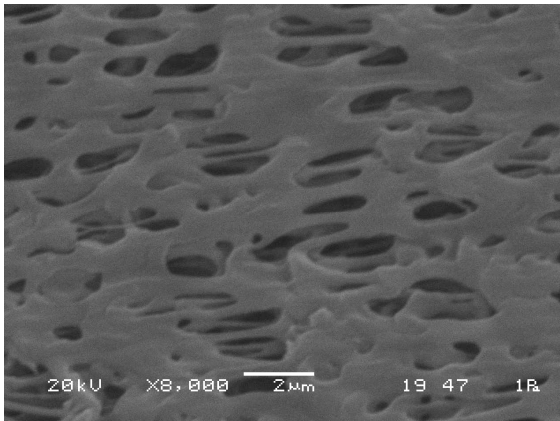
For used–processed fibers in Figure 2.5.3.2 (b) and (d), the ruptures look like as if they are deeper compared to the virgins; (a) and (c), regardless of which tensile test is applied. In the cross–section of the cyclically loaded virgin polysulfone hemodialyzer fiber, shown in (c), textural distribution is more regular compared to the cyclically loaded used–processed fiber, shown in (d).

Figure 2.5.3.3 shows the lateral SEM micrographs of the outer surfaces of the virgin, monotonically loaded virgin, monotonically loaded used–processed, cyclically loaded virgin, and cyclically loaded used–processed polysulfone hemodialyzer fiber at 2000× magnification, respectively.

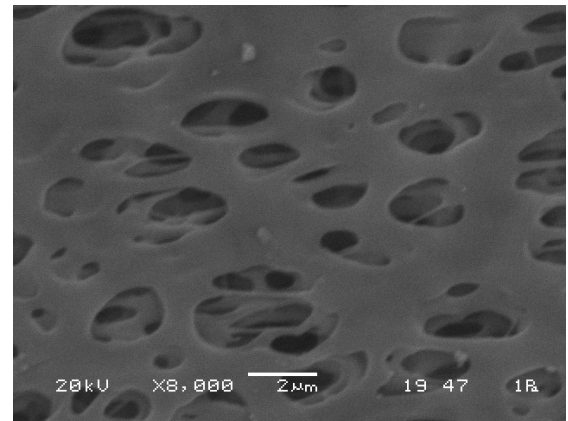
It is seen that the pore sizes in the dialysate surfaces of the polysulfone hemodialyzer fibers increases with mechanical effects and/or reprocessing. In figure 2.5.3.3 (b) and (c), the virgin membranes with pure mechanical effects are shown. In addition to increase in pore size, because of the monotonic and cyclic loading, the pores lose their circular shape, and become more elliptic. This kind of strain induced morphological change in the polysulfone fibers can be followed by merging of pores and possibly decreases the performance of the hemodialyzer.



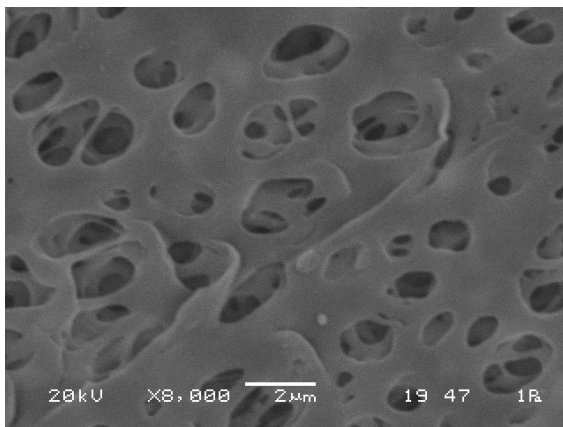
(a)



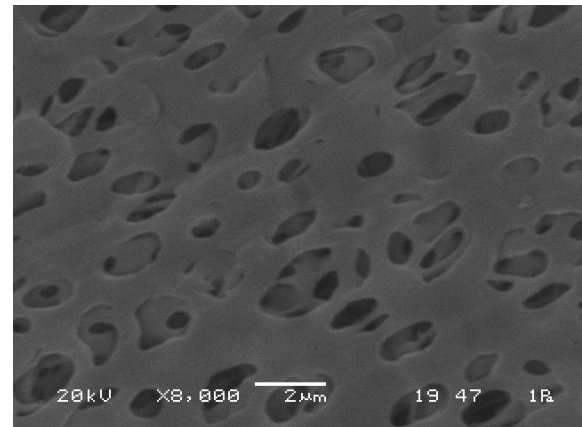
(b)



(c)



(d)



(e)

Figure 2.5.3.3 SEM micrographs of the lateral outer surfaces of: (a) virgin, (b) monotonically loaded virgin, (c) cyclically loaded virgin, (d) monotonically loaded used-processed, (e) cyclically loaded used-processed polysulfone hemodialyzer fiber at 2000× magnification.

Figure 2.5.3.3 (d) and (e) shows the hemodialyzer hollow fibers with blood and formaldehyde/bleach exposure also with mechanical effects. Compared to its initial structure, the changes in the used–processed fibers can be listed as; increase in pore size, merging of pores, formation of ligaments and hindered passages. Figure 2.5.3.4 and Figure 2.5.3.5, from the lateral view of outer side nearer to fracture surface, can better show the morphological difference in monotonically loaded used–processed and virgin fibers.

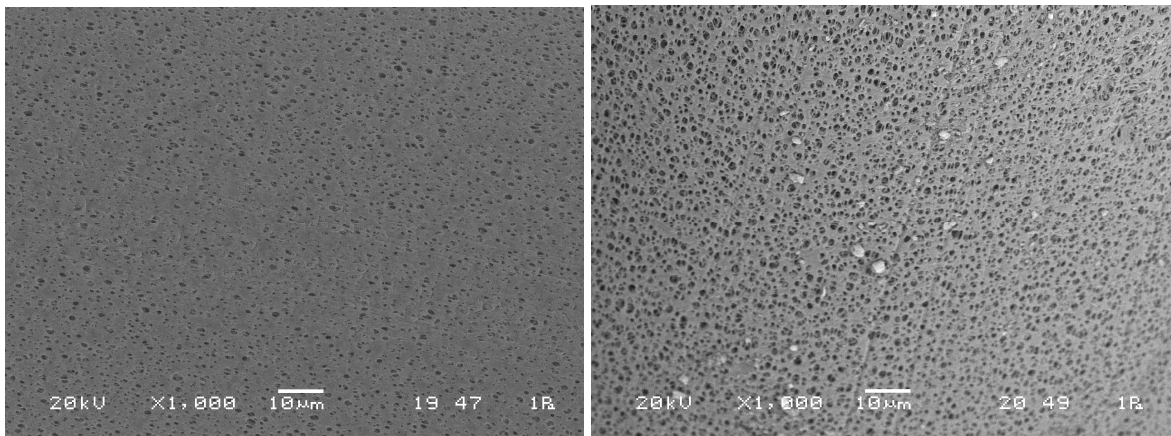


Figure 2.5.3.4 SEM micrographs of the lateral outer surfaces of the (untreated) virgin (left) and monotonically loaded used–processed (right) polysulfone hemodialyzer fiber at 1000× magnification.

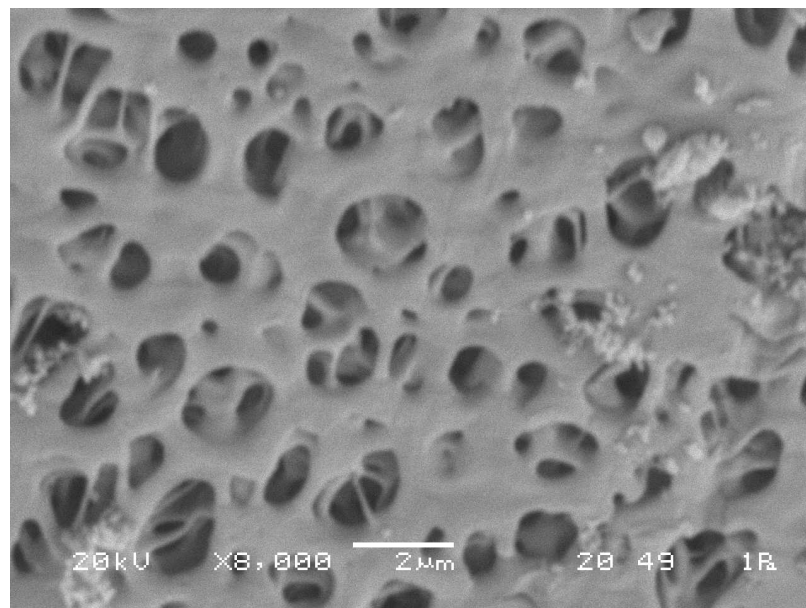


Figure 2.5.3.5 SEM micrograph of the lateral outer surface of monotonically loaded used–processed polysulfone hemodialyzer fiber at 8000× magnification.

Similarly, Figure 2.5.3.6 show the morphological difference in cyclically loaded used–processed and virgin fibers. Figure 2.5.3.7 depicts the lateral outer surface of cyclically loaded used–processed polysulfone hemodialyzer fiber near fracture at 8000× magnification. In addition, although all used–processed fibers were rinsed with ultra–pure water after reprocessing procedure, their SEM images include some residual materials on the surfaces.

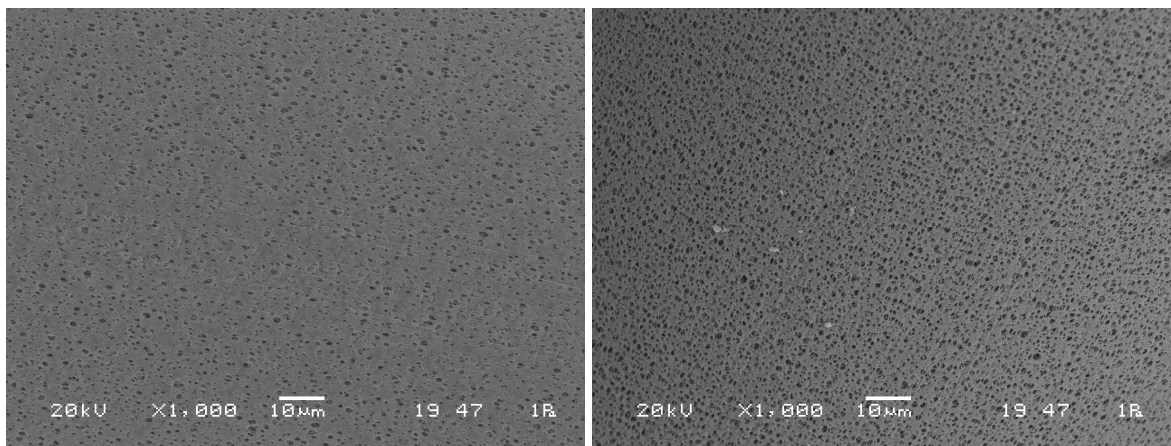


Figure 2.5.3.6 SEM micrographs of the lateral outer surfaces of the (untreated) virgin, cyclically loaded used–processed polysulfone hemodialyzer fiber at 1000× magnification.

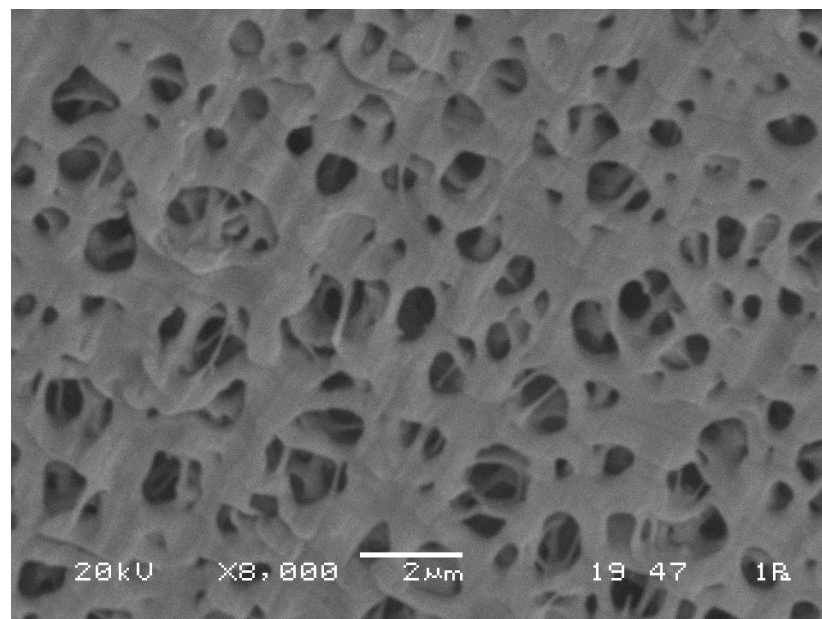


Figure 2.5.3.7 SEM micrograph of the lateral outer surface of cyclically loaded used–processed polysulfone hemodialyzer fiber at 8000× magnification.

2.5.4 Conclusions

In this study, the polysulfone hemodialyzer fibers are investigated by the use of SEM before and after the reprocessing. The microstructures of the fracture and outer surfaces of the fibers are determined by means of change in pore size and pore geometry, existence of pore merging or ruptures and hindrance of passages.

The blood and dialysate flow, the changes in the flow rates, and accordingly the alternation in pressure are the stress factors in dialysis, which may affect the performance of the dialyzer for reuse applications. Additionally, during hemodialysis, blood proteins coat the inner lumen of hemodialyzer fibers and reduce the effective membrane pore size and resultant ultrafiltration [61]. In reuse applications, in order to prevent the reduction in ultrafiltration, adequate removal of coagulants must be achieved during disinfection process. Previously, chlorine-based solutions have been shown to be effective at removing blood proteins from hemodialyzer membranes [61]. However, bleach solutions play a significant role on the membrane porous structure as on its transport properties which can also affect performance of the membrane [54]. This study investigates the effect of disinfection agents together with mechanical effects in order to mimic the environment in which dialysis fibers encountered during reuse procedures.

Wolff and Zydney, who studied the effect of bleach on the transport characteristics of a polysulfone hemodialyzer (F80B), underlined, without knowing its origin, the fact that bleach causes significant changes in the membrane properties [62]. Similarly, Cheung et al, measured β_2 -microglobulin clearance of reprocessed Fresenius F80B polysulfone membranes and hypothesized that reuse with bleach increases the pore size of the membrane. However, continuous increases in pore size may pose a health risk to the patient if significant amounts of albumin are lost and/or the integrity of the hemodialyzer fibers is altered [61].

In this study, the cross-sectional microscopic view of polysulfone membrane showed that the fiber is constituted of a very thin internal skin and an external surrounding support structure with relatively increased pore size. The fracture surfaces of

monotonically or cyclically loaded virgin and used–processed fibers showed that the mechanical and chemical exposure causes non–uniform increasing in pore size towards the outside of the fiber because of merging. The most damaged fiber is the cyclically loaded used–processed fiber with some ruptures in the lumen perimeter.

It can be said that there is an increase in pore size in the outer surfaces of the mechanically and/or chemically affected fibers, compared to the virgin. Although greater pore size seems to be beneficial by means of transportation of larger molecules, it can be accompanied by albumin loss if the pore size exceeds the desired dimension. In addition, it is observed that stress causes the pores to lose their circular shape and become more elliptic. The formation of stress concentrated tips along the axis of elliptic pores is the preliminary stage of pore merging. Accordingly, ruptures may probably occur after increased number of reprocessing.

In addition, although the used fibers are rinsed with ultra–pure water before and after reprocessing procedure, the SEM images of all used–processed fibers include some residual materials on the surfaces. Therefore, the manual application of disinfecting agents is not recommended.

In conclusion, SEM micrographs showed that, compared to its initial structure, the used–processed fibers have increased pore size on the outer surface, however some passages seem to be hindered.

2.6 X– Ray Diffractometry (XRD)

The crystallographic structure of virgin and used–processed polysulfone hemodialyzers were studied by X–ray diffraction (XRD) method, which is a primary technique to determine the degree of crystallinity in polymers. Through this analysis it is possible to detect the structural modification caused by the patient contact and reprocessing procedure on polysulfone hemodialyzer.

2.6.1 Introduction

Crystallinity is one of the most important parameters of polymer structure, which is defined as the ratio of the mass of crystalline phase to the total mass of the polymer. The physical and mechanical properties of polymers are profoundly dependent on the crystallinity and XRD method has been elaborated to determine this parameter [63].

The most common arrangement of XRD apparatus is illustrated in Figure 2.6.1.1. The surface of sample is mounted to the stage with parallel [56]. A collimated beam of X-rays, is incident on a specimen and is diffracted by the crystalline phases in the specimen according to Bragg's law:

$$n\lambda = 2d \sin \theta \quad (2.6.1.1)$$

where d is the spacing between adjacent lattices in the crystalline phase and λ is the X-ray wavelength.

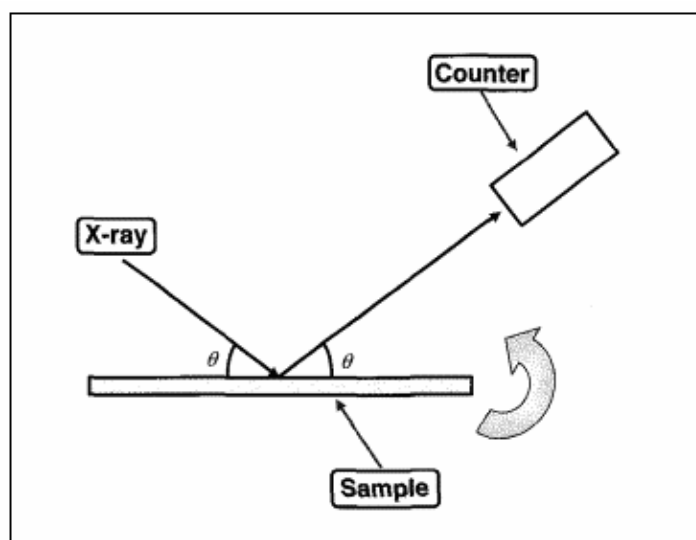


Figure 2.6.1.1 The principle of X-ray diffraction [56].

The signal coming from the counter is amplified and displayed on a meter and provide a continuous trace of intensity versus 2θ [56]. This diffraction pattern is used to identify crystallinity and the specimen's crystalline phases [60].

Since polymers may possess range order in some regions of the solid, with chains line up regular array, it can be said that the extent of such ordering is indicated by the degree of crystallinity of the polymer and the crystallinity of a polymer can frequently be changed by mechanical stretching [64]. Therefore, in the aggressive environment that arises during dialysis, the degree of crystallinity of the polymer may change under stress and that results in changes of mechanical properties.

In general, the scattering pattern of amorphous materials display broad, low intensity peaks characteristic of the average local atomic environment. As the crystal size gets smaller, diffraction peaks in the intensity versus 2θ curve get broader [36]. Conversely, if the crystalline portion increases, the peaks become narrower and extent to higher intensities. The areas under the crystalline and amorphous peaks are proportional to their volume fraction in the sample [65].

2.6.2 Materials And Methods

The XRD studies were performed at Materials Laboratories of Gebze Institute of Technology. The experiment was run with Rigaku D–Max 2200 X–ray diffractometer (Figure 2.6.2.1) with Cu K–alpha 1 radiation. The mechanically tested virgin and used–processed hollow fibers were placed into the sample holder and the specimen plane was adjusted with the goniometer.

The intensity (count per second) versus diffraction angle 2θ (degrees) were recorded by the PC connected to XRD. The diffractometer was running at 40 kV and 40 mA. The data were smoothed with a 33–pt parabolic filter. The wavelength of the characteristic X–rays of Cu to compute d–spacing was 1.54059 Å. The scanning speed and the width of the step of sampling kept constant in each scanning.



Figure 2.6.2.1 Rigaku D-Max 2200 X-ray diffractometer.

2.6.3 Results And Discussions Of XRD Studies

The effect of dialysis and reuse procedure on polysulfone hemodialyzers was studied by microstructure analysis of fibers with XRD. The X-ray diffraction pattern of virgin polysulfone hemodialyzer, which is in its original state, is given as Intensity (counts per second) versus 2θ (degrees) in all figures in order to observe the effects of mechanical tests and reuse applications.

X-ray diffraction pattern of virgin polysulfone hemodialyzer fiber on which monotonic tensile loading is applied together with the diffraction pattern of virgin (untreated) fiber is given in Figure 2.6.3.1.

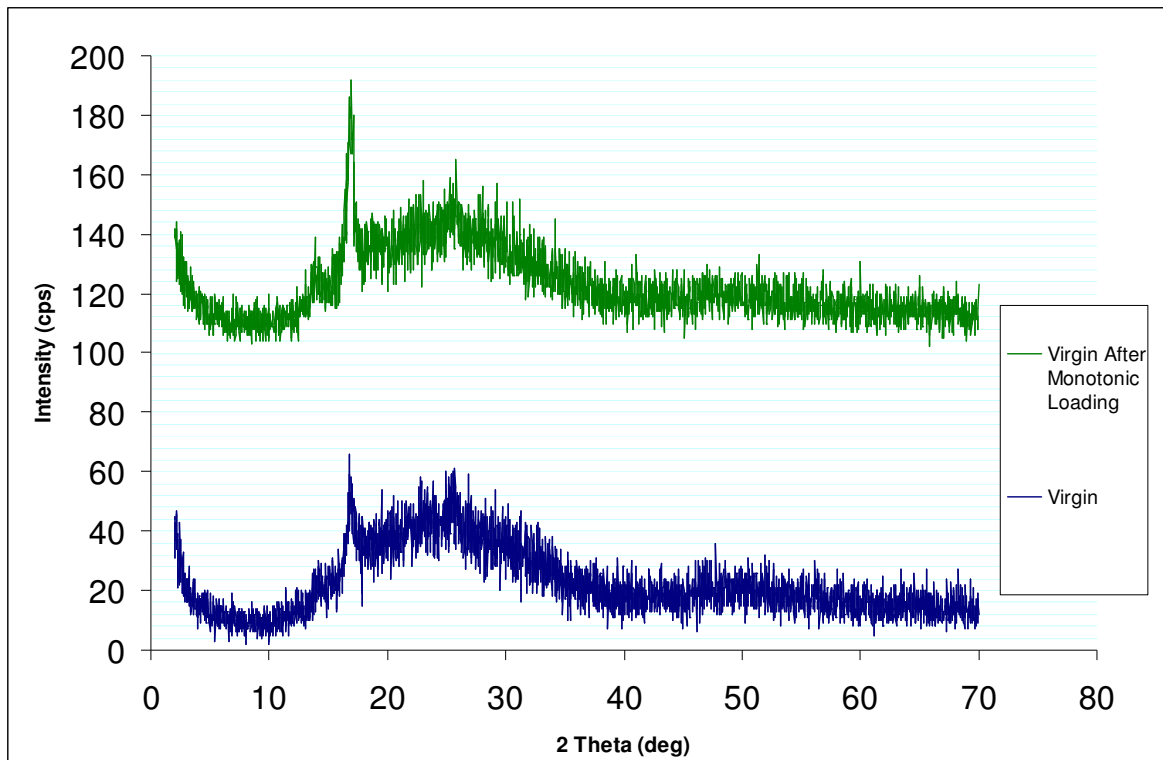


Figure 2.6.3.1 X-ray diffraction patterns of virgin polysulfone hemodialyzer fibers (upper belongs to the fiber on which monotonic tensile loading is applied).

X-ray diffraction pattern of virgin polysulfone hemodialyzer fiber is in the typical trend of a partially crystalline polymer with a main peak at 2θ of 16.8 degrees and intensity of 65 cps. Figure 2.6.3.1, shows the increase in the contribution of crystalline part of the virgin fiber after monotonic loading. As evidence, the main peak at 2θ of 16.8 has a height of 86cps. In other words, main peak height in the diffraction pattern of monotonically loaded virgin fiber is greater than in untreated virgin fiber. Additionally, another distinct peak is seen at 2θ of 14.1, which is broader in the diffraction pattern of untreated virgin fiber.

X-ray diffraction pattern of used-processed polysulfone hemodialyzer fiber on which monotonic tensile loading is applied together with the diffraction pattern of virgin (untreated) fiber is given in Figure 2.6.3.2.

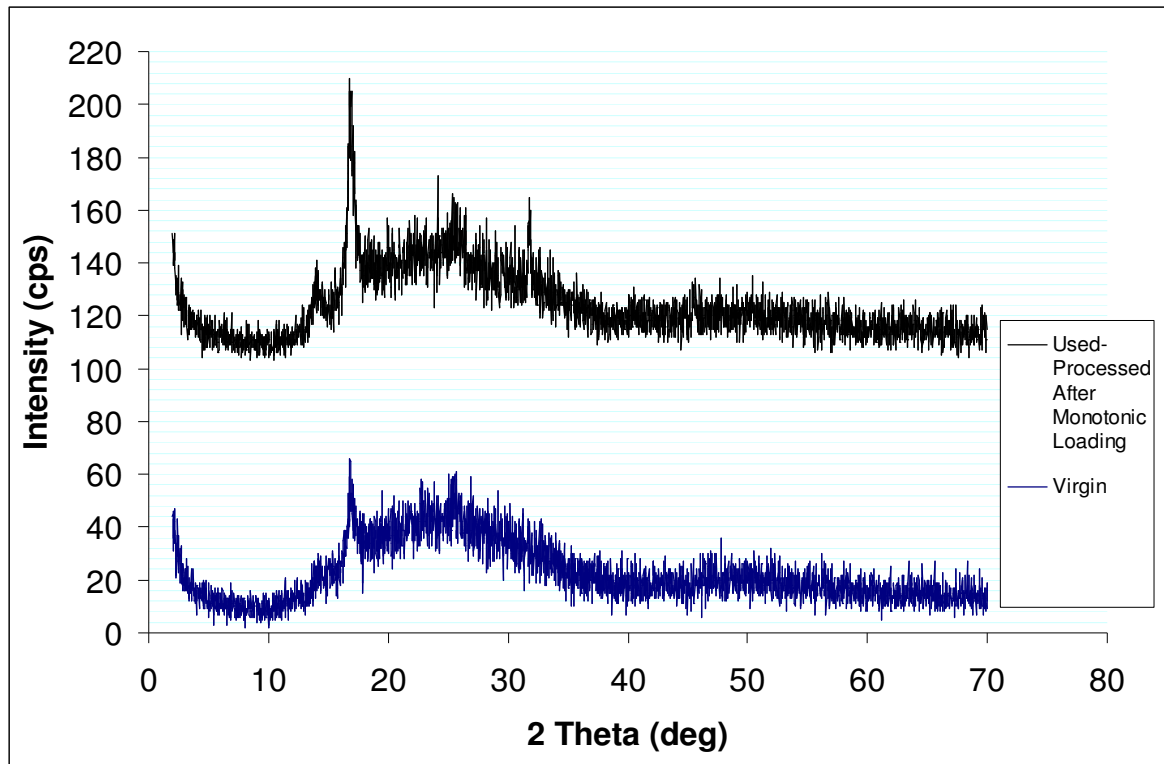


Figure 2.6.3.2 X-ray diffraction patterns of used-processed polysulfone hemodialyzer fiber on which monotonic tensile loading is applied (upper) and untreated virgin membrane (lower).

The crystallinity pattern of monotonically loaded used-processed hemodialyzer fiber has a main peak at 2θ of 16.8 with a height of 110 cps. When compared to virgin fiber, addition of a new peak is clearly seen at 2θ of 31.8. The peak at 2θ of 14.1 becomes more obvious, because its intensity is 21cps in the pattern of virgin fiber while it is 41cps in the pattern of monotonically loaded used-processed fiber. Therefore, compared to the virgin, the monotonically loaded used-processed fiber becomes apparently more crystalline.

In order to see the crystallinity difference, the X-ray diffractograms of used-processed polysulfone hemodialyzer fiber after monotonic loading, virgin fiber after monotonic loading, and virgin fiber without any application is given together in Figure 2.6.3.3.

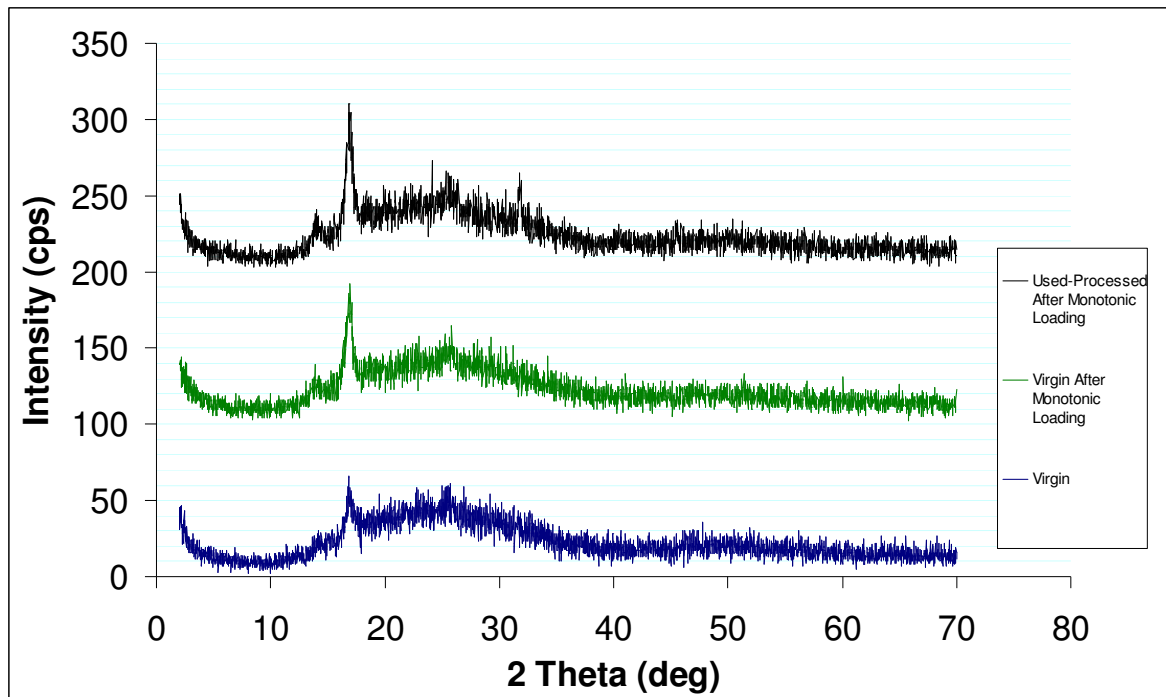


Figure 2.6.3.3 The X-ray diffractograms of used–processed polysulfone hemodialyzer fiber after monotonic loading (upper), virgin polysulfone hemodialyzer fiber after monotonic loading (middle), and virgin polysulfone hemodialyzer fiber without any application (lower).

From Figure 2.6.3.3, it is obvious that the diffractogram of used–processed hemodialyzer fiber after monotonic loading gives the highest intensity peaks. At the same time, it has additional crystalline peaks. The intensity values of the peaks belong to the diffraction patterns of virgin, monotonically loaded virgin and monotonically loaded used–processed fibers are summarized in Table 2.6.3.1.

Table 2.6.3.1

The intensity values of the main peaks of the diffractograms of given membranes.

Membrane Type		Peaks		
		$2\theta = 14.1$ (deg)	$2\theta = 16.8$ (deg)	$2\theta = 31.8$ (deg)
Virgin Polysulfone Hemodialyzer	Peak Height (cps)	21	65	No peak
Virgin Polysulfone Hemodialyzer After Monotonic Loading		29	86	No peak
Used–processed Polysulfone Hemodialyzer After Monotonic Loading		41	110	65

To conclude, both monotonic loading and disinfection process together with patient contact increases the contribution of the crystalline portion to the structure of polysulfone hemodialyzer fiber.

For the cyclically loaded virgin and used–processed polysulfone hemodialyzer fibers, the change in the internal structure is different. X–ray diffraction pattern of virgin polysulfone hemodialyzer fiber on which cyclic tensile loading is applied together with the diffraction pattern of virgin (untreated) fiber is given in Figure 2.6.3.4.

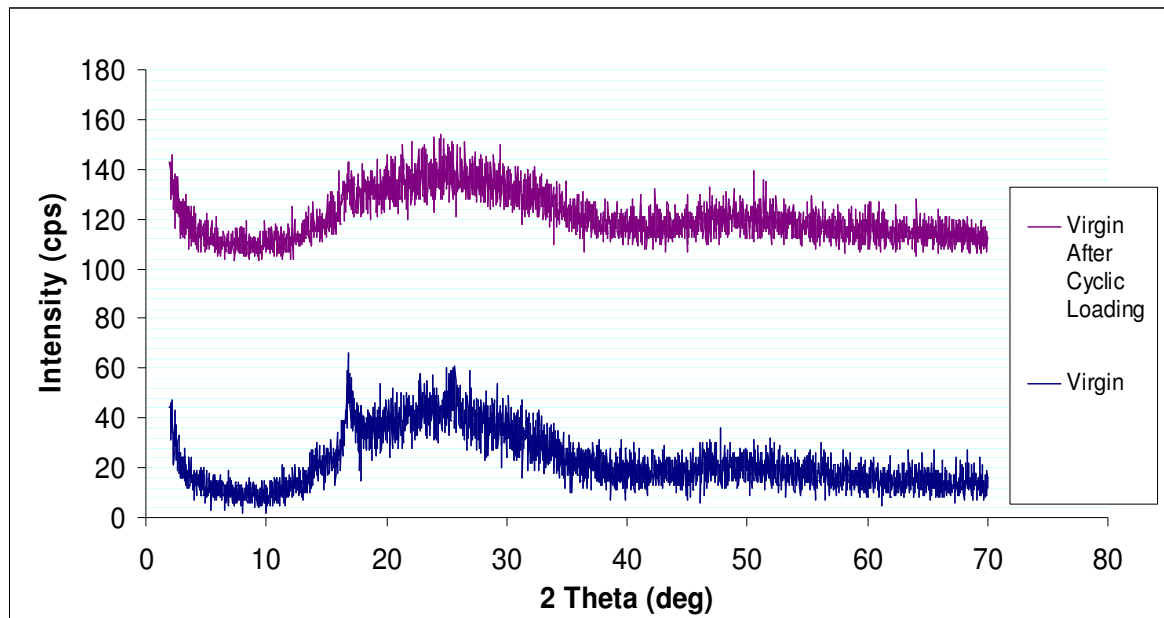


Figure 2.6.3.4 The X–ray diffractograms of virgin polysulfone hemodialyzer fiber after cyclic loading (upper), and virgin polysulfone hemodialyzer fiber without any application (lower).

X–ray diffraction pattern of used–processed polysulfone hemodialyzer fiber on which cyclic tensile loading is applied together with the diffraction pattern of virgin (untreated) fiber is given in Figure 2.6.3.5.

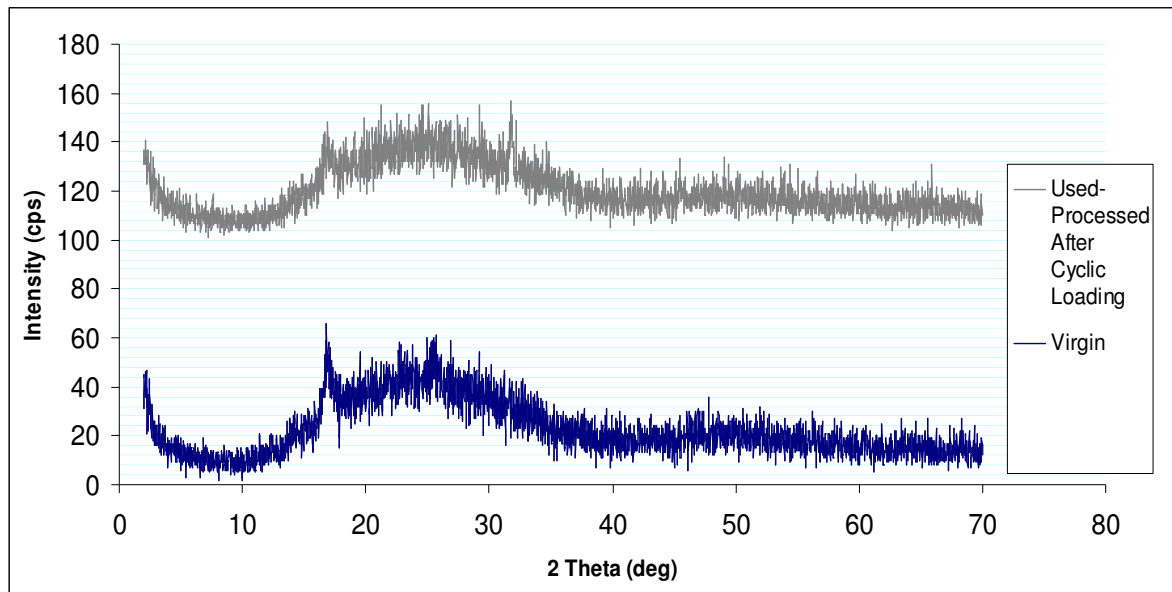


Figure 2.6.3.5 The X-ray diffractograms of used-processed polysulfone hemodialyzer fiber after cyclic loading (upper), and virgin polysulfone hemodialyzer fiber without any application (lower).

From Figure 2.6.3.4, it is seen that the X-ray diffractogram of cyclically loaded virgin polysulfone hemodialyzer fiber is broader than the diffractogram of untreated virgin fiber. The main peak gets smaller, that is, the fiber probably becomes more amorphous after cyclic loading. To remind, the cycles of the tensile test was remained in the elastic range and the material did not deform plastically, i.e. permanent deformation was not allowed in the bulk of the material.

Similarly, the X-ray diffractogram of cyclically loaded used-processed polysulfone hemodialyzer fiber is broader than the diffractogram of untreated virgin fiber, as seen in Figure 2.6.3.5. It has only two distinct peaks at 2θ of 16.8 and 31.8 cps.

The difference between the X-ray diffractograms of cyclically loaded virgin and used-processed polysulfone hemodialyzer fibers is seen in Figure 2.6.3.6.

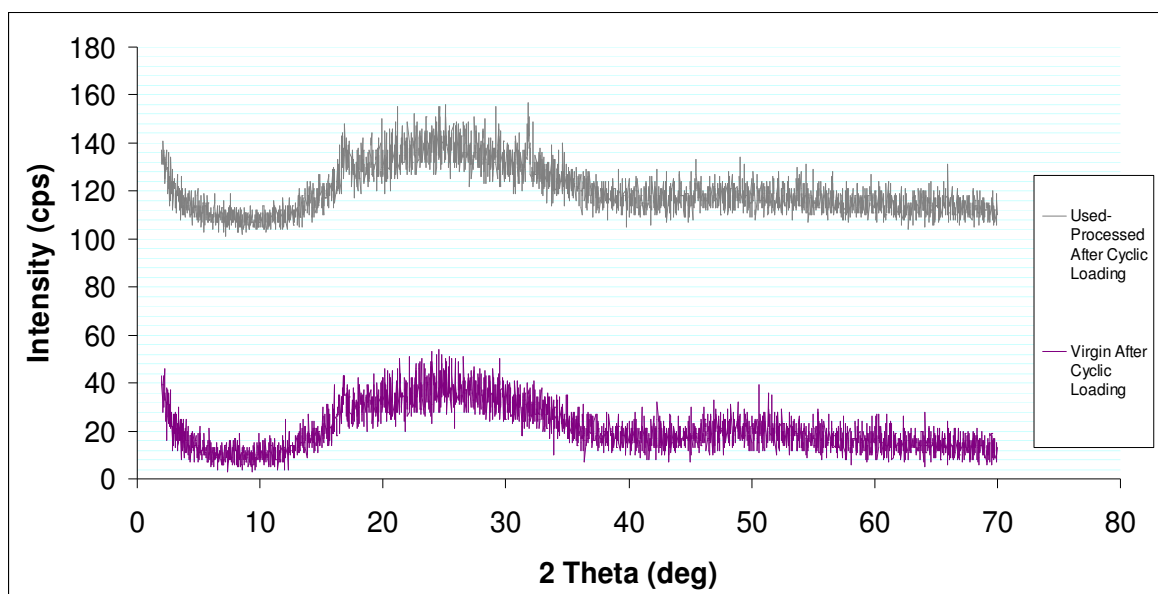


Figure 2.6.3.6 The X-ray diffractograms of cyclically loaded polysulfone hemodialyzer fibers; used-processed fiber (upper) and virgin (lower).

It is remarkable that cyclically loaded used-processed has greater contribution of crystalline portion in its structure compared to the cyclically loaded virgin polysulfone hemodialyzer fiber. In this sense, the effect of chemical environment in disinfection process and dialysis, together with the effect of cyclic tensile loading on polysulfone hemodialyzer fiber is seen.

2.6.4 Conclusions

For materials that are partially crystalline, e.g. polysulfone hemodialyzer fibers, the amorphous and crystalline contributions to the X-ray diffraction can be interpreted to determine the degree of crystallinity. The sharpening of the distinct peaks or addition of new peaks to the X-ray diffractograms is associated with the increase in the amount of crystal structure in the membrane. In general, the scattering pattern of amorphous materials shows broad and low intensity peak characteristics.

Dialyzer membranes function under pressure, which results in exertion of tensile, compressive and torsional forces to the fibers [59]. In general, when a polymer is stretched,

the degree of crystallinity increases. Therefore, it is expected that usage of a hemodialyzer by itself (only patient contact) would affect the molecular orientation of the fiber towards crystallization. However, before being used again, the hemodialyzers are needed to be sterilized and the change in crystal structure must be discussed by means of both usage and reprocessing procedures. However, systematic studies on the crystallization behavior and mechanical fracture characteristics of dialyzer fibers and the interrelationships between them are in its early stages.

The studies of Konduk, B.A. showed that, after a dialysis session, hemophan, cupropan and cellulose acetate type hemodialyzer fibers undergo polymorphic changes resulting in an increase in the amount of crystallinity. However, compared to these dialyzers the effect of dialysis on polysulfone membrane is very small [59]. In this study, some morphological changes between virgin and used-processed fibers, on which different tensile tests are applied, are verified. This suggests that structure of polysulfone hemodialyzer fibers undergoes reorganization under stress.

In this study, each spectrum of polysulfone fibers shows typical broadband of amorphous polymer with some peaks of crystallinity. From these diffractograms, it is concluded that both monotonic loading and disinfection process together with patient contact increases the contribution of the crystalline portion to the structure of polysulfone hemodialyzer fiber.

Although, the cyclically loaded used-processed fiber is more crystalline than cyclically loaded virgin fiber, both of them is more amorphous compared to untreated virgin fiber or other types, interestingly. This is important for understanding the effect of cyclic loading on the fibers. The fact that cyclic loading was applied in the elastic margin without permanently deforming the fiber must not be ignored. In addition, from SEM studies it is known that the route of pores converted from circular to elliptical and there must be high amount of plastic deformation in the axes of ellipses. However, the X-ray diffraction method investigates the structure of bulk and therefore these plastically deformed areas might have been undetected. Further studies covering plastic range cyclic loading and several reuses will be beneficial to understand the behavior of porous polymeric material.

In general, by increasing the contribution of crystal part in a polymer, the material tends to become more brittle and its fracture strength would decrease. Supporting tensile tests, SEM and AFM findings, XRD results show that the performance of polysulfone hemodialyzer fibers would be negatively affected because of the decrease in its resistance to fracture. Additionally, it is known that crystallinity in polymers tends to reduce both penetrant solubility and diffusivity, thereby reducing the permeance [66]. In the present case, since the membrane becomes more crystalline, loss of permeance can be expected. Therefore, increase in crystallinity can be a risk to perform dialysis procedure in a healthy way if it is not in a safety margin.

3. DISCUSSION

The kidney serves multiple complex physiologic functions and in the case of chronic renal failure, these functions are needed to be implemented at least partially by artificial kidneys, which goals to remove the toxins and excess fluid from the patient's blood. By 2006, only in our country, more than 33,500 patients are suffering from end stage renal disease and treated with hemodialysis [11]. Therefore, hemodialysis plays an important role in renal replacement management in Turkey, as it is throughout the world.

The need to improve the dialysis quality and treatment efficiency brings out the necessity of researches in determining the biocompatibility and performance of the dialyzers. Most clinical researches have concerned the membrane biocompatibility, clearance, patient's symptoms and survival. In parallel to these clinical studies, in vitro determination of characteristics of the hemodialyzers under different conditions is essential. In this thesis, the performance of the membrane for first and reuse applications was evaluated by focusing on mechanical stability, crystallinity degree and microscale structure in terms of pore dimension, geometry and distribution. The studied membrane type was chosen as an example of a widely used hemodialyzer representing the recent technical innovations in the field of membrane technology.

The stereomicrographs depicted different components of the polysulfone dialyzers in relatively low magnification and proved the necessity of AFM and SEM studies while examining the detailed morphology of the fibers. It is known that blood and dialysate entrance and pathway determines the homogeneity of the flow distribution, which makes the contact of the countercurrent flows with the membrane more effective [31]. The micro undulation of the fibers, that avoids dead zones and channeling phenomena [31], can be seen by naked eyes. The special dialysate entrance with the pinnacle structure and distribution of the fibers in the potting material (polyurethane) is observed with the help of stereomicroscopy.

Multiple use (reuse) of hemodialyzers is practiced in many countries to reduce costs in the treatment of end stage renal disease (ESRD). Although it has emerged as a practical tool, little is known about the effects of reprocessing on dialyzer fibers or on the interactions that occur during blood contact [32]. In addition to the chemically aggressive environment created by blood, dialysate and mostly by sterilants, the dialyzer fibers have to function under fluctuating mechanical stress arising from the fluid flow. Under these circumstances, the predicted stress concentration around the imperfections (pores) of the material may result in inadequate solute removal, inefficient dialysis, more importantly, blood leakage due to the small fractures. Therefore, determination of mechanical properties of the hemodialyzer membranes is critically important in reducing dialysis risks.

The monotonic and cyclic tensile loading stress–strain curves of the virgin and used–processed polysulfone fibers are plotted in Figures 2.3.3.1 – 2.3.3.4, in order to show the mechanical behavior of the membrane after different treatments. The results of tensile tests show that the used–processed fibers fractures at lower stresses and strains compared to virgin fibers after monotonic or cyclic loading. Both of the virgin and used–processed fibers that are exposed to cyclic loading become stiffer compared to monotonically loaded fibers. Since cyclic loading resembles the alteration in pressure due to the interferences in dialysis session that depends on the complications in the patient, this result is important for showing the increase in resistance to elongation after patient contact.

The energies required to fracture monotonically loaded virgin fiber, cyclically loaded virgin fiber, monotonically loaded used–processed fiber and cyclically loaded used–processed fiber are; 219.46, 173.79, 140.13, 40.45 MPa, respectively. Therefore, it can be said that the toughness of the polysulfone membrane decreases dramatically after patient contact and disinfection process. Additionally, the toughness of cyclically loaded virgin or used–processed fibers is less than the toughness of monotonically loaded fibers. In conclusion, the used membranes cannot resist high loads as much as the virgin membranes. Reprocessing reduces the membrane's toughness, ultimate tensile stress and yield strength and membrane becomes more brittle resulting in an increase in the possibility of membrane damage.

The changes in the membrane's outer surface morphology between virgin and used-processed fibers are determined by the AFM studies including three dimensional micrographs and height histograms, from which detailed information about the surface roughness of the fibers can be obtained. The results of AFM studies revealed that the surface morphology of the polysulfone hemodialyzer fiber become rougher after dialysis and reprocessing procedure. The appearance of interconnected cavity channels on the virgin polysulfone hollow fiber can be seen obviously, however, it is seen that there is a decrease in the number of clearly open channels after reprocessing. In conclusion, AFM studies showed that surface degradation occurs on the outer surfaces polysulfone hemodialyzer fibers after patient contact and disinfection procedure, which is important in terms of performance and possible also for the inner (separating) surface.

As stated before, SEM and AFM are complementary techniques for investigating the surface features and morphology. The SEM images of the polysulfone hemodialyzer fibers showed the dense skin layer in the internal surface of the membrane. The number of pores decreases and the size of pores increases toward the exterior of the membrane in order to form a support structure.

Figure 2.5.3.1, Figure 2.5.3.2 show the scanning electron micrographs of the fracture surfaces of the monotonically or cyclically loaded virgin and used-processed fibers. It is seen that the cyclically loaded use-processed fiber, which demonstrates both of the chemical and mechanical effects, has some ruptures in the blood side, which may lead to protein loses. Additionally, from Figure 2.5.3.3, in the lateral surface (dialysate side), pore size is considerably larger in all types of fibers compared to the initial structure. Figure 2.5.3.4 – Figure 2.5.3.7 are the clear evidences of the change in pore geometry and the increase in diameter after mechanical stress and blood/sterilant contact of the membrane.

Previous studies with bleach reprocessing have already hypothesized that hemodialyzer reprocessing results in increased pore size and increased potential for loss of proteins, such as albumin [61]. On the other hand, the increase in pore size may be attributed to the increase in solute clearance during the treatment. However, continuous increase in the pore size may pose a health risk to the patient if the integrity of the fibers is

altered [61]. Therefore, the porosity of a membrane, which is expressed by the number of pores per unit of surface area and the curve of pore size distribution, must be optimized in dialysis in order to achieve the maximal permeability for solutes up to 40,000 Da and with a minimal or no leak of albumin (MW 48,000 Da) [67]. This optimized structure must not lose its integrity in reuse applications and minimal loss of proteins in the presence of high sieving coefficients must be achieved after multiple uses also. However, in this thesis, it is seen that, compared to its initial structure, the structure of used–processed fibers changes and these changes can be listed as; increase in pore size, merging of pores, formation of ligaments and hindered passages. In addition, although they are rinsed with ultra–pure water after reprocessing procedure, the SEM images of all used–processed fibers include some residual materials on the surfaces that can coat the inner lumen of hemodialyzer fibers and reduce the number of effective pores in the separating (inner) side. In conclusion, the dialysis session and reprocessing does alter the membrane surface, which may result in different patient responses and increased risk for the multiple use of the same membrane.

The crystallographic structures of virgin and used–processed polysulfone hemodialyzers were determined and compared by X–ray diffraction (XRD) method. When the X–ray diffractograms of used–processed polysulfone hemodialyzer fiber after monotonic loading, virgin fiber after monotonic loading, and virgin fiber without any application are compared, it is obvious that the diffractogram of used–processed hemodialyzer fiber after monotonic loading gives the highest intensity peaks. At the same time, it has additional crystalline peaks. In other words, monotonic loading increases the crystalline portion in the structure of polysulfone hemodialyzer fiber and addition of the effects of reprocessing further increases the crystallinity.

However, for the cyclically loaded virgin and used–processed polysulfone hemodialyzers, the change in the membrane structure is different from the monotonically loaded fibers. X–ray diffractograms of cyclically loaded virgin or used–processed fibers are broader than the diffractogram of untreated virgin fiber, i.e. the main peaks have lower heights that bring a decrease in crystalline portion into mind. On the other hand, the used–processed fiber after cyclic loading has two more distinct peaks in its diffractogram compared to the virgin fiber, which can be deduced as an evidence of increase in the

crystallinity. It can be said that cyclic loading results on new orientations and phases in the structure of the fibers. In the used–processed fibers, the effect of cyclic loading and the chemical ageing due to reprocessing is seen together. It must be noted that during cyclic tensile loading, the load cycles were in the elastic range. Although this might even be related to microdamage, the prolonged cyclic loading applied in the plastic range may result different responses in the material. At this point, further studies are needed to be performed in order to investigate the effect of cyclic loading in plastic region after multiple uses. In addition, it must be noted that the X–ray diffractometer investigates the bulk material. The plastic deformation on the pore tips might have been ignored, although, it increases the contribution of the crystalline part into the membrane’s structure.

4. CONCLUSION

The performance of a widely used high flux polysulfone hemodialyzer was evaluated in order to determine the effect of hemodialysis and reprocessing procedures. The results showed that the chemically and mechanically aggressive environment arising from hemodialysis and reprocessing procedures alters the mechanical, crystallographic and microstructural properties of high flux polysulfone hemodialyzers. The toughness, ultimate stress and yield strength of used–processed fibers decrease and they become stiffer than their initial structure. The surface morphology changes only after one dialysis session and reprocessing. It appears that the pore geometry, size and distribution alter and this can be connected with an increased risk in disturbance of ideal filtration characteristics. Furthermore, the membrane material undergoes some changes in the way of increased crystalline portion in its structure after monotonic loading. The cyclically loaded fibers become more amorphous regardless of being virgin or used and reprocessed.

As stated before, this study takes no position for or against the practice of dialyzer reuse since the impact of reused dialyzers on patient safety is not still completely determined. However, as a matter of fact, the performance polysulfone hemodialyzer differs from the initial use after multiple reprocessing. Although it is believed that membrane reuse should be adopted in Turkey in order to reduce the costs [13], the risks for patients and also for the dialysis staff must be taken into account.

It is obvious that additional research is needed to evaluate the impact of reprocessing on the performance of high flux polysulfone dialyzers in parallel with clinical studies, with regard to solute removal and biocompatibility. Laboratory studies should be aimed at increasing understanding of membrane–protein interactions, how these interactions are modified by different germicides, and the consequences of any modification on dialyzer performance and subsequent interactions with blood components [39]. The most important step for increasing the lifetime and quality of hemodialysis patients is the implementation of the results of these studies to the newer membrane technologies and manufacture innovative hemodialyzers that can approach to ideality.

REFERENCES

1. Guyton, A.C., and Hall, J.E., *Textbook of Medical Physiology*, USA: Elsevier Inc., 11th Edition, 2006.
2. Sobh, M.A., *Essentials of Clinical Nephrology*, Egypt: Dar El Shorouk, 1st Edition, 2000.
3. Brenner, B.M., Rector, F.C., and Livine, S.A., *Brenner & Rector's the Kidney*, USA: W. B. Saunders, 7th edition, 2004.
4. Fresenius Medical Care GmbH, "FX class high flux dialyzers for the future–Brochure", Fresenius Medical Care Releases, 2004. Available: www.fmc-ag.com.
5. Truskey, G.A., Yuan, F., and Katz, D.F., *Transport Phenomena in Biological Systems*, NJ: Pearson Prentice Hall, 2004.
6. Fauci, A.S., Kasper, D.L., Longo, D.L., Braunwald, E., Hauser, S.L., Jameson, J.L., and Loscalzo, J., *Harrison's Principles of Internal Medicine*, USA: The McGraw–Hill Companies, Inc., 17th Edition, 2008.
7. Fresenius Medical Care GmbH, "Dialysis compact: The invention, development and success of the artificial kidney", Fresenius Medical Care Releases, 2007. Available: www.fmc-ag.com.
8. Ronco, C., and La Greca, G., "The role of technology in hemodialysis", *Hellen Nephrol.*, Vol.14 Suppl. 1, pp. 66–74, 2002.
9. Grassmann, A., Gioberge, S., Moeller, S., and Brown, G., "ESRD patients in 2004: global overview of patient numbers, treatment modalities and associated trends" *Nephrology Dialysis Transplantation*, Vol. 20, pp. 2587–2593, 2005.
10. Reuß, M., "Gesundheitsindustrie – ein Wachstumsmarkt am Beispiel Dialyse," Fresenius Medical Care, Schweinfurt, pp. 6–7, 2007.
11. Turkish Society of Nephrology, "National hemodialysis, transplantation and nephrology registry report of Turkey, 2006", Turkey: Turkish Society of Nephrology, 2007.
12. U.S. Renal Data System, "USRDS 2007 Annual data report: Atlas of end–stage renal disease in the United States", National Institutes of Health, National Institute of Diabetes and Digestive and Kidney Diseases, 2007.
13. Ereğ, E., Sever, M.S., Akoglu, E., Sariyar, M., Bozfakioğlu, S., Apaydin, S., Ataman, R., Sarsmaz, N., Altıparmak, M.Z., Seyahli, N., and Serdengeçti, K., "Cost of renal replacement therapy in Turkey", *Nephrology*, Vol. 9, pp.33–38, 2004.
14. Ronco, C., *Sepsis, Kidney and Multiple Organ Dysfunction: Proceedings of the Third International Course on Critical Care Nephrology*, Farmington, CT, USA: Karger Publishers, 2004.
15. Ratner, B.D., Hoffman, A.S., Schoen, F.J., and Lemons, J.E., *Biomaterials Science, an Introduction to Materials in Medicine*, 2nd Edition, Elsevier Inc., 2004.

16. Davison, A. M., Cameron, J.S., Grunfeld, J.P., Kerr, D.N.S., Ritz, E., and Winearls, C.G., *Oxford Textbook of Clinical Nephrology*, Oxford University Press, 2nd edition, 1998.
17. Malluche H.H., Sawaya, B.P., Hakim, R.M., and Sayegh, M.H., *Clinical Nephrology, Dialysis and Transplantation*, Dustri-Verlag, 1999.
18. Association for Advancement of Medical Information (AAMI): American National Standard. "Reuse of Hemodialyzers" Arlington, VA: AAMI, 2003.
19. Morti, S., "Mass transport during hemodialysis, effects of plasma contacting, reprocessing and uremia", PhD Thesis, University of Delaware, USA, 1999.
20. Cheng, C.T., Wu, M.H., Lin, L.L., Hsu, H.P., Chang, H.Y., Hsu, S.W., and Yang, H.M., "Clinical study of a nano structure FX80 hollow fiber dialyzer", *Acta Nephrologica*, Vol. 16, pp. 73–78, 2002.
21. National Kidney Foundation (NKF), "NKF-KDOQI clinical practice guidelines and clinical practice recommendations for hemodialysis adequacy 2006", National Kidney Foundation, Inc., USA, 2008. Available: <http://www.kidney.org/professionals/KDOQI/>.
22. Schrier, R.W., *Atlas of Diseases of the Kidney*, Vol. 5, Current Medicine, Inc. Blackwell Science, 1999. Available: <http://www.kidneyatlas.org>.
23. Ward, R. A., and Ouseph, R., "Impact of bleach cleaning on the performance of dialyzers with polysulfone membranes processed for reuse using peracetic acid", *Artificial Organs*, Vol. 27, pp. 1029–1034, 2003.
24. Lameire, Norbert, *Complications of Dialysis*, New York, USA: Marcel Dekker Inc., 2000.
25. Budinsky, K.G., *Engineering Materials, Properties and Selection*, USA: Prentice Hall, 4th Edition, 1992.
26. Hongu, T., *New Millennium Fibers*, Cambridge, GBR: Woodhead Publishing Limited, p.53, 2005.
27. Külz, M., Nederlof, B., and Schneider, H., "In vitro and in vivo evaluation of a new dialyzer", *Nephrology Dialysis Transplantation*, Vol. 17, pp. 1475–1479, 2002.
28. Mudge, D.W., et.al. "Randomized trial of FX high flux vs standard high flux dialysis for homocysteine clearance" *Nephrology Dialysis Transplantation*, Vol. 20, pp. 2178–2185, 2005.
29. Mintech Corporation, "How a dialyzer is made, In: *Renews*, A publication on dialyzer reprocessing", Mintech Corporation, Vol. 12, 2007.
30. Ronco, C., Ballestri, M., and Brendolan, A., "New developments in hemodialyzers", *Blood Purification*, Vol. 18, pp. 267–275, 2000.
31. Ronco, C., et al. "Hemodialyzer: From macro-design to membrane nanostructure; the case of the FX-class of hemodialyzers", *Kidney International*, Vol. 61, Suppl. 80, pp. 126–142, 2002.
32. Cornelius, R.M., et al. "Effects of reuse and bleach/formaldehyde reprocessing on polysulfone and polyamide hemodialyzers", *ASAIO Journal* Vol. 48, pp. 300–311, 2002.

33. Blagg, C., "How should dialyzers be reprocessed?", *Seminars in Dialysis*, Vol. 11, pp. 279–28, 1998.
34. Association for Advancement of Medical Information (AAMI): American National Standard. "Current concepts in hemodialyzer reprocessing" Arlington, VA: AAMI, 2nd Edition, 1998.
35. Seymen, P.S., "Nefroloji Yandal Uzmanlık Tezi–Diyalizör Reuze'un İnflamasyon ve Nutrisyon Üzerine Etkisi", Specialization Thesis, Cerrahpaşa Tıp Fakültesi, İstanbul, Turkey, 2004.
36. Stragier, A., Wenderickx, D., and Jadoul, M., "Rinsing time and disinfectant release of reused dialyzers: comparison of formaldehyde, hypochlorite, Warexin, and Renalin", *American Journal of Kidney Diseases*, Vol. 26, pp. 549–553, 1995.
37. Levin, N. W., "Effects of reuse on dialyzer function", *Seminars In Dialysis*, Vol. 13, pp. 286–288, 2000.
38. Metrex Research Corporation, "Patent on cleaning and decontaminating dialyzers by per-compound solution", WO/2001/019414, Publication Date: 22.03.2001.
39. Ward, R. A., and Feldman H.I., "Dialyzer reuse: lingering doubts", *Seminars in Dialysis*, Vol. 11, pp. 276–278, 1998.
40. Twardowski, Z.Y., "Dialyzer reuse – Part II: Advantages and disadvantages", *Seminars in Dialysis*, Vol. 19, pp. 217–226, 2006.
41. Levin, N. W., Levin, R., and Folden, T., "How should dialyzers be reprocessed?", *Seminars in Dialysis*, Vol. 11, pp. 281–282, 1998.
42. Murthy B.V.R., Sundaram, S., Jaber, B.L., Perrella, C., Meyer, K.B., and Pereira, B.J.G., "Effect of formaldehyde/bleach reprocessing on in vivo performances of high–efficiency and high–flux polysulfone dialyzers", *Journal Of American Society Of Nephrology*, Vol. 9, pp. 464–472, 1998.
43. San, A., Tonbul, H.Z., İka, D., and Selçuk, N.Y., "Diyaliz merkezimizde çeşitli membranlarla yapılan reuse uygulama sonuçları", *Official Journal Of The Turkish Nephrology Association*, Vol. 3, pp. 93–96, 1994.
44. Ereğ, E., "Çöpe atılan dövizler ve aynı diyaliz filtresinin aynı hastada 5–10 defa kullanılması", *Official Journal of the Turkish Society of Nephrology*, Vol. 10, pp.196–202, 2001.
45. Port, F.K., Wolfe, R.A., Hulbert–Shearon T.E., Daugirdas, J.T., Agodoa, L.Y.C., Jones, C., Orzol, S.M., and Held, P.J., "Mortality risk by hemodialyzer reuse practice and dialyzer membrane characteristics: Results from the USRDS dialysis morbidity and mortality study", *American Journal of Kidney Diseases*, Vol. 37, pp. 276–286, 2001.
46. Bart, J.C.J., *Plastics Additives*, Amsterdam, Netherlands: IOS Press, 2006.
47. McMahon, C.J., *Structural Materials, a Textbook with Animations*, Merion Press, 2004.
48. Roylance, D., "Stress–strain curves", Massachusetts Institute of Technology: MIT Open Course Ware, 2001. Available: <http://ocw.mit.edu>.
49. Mark, J. E., *Inorganic Polymers*, Cary, NC, USA: Oxford University Press, Incorporated, 2005.

50. Perez, N., *Fracture Mechanics*, Hingham, MA, USA: Kluwer Academic Publishers, 2004.
51. Solvay Advanced Polymers, “UDEL polysulfone design guide”, L.L.C., USA: Solvay Advanced Polymers, 2002. Available: <http://www.solvayadvancedpolymers.com>.
52. Shao, J., Wolff, S., and Zydney, A. L., “In vitro comparison of peracetic acid and bleach cleaning of polysulfone hemodialysis membranes”, *Artificial Organs*, Vol. 31, pp. 452–460, 2007.
53. Causserand, C., Rouaix, S., Lafaille, J.P., and Aimar, P., “Degradation of polysulfone membranes due to contact with bleaching solution” *Desalination*, Vol. 199, pp.70–72, 2006.
54. Maurin, E., and ThomINETTE, F., “Ageing of polysulfone ultrafiltration membranes in contact with bleach solutions”, *Journal of Membrane Science*, Vol. 282, pp.198–204, 2006.
55. Khulbe, K. C., Feng C. Y., and Matsuura, T., *Synthetic Polymeric Membranes–Characterization by Atomic Force Microscopy*, Berlin: Springer, 2008.
56. Ramakrishna, S., *Introduction to Electrospinning and Nanofibers*, River Edge, NJ, USA: World Scientific Publishing Company, Incorporated, 2005.
57. Ambios Technology, “USPM Brochure–Q–Scope Series Scanning Probe Microscopes”, Ambios Technology, Inc. Releases, 2006.
58. Boussu, K., Van der Bruggen , B., Volodin, A., Snauwaert , J., Van Haesendonck, C., and Vandecasteele, C., “Roughness and hydrophobicity studies of nanofiltration membranes using different modes of AFM”, *Journal of Colloid and Interface Science*, Vol. 286, pp. 632–638, 2005.
59. Konduk, B.A., “Comparative analysis of artificial kidney membranes and influences of in vivo utilization on their properties and performances in terms of the quality of the materials and hemodialysis treatment”, PhD. Thesis, Boğaziçi University, Istanbul, Turkey, 2004.
60. Cao, G., *Nanostructures and Nanomaterials*, Singapore: World Scientific Publishing Company, Incorporated, 2004.
61. Johnson, A., Mishkin, G. J., Lew, S.Q., Mishkin, M., Abramson, F., and Lecchi, P., “In vitro performance of hemodialysis membranes after repeated processing”, *Am. Journal of Kidney Dis.*, Vol. 42, pp. 561–566, 2003.
62. Wolff, S.H., and Zydney, A.L., “Effect of bleach on the transport characteristics of polysulfone hemodialyzers”, *Journal of Membrane Science* 243, pp. 389–399, 2004.
63. Rabiej, S., et.al., “ Investigations of the crystallinity of polyamide–6/sulfonated polysulfone blends by X–ray diffraction and DSC methods” *Eur. Polymer. J.*, Vol. 33, pp. 1031–1039, 1997.
64. Brown, T.L., LeMay, E., and Bursten, B.E., *Chemistry–The Central Science*, UK: Prentice–Hall International Inc., 7th Edition, 1997.
65. Treska, M., “Polymer structure”, Massachusetts Institute of Technology: MIT Open Course Ware, 2006. Available: <http://ocw.mit.edu>.
66. Sridhar, S. et.al., “Gas permeation properties of polyamide membrane prepared”, *Journal of Material Science*, Vol. 42, pp. 9392–9401, 2007.

67. Ronco, C., and Nissenson, A.R., "Does nanotechnology apply to dialysis?", *Blood Purification*, Vol. 19, pp. 347–352, 2001.